Università degli Studi di Ferrara

DOTTORATO DI RICERCA IN

"MEDICINA MOLECOLARE"

CICLO XXXIV

COORDINATORE Prof. Francesco Di Virgilio

Tofacitinib improves mitochondrial function in psoriatic arthritis fibroblast-like synoviocytes via autophagy modulation

Settore Scientifico Disciplinare MED/16

Dottorando

Dott. Ettore Silvagni

_____

Tutore

Prof. Marcello Govoni

_____

Co-Tutore

Dott.ssa Sonia Missiroli

_____

Anni 2018/2021

Index

Abbreviations

In order of appearance in the text:

PsA, Psoriatic arthritis

JAKs, Janus kinases

FLS, fibroblast-like synoviocytes

PBMCs, peripheral blood mononuclear cells

ROS, reactive oxygen species

OCR, Oxygen consumption rate

SD, Standard deviation

TNF, tumor necrosis factor-α

IL; interleukin

RA, rheumatoid arthritis

DMARDs, disease-modifying antirheumatic drugs

RCTS, randomized controlled trials

SLRs, systematic literature reviews

NSAIDs, nonsteroidal anti-inflammatory drugs

GCs, glucocorticoids

cs, Conventional synthetic

MTX, methotrexate

b, biological

ts, targeted synthetic

JAKis, JAK inhibitors

TNFis, TNF inhibitors

IFX, infliximab

ETA, etanercept

ADA, adalimumab

CTZ, certolizumab pegol

GOL, golimumab

SEC, secukinumab

IXE, ixekizumab

FDA, Food and Drug Administration

EMA, European Medicine Association

PDE4, phosphodiesterase-4

IFNs, interferons

EULAR, European League Against Rheumatisms

ACR, American College of Rheumatology

PASI, Psoriasis Area Severity Index

GRAPPA, Group for Research and Assessment of Psoriasis and Psoriatic Arthritis

SF, synovial fluid

TGF, transforming growth factor

IFN-γ, interferon-gamma

MMP-3, matrix metalloproteinase 3

CRP, C-reactive protein

VEGF, vascular endothelial growth factor

YKL-40, chitinase-3 like-1

COMP, cartilage oligomeric matrix protein

Th1, T helper 1

SDAI, Simplified Disease Activity Index

DAS28, Disease Activity Score on 28 joints

PMN, polymorphonuclear

SFMC, synovial fluid mononuclear cell

MCP-1, monocyte chemoattractant protein 1

IL-17RA, IL-17-receptor A

Tm, transmembrane

TACE, TNF-alpha-converting enzyme

NF-κB, nuclear factor kappa-B

RANKL, receptor activator of nuclear factor-kB ligand

TRAF, TNFR-associated factor

GM-CSF, Granulocyte-Macrophage Colony-Stimulating Factor

TYK2, tyrosine kinase 2

ECM, extracellular matrix

OSM, Oncostatin M

ECAR, extracellular acidification rate

MRC, maximal respiratory capacity

ER, endoplasmic reticulum

mTOR, mammalian target of rapamycin

mTORC1, mammalian target of rapamycin (mTOR) complex 1

PI3K-III, phosphatidylinositol 3-kinase

LC3, microtubule-associated protein 1 light-chain 3

PE, phosphatidylethanolamine

GWAS, genome-wide association

HLA, human leukocyte antigens

ATG, autophagy related

PAD, peptidyl-arginine deiminase

APCAs, anti-citrullinated peptides autoantibodies

3-MA, 3-methyladenine

MHC, major histocompatibility complex

APCs, antigen presenting cells

OA, osteoarthritis

TUNEL, terminal deoxynucleotidyl transferase-mediated dUTP nick end labeling

PARP, PolyADP-ribose polymerase

DNM1L, Dynamin 1-like protein

TRAP, tartrate-resistant acid phosphatase

SpA, spondyloarthritis

DCs, dendritic cells

ANA, anti-nuclear antibodies

CE-AVEC, Ethics Committee of Area Vasta Emilia Centro - Regione Emilia-Romagna

CASPAR, Classification Criteria for Psoriatic Arthritis

US, Ultrasound

BMI, body mass index

HAQ-DI, Health Assessment Questionnaire–Disability Index

PGA, patient global activity

PhGA, physician global assessment

ESR, erythrocytes sedimentation rate

DAPSA, Disease activity in psoriatic arthritis

LEI, Leeds Enthesitis Index

BSA, Body Surface Area

MSK, musculoskeletal

GLOESS, Global OMERACT–EULAR Synovitis Score

OMERACT, Outcomes Measures for RheumAtology Clinical Trials

PD, Power-Doppler

IHC, immunohistochemistry

H&E, haematoxylin/eosin

DMEM, Dulbecco's modified Eagle's medium

FBS, foetal bovine serum

RPMI, Roswell Park Memorial Institute

PBS, Phosphate Buffered Saline

DMSO, dimethyl sulfoxide

rpm, revolutions per minute

ELISA; enzyme-linked immunosorbent assay

NH_4Cl, ammonium chloride

NAC, N-Acetyl-L-Cysteine

p, phosphorylated

FCCP, carbonyl cyanide-4-(trifluoromethoxy) phenylhydrazone

ALP, alkaline phosphatase

SLE, systemic lupus erythematosus

PsO, psoriasis

JIA, juvenile idiopathic arthritis

AS/nrAS, ankylosing spondylitis/nonradiographic axial spondylarthritis

SH, suppurative hidradenitis

CD, Crohn's disease

UC, ulcerative colitis

BD, Behcet's disease

JAK, Janus Kinase

AD, atopic dermatitis

NAFLD, non-alcoholic Fatty Liver Disease

COPD, chronic obstructive pulmonary disease

CKD, chronic kidney disease

TAK1, Transforming growth factor-alpha-activated kinase 1

NEMO, NF-κB essential modulator

IKK, inhibitor of IκB kinase

IκBs, inhibitory proteins of NF-κB

Abstract

Introduction: Psoriatic arthritis (PsA) is a chronic inflammatory systemic disease, and peripheral joints involvement is responsible of significant morbidity for patients, leading to damage accrual. Different drugs are available for the systemic management of this condition, with different mechanisms of action. Nevertheless, the rules driving the correct therapeutical choice in each individual patient are not completely defined. Janus kinases (JAK) inhibitors are a class of drugs able to reduce synovial inflammation in patients, and tofacitinib, a JAK1/3 inhibitor, is the most studied. Preliminary evidence suggest an effect of tofacitinib on fibroblast-like synoviocytes (FLS), reducing pro-invasive and pro-inflammatory properties, as well as improving mitochondrial function. The link between JAK inhibition and mitochondrial function improvement at synovial level is not completely understood.

Materials and Methods: This is an *in vitro* study. Patients with active PsA underwent ultrasound-guided synovial biopsy in the context of a tertiary-referral outpatient clinic. Histological evaluation was performed according to Krenn's synovitis score. FLS, peripheral blood mononuclear cells (PBMCs), and synovial explants cultures were set up, and cells were treated *in vitro* with tofacitinib 1 μM or vehicle control for 24h. For some experiments, the autophagy-inducer rapamycin was utilized, as well. Protein levels in cellular homogenates were analysed by western blot for relevant autophagy markers, and chemokines/cytokines into culture supernatants were quantified by ELISA. Migration assays were used to investigate the effect of tofacitinib on invasive properties of FLS, while specific mitochondrial probes were used to measure intracellular reactive oxygen species (ROS), mitochondrial potential, and mitophagy. Oxygen consumption rate (OCR), reflecting oxidative phosphorylation, was quantified using the Seahorse technology. Differences were determined adopting the non-parametric Wilcoxon signed rank test.

Results: 16 patients with moderately active PsA were enrolled. Mean (SD) Krenn's synovitis score was 4.4. (1.9). Tofacitinib significantly increased LC3-II (p=0.0002) and ATG7 (p=0.0001) levels in PsA FLS compared to vehicle control, suggesting an increase in spontaneous autophagy activity. No effect was highlighted in PBMCs and synovial explants cultures. Tofacitinib reduced migration properties of PsA FLS (p=0.0024), and a similar trend was documented using rapamycin. Moreover, tofacitinib reduced MCP-1 and IL-6 release into FLS supernatants (p=0.0007 and p=0.0022, respectively), reduced intracellular ROS production (p=0.0180), increased basal OCR (p=0.02809), ATP production (p=0.0280) and maximal respiratory capacity (p=0.0180), and enhanced mitophagy (p=0.0156).

Conclusion: The JAK inhibitor tofacitinib reduces pro-invasive and pro-inflammatory properties of PsA FLS and improves mitochondrial function. The induction of autophagy/mitophagy by tofacitinib might permit the removal of damaged mitochondria and a better functioning of the remaining ones.

Introduction

Psoriatic arthritis (PsA) is a chronic systemic immune-mediated inflammatory disease, occurring at frequencies ranging from 6 to 42% of patients with skin psoriasis [1,2], or affecting family members of psoriatic patients [3]. Skin disease is considered the main risk factor for PsA development and, although the occurrence of joint disease is not predictable, an incidence risk of 20% is approximated after more than 30 years of skin psoriasis, with higher rates in the context of nail, scalp, or inverse psoriasis; this risk is also affected by the severity of the cutaneous manifestations. In the context of PsA, involvement of the joints, entheses, and skin is challenging for clinicians, and dactylitis, nail dystrophy, uveitis, and spine manifestations represent clinical endotypes susceptible to different management approaches. Progressive damage accrual, along with inflammatory manifestations of the disease, is highly disabling for patients, with impacts on quality of life and healthcare costs [4]. Comorbidities associated with repercussions related to cardiovascular risk, such as obesity and metabolic syndrome, are intrinsic parts of the psoriatic "disease".

This clinical heterogeneity is reflected in complex pathophysiology, knowledge of which is crucial to hypothesizing a therapeutic approach targeting the ongoing pathological process [1,5–7]. Infiltration of both innate and adaptive immune cells in different target organs and tissues results in significant production of different proinflammatory cytokines, including tumor necrosis factor-α (TNF), interleukin (IL)-1β, IL-6, IL-22, IL-23, IL-17A, and IL-18, inducing further inflammatory mediators release and damage progression. New evidence in PsA pathogenesis has provided further insights into the molecular pathways involved in either cutaneous or articular manifestations of the disease, and genetic, epigenetic, environmental, cellular and molecular aspects have been clarified, driving the development of different targeted therapies [8]. From a clinical point of view, drugs targeting different molecules primarily involved in chronic inflammation, such as TNF, the IL-23 and IL-17A axis, or Janus Kinases/Signal Transducers and Activators of Transcription (JAK/STATs), are now available [9–11]. This multiplicity of treatment options poses relevant questions about how to best interfere with different pro-inflammatory processes in individual PsA patients, since clinicians lack reliable tools to select the best therapeutic pathway to target to optimize clinical response [8]. *A priori*, tissue-specific biomarkers are the most promising candidates to stratify patients based on the actual ongoing pathogenic process, as demonstrated by some attempts in other chronic inflammatory joint diseases, such as rheumatoid arthritis (RA) [12,13], and the recognition of the specific effects of different disease-modifying antirheumatic drugs (DMARDs) is crucial to hypothesize a biomarkers-driven therapeutical strategy.

Targeted therapies for PsA

Adapted from: Silvagni E. et al. From Bed to Bench and Back: TNF-α, IL-23/IL-17A, and JAK-Dependent Inflammation in the Pathogenesis of Psoriatic Synovitis. Front Pharmacol. 2021 Jun 15;12:672515 [7].

Data on the efficacy of treatments for PsA come from randomized controlled trials (RCTs) and observational studies, as well as systematic literature reviews (SLRs) [14] informing current clinical practice guidelines [9–11,15]. First-line pharmacological treatment strategies include nonsteroidal anti-inflammatory drugs (NSAIDs) and/or local injection of glucocorticoids (GCs). Conventional synthetic (cs)DMARDs (e.g., methotrexate (MTX)) are selected in cases of elective peripheral joint involvement, while PsA patients refractory to csDMARDs should be treated with biological (b) DMARDs or oral targeted synthetic (ts) DMARDs. Current treatment guidelines suggest the use of JAK inhibitors (JAKis) in cases of bDMARD treatment failure or when other biologics are contraindicated. Since the amount of data on JAKis adoption in PsA will increase in the coming years, the positioning of these drugs might be revised when treatment recommendations are updated. This stepwise approach is generally accepted worldwide. Currently available bDMARDs for the management of PsA, which were designed based on the growing knowledge of disease pathogenesis, include 5 different TNF inhibitors (TNFis) (infliximab (IFX), etanercept (ETA), adalimumab (ADA), certolizumab pegol (CTZ), golimumab (GOL)) and their available biosimilars, the anti-IL-12/IL-23 p40 common subunit antibody ustekinumab, the anti-IL-17A antibodies secukinumab (SEC) and ixekizumab (IXE), and the selective T cell costimulation modulator abatacept. Recently, the selective IL-23 p19 subunit inhibitor guselkumab [16,17] has been approved for the management of PsA, as well. Additionally, apremilast, tofacitinib and upadacitinib are the oral tsDMARDs available for PsA approved by the Food and Drug Administration (FDA) and European Medicine Association (EMA). The first inhibits phosphodiesterase-4 (PDE4). Tofacitinib blocks JAK1 and JAK3, with a functional effect on JAK2 [18,19], while upadacitinib is a selective JAK1 inhibitor [20]. Moreover, other drugs for the systemic management of PsA are in different phases of development, and some of these are already available for the systemic management of skin psoriasis. The anti-IL-23 biologics risankizumab [21–23], tildrakizumab [24,25], and the anti-IL17 receptor (IL-17R) antibody brodalumab [26] are under investigation in PsA, and the bispecific immunoglobulin bimekizumab, which targets IL-17A and IL-17F, is also being studied [27]. Among tsDMARDs, filgotinib is promising [28,29]. Table 1 summarizes the drugs for the management of PsA that are currently approved or in different phases of development.

Among the high number of drugs registered for the management of PsA in recent years, the majority of available therapeutic options act against the TNF pathway, while others are directed against the IL-23/IL-17A axis, and JAKis virtually encompass the intersections of a number of pathways based on their potential 'broad-spectrum' mechanism of action, blocking different type I and II cytokines (e.g., IL-6, IL-23, IL-22, and interferons (IFNs)). This wide availability of drugs enables interference with the most important cytokines

and nodes involved in disease pathogenesis, with the clinical aim of reducing signs and symptoms of the disease and preventing joint/bone damage and disability accrual. From a pathogenetic point of view, instead, the possibility of interfering with single or multiple crossroads directly involved in disease susceptibility and synergism could reduce inflammation in its entirety at the site of the disease (i.e., the skin, entheses, and synovium), decelerating the progression to more advanced stages of illness.

From a clinical perspective, the choice of the preferred bDMARD as a first-line biological in patients with peripheral arthritis, as well as selection of the correct strategy after failure of the first bDMARD (historically a TNFi), are aspects of interest, despite available evidence supporting clinical decisions being scant [30,31]. Indeed, after almost 20 years of TNFi availability in the field of PsA, the capability to treat PsA with this class of drugs in the clinic has been reinforced by long-term efficacy and safety data [32,33]. TNFis are usually considered among first-line biological treatment strategies in different clinical settings, while experience with recently developed anti-IL-17A agents is obviously lower. However, similar efficacy rates have been shown between TNFis and non-TNFis in RCTs, with higher responses in first-line treatment strategies [34,35] than in second-line options [36–39]. Moreover, the recent European League Against Rheumatisms (EULAR) recommendations suggested preferring an anti-IL17A or anti-IL12/23 agent in cases with relevant skin involvement [10], and this remains, at present, the only acknowledgment of personalized systemic treatment in this context. However, in the 2018 American College of Rheumatology (ACR) guidelines, TNFis are conditionally suggested as the first-line treatment strategy over anti-IL-17A and anti-IL-12/23 antibodies [11] on the basis of the more robust amount of clinical data.

Information regarding the comparative effectiveness of drugs with different modes of action in PsA is steadily increasing. Indirect evidence from RCTs and observational studies cautiously suggests a higher efficacy for IL-17A inhibition at the cutaneous level, with respect to joint involvement, while the use of TNFis has produced more comparable rates of response between the skin and joints [40]. This was confirmed by network meta-analyses. TNFis demonstrated substantially higher ACR responses (i.e., articular symptoms) than other biologics and tsDMARDs, although the differences were numerically low [41,42], and the effect of prior exposure to bDMARDs did not result in higher efficacy for other drugs with different mechanisms of action. On the other hand, both TNFis (except for etanercept) and anti-IL17A agents produced consistent cutaneous responses (i.e., Psoriasis Area Severity Index (PASI) response) compared to placebo. Recently, head-to-head RCTs directly comparing different active treatment strategies have provided relevant practical information. In the EXCEED trial [43], 853 active bDMARD-naïve PsA patients were randomly assigned to the anti-IL17A SEC (300 mg monthly) or the TNFi ADA, with the primary objective of demonstrating the superiority of SEC over ADA at 52 weeks (ACR20 response). The primary endpoint was not reached; however, SEC demonstrated an efficacy profile similar to that of ADA (odds ratio (OR) 1.30, 95% confidence interval (95% CI) 0.98-1.72) with no new safety signals with respect to registration RCTs. In the SPIRIT-H2H trial [44,45], the primary

objective was the simultaneous achievement of joint and skin responses (ACR50 and PASI100) with IXE compared to ADA. IXE was superior to ADA in terms of the combined skin and joint primary endpoint ($p=0.036$ at 24 weeks, $p<0.001$ at 52 weeks) and non-inferior to ADA in ACR responses. Additional RCTs compared TNFis with non-TNFis, and although these trials were not designed to primarily evaluate the comparison, numerical differences in terms of efficacy endpoints, at least for the peripheral joints involvement, were not clinically meaningful [35,46]. On the contrary, the level of knowledge on comparative effectiveness of tsDMARDs with respect to TNFis is significantly lower.

In line with these results, the decision on the biologic to adopt in each PsA patient is substantially empirical, and guidelines are not restrictive in this sense, with even more elusive data on the sequencing of therapies. EULAR recommendations [10] suggest a preferred option for an anti-IL17A or anti-IL12/23 agent over TNFis and JAKis in cases with severe skin involvement, while the 2015 Group for Research and Assessment of Psoriasis and Psoriatic Arthritis (GRAPPA) guidelines tried to enlist specific treatments for individual clinical domains (e.g., axial, enthesis, dactylitis, and peripheral joint) and in cases with selected comorbidities [47]. However, individual treatment decisions remain based on 'heuristic' approaches, being not tailored to the biological features of the disease. Based on these issues, this approach exposes patients to possible primary inefficacy, unexpected side effects or several failed biological treatments before achieving clinical amelioration. As almost 40% of patients do not appropriately respond to their first-line biological treatment [48], the search for predictive biomarkers able to depict treatment response *a priori* is one the major unmet needs in the field, and addressing this need includes a global reconsideration of RCT development, aiming to tailor treatment decisions at the 'single-patient' level [49–51].

Treatment response biomarkers in PsA

Adapted from: Silvagni E. et al. From Bed to Bench and Back: TNF-α, IL-23/IL-17A, and JAK-Dependent Inflammation in the Pathogenesis of Psoriatic Synovitis. Front Pharmacol. 2021 Jun 15;12:672515 [7].

As underlined above, determining biomarkers related to early diagnosis, damage, prognosis and treatment response is one of the major unmet needs in the field of PsA; as such, it is included in the research agendas of the most relevant international treatment guidelines [47]. Biomarkers are currently defined as measurable indicators of disease status. Despite the growing number of studies aimed at identifying diagnostic, prognostic and treatment selection biomarkers [52–54], no validated biomarkers are yet available for clinical use in PsA [1]. Special interest lies in identifying peripheral blood, synovial fluid (SF) and synovial membrane biomarkers of response to drugs with different mechanisms of action [8].

Genetic biomarkers

Genetic biomarkers to predict clinical response, mostly to TNFis, have been investigated in both psoriasis and PsA [55]. Early reports require confirmation in defined clinical subsets, with homogenization of inclusion criteria in clinical presentation, course of the disease, and the genotyping and molecular expression of specific cells and tissues. Polymorphisms in the TNFAIP3 [56], TNF308A, IL-6174 [57] and TNF489A [58] alleles were related to the clinical efficacy of different TNFis in observational studies. Genetic and epigenetic modifications have also been exploited to highlight the treatment response to other bDMARDs, such as ustekinumab, but the evidence is mostly available in psoriasis rather than PsA [59,60]. Since the amount of research data will increase as the availability of new b/tsDMARDs increases, the amount of genetic biomarker data will rise accordingly. However, PsA is a multifactorial disease, and genetic predisposition accounts for only a portion of the pathogenic process, with environmental factors significantly influencing the course of this disease [5]. Thus, it is not surprising that genetic biomarkers have not yet entered clinical practice.

Serum biomarkers

Since serum biomarkers are the most easily accessible measures, a relatively high number of studies have focused on serum levels of different proinflammatory molecules, clearly demonstrating increased levels of IL-17A, IL-23, IL-6, IL-1β, IL-21, transforming growth factor (TGF)-β, TNF, and interferon-gamma (IFN-γ) in the serum and SF of patients with SpA, including PsA, compared to those of controls [61,62]. Among biomarkers of response to treatment, baseline C-reactive protein (CRP), IL-6 [63], matrix metalloproteinase 3 (MMP-3) [64], low-molecular-mass hyaluronan [65], and C3 levels [66] were found to be predictive of TNFi therapy response in prospective studies [67–69]. Lower IL-6 levels were associated with clinical response to ustekinumab [63]. Longitudinal decreases in the plasma concentrations of IL-6, vascular endothelial growth factor (VEGF), MMP3, and chitinase-3 like-1 (YKL-40) [70] and increases in serum cartilage oligomeric matrix protein (COMP) [64] levels were linked to clinical response to TNFis. Moreover, from a panel of 92 serum

proteins, pyridinoline, adiponectin, prostatic acid phosphate (PAP) and factor VII were identified as predictors of response to golimumab in a prospective observational study [71]. However, the serum concentrations of metabolites are influenced by several factors, and although PsA is a systemic condition, none of these biomarkers have been validated in clinical trials. Therefore, their roles are mostly mechanistic rather than decisional.

Peripheral blood cellular biomarkers

Within the cellular compartment, several studies have demonstrated elevated frequencies of IL-17-positive T cells in patients with PsA [72,73], with even higher numbers in the SF [74,75]. Peripheral T cell phenotyping was exploited in one of the first attempts to apply a precision medicine approach in PsA. Miyagawa and colleagues [49] directly compared, across a proof-of-concepts open-label study, two different treatment strategies in a population of patients with active PsA and an insufficient response to MTX (26 patients in a strategic treatment group versus 38 in a standard administration group following EULAR recommendations). Before starting therapy, FACS analysis of peripheral blood lymphocytes was performed to phenotypically characterize circulating T cells. Patients with a higher T helper 1 (Th1) cell status received the anti-IL-12/IL-23 antibody ustekinumab, while those with a higher Th17 cell level were treated with the IL-17A blocker SEC. A TNFi or SEC was given if the peripheral blood T cell population was enriched in both the Th1 and Th17 clusters, while only the TNFi was administered when both were downregulated. This tailored approach with specific interventions based on distinct T cell phenotypes and presumed activated proinflammatory pathways resulted in better clinical outcomes at 6 months. Specifically, low disease activity measured by the Simplified Disease Activity Index (SDAI) and Disease Activity Score on 28 joints (DAS28) and ACR20 responses were achieved more often in the group of PsA patients receiving a tailored approach than in the conventional treatment approach group, in which no relevant biologic-dependent treatment decision was made. Similar outcomes were not obtained for cutaneous manifestations, for which the proportions of patients achieving PASI75 and PASI90 were not significantly different between the groups. According to the authors, it was the strategy itself that contributed to the achievement of a favorable response to treatment, instead of the type of bDMARD selected. This study, even if preliminary, is a forerunner in the application of a biomarker-driven approach to address conditions such as PsA.

Synovial biomarkers

The analysis of cells and pathways in synovial tissue reveals findings that are not always exhibited by peripheral blood sampling. The anatomical proximity of the synovial membrane to the hypothesized inflammatory source emphasizes the putative roles of synovial biomarkers and their early modifications after treatment initiation. When chronic inflammatory arthritis occurs in the context of psoriatic disease, histological features include marked hyperplasia of the intimal lining layer containing fibroblast-like

synoviocytes (FLS) and macrophages and infiltration of the synovial sublining by both innate and adaptive immune cells, which are responsible for inflammatory mediator release, neoangiogenesis induction and cartilage and bone destruction. Inflammatory infiltrates in PsA consist of different immune cells, including macrophages, mast cells, polymorphonuclear (PMN) cells, and lymphocytes (B cells, T cells, and plasma cells), responsible for the significant production of different proinflammatory cytokines, including TNF, IL-1β, IL-6, IL-22, IL-23, IL-17A, and IL-18 [5,76] (Figure 1). Based on these observations, tracing inflammatory cells driving synovial inflammation in patients with undifferentiated inflammatory arthritis helped in the identification of tissue-dependent markers for predicting the development of defined chronic arthritis, such as PsA, within 1-year of follow-up [77]. PsA synovitis partially differs from RA, as it is characterized by prominent neoangiogenesis with tortuous, immature and elongated vessels [78,79]; numerous macrophages in the lining (but not the sublining) layer [80,81]; and an increase in IL-17-positive infiltrating mast cells [82]. The presence of clonally expanded populations of CD8 T cells resistant to effective treatment [83,84] suggests an antigen-driven T cell response promoting inflammation. Although lymphoid aggregates and plasma cells are generally less represented in PsA than in RA [85,86], follicle-like structures found in the synovial tissue of treatment-naïve PsA patients are active, as shown by the presence of $CD21^{pos}$ or $CD23^{pos}$ follicular dendritic cells, together with the expression of activation/proliferation markers such as Ki67 and Bcl6, and are associated with the presence of autoantibodies in PsA patients at disease onset [87]. Moreover, consistent remodeling of bone metabolism is found in PsA, with bone neo-formation markers interconnected with catabolic markers (allowing the presence of erosions along with new bone growth) [88,89]. The research utility of synovial biomarker discovery relies on the development of short-term clinical trials testing new drugs in early stages of pharmacological development [90,91], limiting the full period of the study to the time course of small proof-of-principle trials (‘to-go-or-not-to-go’) [92]. With this design in mind, studies investigating predictive synovial biomarkers of response to treatments have identified, in PsA, a reduction in sublining macrophages after effective TNFi treatment [81,93–97]. However, $CD3^{pos}$ T cell and MMP (MMP-3 and MMP-13) reductions appear to be the most sensitive biomarker variations associated with an effective treatment response to TNFis [76,93,95,97]. Recent studies have used protein profiles generated from proteomic analysis of powdered synovial tissues to compare patients with a response to ETA and ADA therapy with non-responders [98,99]. Different sets of biomarkers have been proposed, involving acute-phase proteins, annexins, cytoskeletal proteins, the hypoxia response, angiogenesis, and apoptotic signaling. Again, validation of baseline synovial predictive biomarkers to demonstrate superiority for a biomarker-driven approach with respect to recommended treatment algorithms has not been undertaken to date.

On the other hand, studies investigating the synovial impact of drugs, mostly TNFis, have helped to elucidate the effects of these drugs at the synovial level. TNFis, as an example, do not enhance apoptotic markers in either RA [100] or PsA [95], but they are able to decrease inflammatory cytokine levels, interfere with inflammatory cell homing from the peripheral circulation via a reduction in chemokine and adhesion

molecule production, and reduce neovascularization of the tissue [91,101,102]. Researchers have found decreases in VEGF [96], von Willebrand's factor, αVβ integrin, and the adhesion molecules ICAM-1 and VCAM-1 [95,96,101,103] after TNFi treatment. Conversely, synovial mechanisms of the response to IL-17A blockers are not as widely understood. Van Mens et al. [104] focused on longitudinal synovial modifications following SEC administration. After 12 weeks, there was a significant decrease in $CD15^{pos}$ neutrophils and in $CD68^{pos}$ macrophages in the sublining layer, with an increase in IL-17A-positive mast cells and reductions in IL-6, MMP-8, CCL-20, and IL-17A mRNA expression [104,105]. The *in vitro* administration of an anti-IL17A agent to FLS cultures was effective in reducing IL-17A-induced IL-6 production, with no differences between PsA and RA FLS [106]. SEC was also tested *in vitro* in SF mononuclear cell (SFMC) cultures and co-cultures of FLS and peripheral blood mononuclear cells (PBMCs), producing a reduction in the release of monocyte chemoattractant protein 1 (MCP-1) after 48 hours [107]. Finally, the adoption of a blocker of IL-17-receptor A (IL-17RA) was tested in PsA FLS cultures, highlighting reductions in IL-6 and IL-8 release into supernatants after stimulation with IL-17A [74]. In addition, studies with similar longitudinal design were also performed to deepen the synovial effects of abatacept [108] and ustekinumab [109].

Despite all these promising findings, there is not enough evidence to allow genetic, serum, cellular or synovial biomarkers to be included in treatment decisions-making in clinical practice, mainly because most studies were performed to assess only one class of drugs, without stratifying patient groups based on different treatment responses. Moreover, explanations for the effect of a single drug might be more complex than simply targeting a soluble molecule or receptor, given the heterogeneity of drugs in terms of structures and pharmacokinetics [110]. Therefore, the main treatment selection rules remain mostly empirical, and treatment outcomes, both in RCTs and in clinical practice, remain essentially based on clinical measures.

TNF-, IL-23/IL-17- and JAK/STAT-dependent signal transduction axes

Adapted from: Silvagni E. et al. From Bed to Bench and Back: TNF-α, IL-23/IL-17A, and JAK-Dependent Inflammation in the Pathogenesis of Psoriatic Synovitis. Front Pharmacol. 2021 Jun 15;12:672515 [7].

The availability of efficacious drugs that directly target specific proinflammatory cytokines means, from a biological point of view, that interfering with TNF, IL-23/IL-17A axis or JAK/STAT-dependent inflammation could disrupt several downstream signal transduction axes, with subsequent positive effects at the systemic and local levels. Knowledge of these signal transduction axes is, therefore, important to understand how each drug could interfere with selected cytokines/nodes, dependent or not dependent on others (Figure 2).

TNF

TNF is a key cytokine in the pathogenesis of SpA, and skin manifestations, as well as enthesis, joint, and spine involvement, represent the epiphenomenon of hyperactivated TNF-dependent inflammation as a result of innate and adaptive immune response activation [111–113]. TNF is part of the TNF superfamily, and its activities in health and pathology are pleiotropic. Many different immune and nonimmune cell types can produce this cytokine, including fibroblasts and keratinocytes. TNF can be found in either a soluble form or a transmembrane (tm) form bound to cells. The soluble form (sTNF) is released after enzymatic cleavage of the cell surface-bound precursor (tmTNF) by TNF-alpha-converting enzyme (TACE) [114]. Both sTNF and tmTNF are biologically active. TNF binds two distinct receptors: type I (TNFR1, also known as p55 and CD120a) and type II (TNFR2, also known as p75 and CD120b). Both receptors are transmembrane glycoproteins with multiple cysteine-rich repeats in the extracellular N-terminal domain. Signal transduction mediated by TNF receptor activation can alternatively lead to activation of nuclear factor kappa-B (NF-κB) or to apoptosis, depending on the metabolic state of the cell [115,116]. It is relevant to note that tmTNF can also act as a signal transducer and not only as a ligand. In this case, binding to tmTNF by TNFRs, or even TNFis, can induce reverse signaling and trigger cell activation or cytokine suppression and apoptosis in tmTNF-expressing cells. TNFR1 is constitutively expressed on virtually all nucleated cell types, whereas TNFR2 is inducible and preferentially expressed on endothelial and hematopoietic cells [117]. The cytoplasmic region of TNFR1 contains a death domain that couples TNFR1 to either of 2 distinct signaling pathways via binding of the adapter protein TNFR-associated death domain. The first pathway leads to the activation of nuclear factor kappa-B1 (NF-κB1), a family of transcription factors that controls many inflammatory genes, while a distinct signaling pathway leads to caspase-8– and caspase-3–dependent apoptosis. In a ‘network concept’ of the role of TNF in inflammation, TNF is considered an early and important trigger and mediator of downstream mechanisms, with a variety of feedback loops managing chronicity. However, it is not the only key cytokine involved in inflammatory pathways at the basis of chronic inflammatory arthritis development and perpetuation.

IL-17

IL-17-dependent signaling has been identified as a key modulator of synovial inflammation and joint destruction in various arthropathies, and its role in PsA pathogenesis, not only in skin manifestations [118], is crucial [62,74,119]. In particular, IL-17 is essential for increased expansion of Th17 cells, amplification and perpetuation of enthesitis, promotion of bone resorption *via* stimulation of receptor activator of nuclear factor-kB ligand (RANKL) expression, and modulation of inflammatory pain. The IL-17 family is composed of 6 different forms. IL-17A is the most active form, with 30-fold higher activity than IL-17F. IL-17A can also be part of an active heterodimer with IL-17F, which is thought to have intermediate activity between IL-17A and IL-17F. Cellular production of IL-17 is complex, and different cells are involved in its production. Naïve $CD4^{pos}$ T cells that differentiate into Th17 cells in response to stimulation by IL-23 are considered the main producers of this cytokine, but other cell types (e.g., $CD8^{pos}$ T cells, γδ T cells, NK cells, mast cells, polymorphonuclear cells, and group 3 innate lymphoid cells) consistently contribute to its production [105,120]. IL-17 receptor is a receptor complex formed by IL-17RA and IL-17RC (a heterodimeric transmembrane IL-17RA and IL-17RC complex). The binding of IL-17 to IL-17R leads to Act1 engagement, activation of the TNFR-associated factor (TRAF) 6 protein and subsequent NF-κB-mediated transcription of proinflammatory cytokines, among which IL-22 increases IL-17 function and activates osteoclasts and IL-21 promotes the differentiation of follicular Th cells. Conversely, IL-17E, also called IL-25, can bind another receptor formed by IL-17RA and IL-17RB, blocking downstream Th1/Th17 activation and, in contrast, increasing Th2 activity.

JAK/STAT-dependent signaling

In contrast, JAK/STAT-dependent signal transduction mediates the responses to a variety of different type I and II cytokines [121]. It is relevant to note that neither TNF nor IL-17A signals via JAK/STAT-coupled receptors. However, IL-23, one of the key cytokines involved in Th17 polarization, and the IL-17-dependent downstream cytokines IL-22 and IL-21 bind to JAK/STAT-associated receptors. The type I cytokines include common gamma-chain cytokines (IL-2, IL-4, IL-7, IL-9, IL-15, and IL-21), common beta-chain cytokines (IL-3, IL-5, and Granulocyte-Macrophage Colony-Stimulating Factor (GM-CSF)), IL-6, IL-23 and IL-12. Among type II cytokines, type I, II and III IFNs and IL-10-related cytokines (IL-10, IL-22, and IL-20) are involved. JAK/STAT-coupled receptors have an extracellular cytokine-binding domain and a cytoplasmic domain that associates with JAKs. JAKs comprise four different proteins (JAK1, JAK2, JAK3, and tyrosine kinase 2 (TYK2)); when cytokines bind to the extracellular portion of their receptors, JAKs start working as phosphotransferases, transferring a phosphate group from ATP to tyrosine residues in their substrates. JAKs can transfer a phosphate group to themselves (auto-phosphorylation) or to other JAKs (transphosphorylation). Once JAKS are phosphorylated, they are recognized by STATs. The primary function of STATs relies on transmitting signals from type I and II cytokine receptors to the nucleus. There are currently seven known STATs: STAT1, STAT2, STAT3, STAT4, STAT5A, STAT5B, and STAT6. Prior to activation, STATs reside in the cytosol, but after

cytokines bind to receptors, STATs bind to their cognate receptors and are phosphorylated by JAKs. After this modification, STATs translocate to the nucleus, where they bind DNA and activate the transcription of target genes, resulting in activation of key interferon response genes, production of pro-inflammatory cytokines and chemokines that perpetuate synovial inflammation, and activation of products that destroy the extracellular matrix (ECM) (e.g., MMPs), mediating cartilage and bone damage. Different JAK and STAT proteins can transmit signals from specific cytokines; however, a certain degree of functional promiscuity exists.

Synovial effects of JAK inhibitors in PsA

JAKis have been recently utilized for *in vitro* experiments in the field of chronic inflammatory arthritis, included PsA, given their broad mechanism of action, and, specifically, tofacitinib was used on several synovial biopsy-derived cells, permitting to deepen its synovial effect.

The first report on the effect of tofacitinib in primary cells isolated from PsA synovium dates back to 2016. Gao et al. [122], in fact, cultured unstimulated PsA-derived FLS (eleven patients), as well as whole-tissue synovial explants, maintaining the synovial architecture and cell–cell contact with spontaneous release of proinflammatory mediators, in the presence or absence of 1 μM tofacitinib citrate. Tofacitinib inhibited pSTAT3 and pSTAT1 expression in PsA FLS after 24h, inducing negative inhibitors of STATs, like SOCS3 and PIAS3, compared with a vehicle control. Furthermore, tofacitinib reduced FLS invasion, migration, and network formation. In synovial explants cultures, tofacitinib reduced spontaneous IL-6, IL-8, MMP-3 and MCP-1 release into supernatants compared with a vehicle control, and inhibited NFkB-P65 expression in tissue homogenates. In this work, the IL-17A levels in PsA synovial explant cultures were undetectable, while TNF levels were not investigated. These findings permitted to confirm the broad anti-inflammatory and anti-invasive effect of this drug in the context of a complex disease like PsA, and, specifically, demonstrated that synovial tissue and synovial tissue-derived cells could be studied *in vitro* without exogenous manipulations (e.g. cytokines addition to supernatants). More recently, the same group deepened the synovial mechanisms of action of tsDMARDs investigating the *in vitro* effect of several different JAKis, the pan-JAK inhibitors baricitinib and peficitinib, and the selective JAK1 inhibitors upadacitinib and filgotinib [123]. Fourteen PsA patients underwent synovial biopsy under arthroscopic guidance, and, in this work, FLS were stimulated with Oncostatin M (OSM) to activate JAK/STAT pathway. Following *in vitro* JAKis+OSM administration, a significant reduction in MCP-1 and IL-6 levels in FLS cultures supernatants was retrieved, as well as a reduction in invasion and migration properties of FLS. The spectrum of activity of JAKis varied depending on the type of the drug, with the most pronounced effects for peficitinib; however, the trend was similar for all of them. Interestingly, the authors analyzed also in real time the two major cellular energy pathways: oxidative phosphorylation (OCR) and extracellular acidification rate (ECAR), using the Seahorse technology. The OCR is indicative of mitochondrial respiration, and it can be employed as an indicator of mitochondrial respiratory capacity and energy production to reveal defects in mitochondrial bioenergetics mechanisms. ECAR, instead, is a measure of glycolysis. The consecutive addition of specific mitochondrial inhibitors to cells allows the measurements of distinct modules of oxygen consumption related to different mitochondrial processes, in particular the ECAR, the basal OCR, the ATP production, and the maximal respiratory capacity (MRC). Globally, JAKis decreased the ECAR:OCR ratio, and in particular, it was the glycolytic counterpart being significantly reduced, with no significant effect on OCR. This signifies a shift away from glycolytic mechanisms and towards a more oxidative phosphorylated/quiescent phenotype of FLS. These results partially confirmed

a previous work in the context of RA [124]. In 2018, in fact, McGarry et al. investigated the effect of tofacitinib on unstimulated RA-derived FLS, demonstrating that this drug was able to increase basal OCR and ATP synthesis, with consequent reduction in ECAR:OCR ratio. Moreover, tofacitinib reduced the production of reactive oxygen species (ROS), as well as the mitochondrial membrane potential. It has to be underlined, however, that not all the experiments were performed after 24h of *in vitro* treatment, with ROS and mitochondrial potential experiments performed up-to 3h, while synovial explant cultures were performed at 72h. Moreover, the *in vitro* dosage of tofacitinib chosen for experiments was 1 μM, but different dosages were chosen in other works [123], and here FLS were left unstimulated. This should be underlined when interpreting the results of different works.

Taken together, these studies have shown that JAKis are able to reduce oxidative stress in chronic inflammatory arthritis-derived FLS, switching the inflammatory profile of synovial cells, partly through metabolic reprogramming, thus reducing proinflammatory milieu. This is not surprisingly, since changes in metabolism have been observed at one of the primary sites of inflammation (e.g. synovium) in both PsA and RA, with a shift to a more glycolytic profile in FLS [125]. This results in a more hypoxic synovial microenvironment [126,127], responsible of the perpetuation of inflammation. Moreover, inflammation is able to induce mitochondrial DNA mutations accrual in FLS [128], and accumulation of damaged mitochondria is common in different types of cells from rheumatic musculoskeletal diseases patients [129], possibly linked to defective mitochondrial biogenesis or impaired clearance mechanisms. Again, the growing role of the metabolic shift in the perpetuation of chronic inflammation is corroborated by the knowledge that anti-oxidant agents might rescue mitochondrial dysfunctions [130], showing potential benefits for the systemic management of arthritis [131]. However, despite all the evidence, the link between JAK inhibition and the metabolic reprogramming in FLS remains not completely explained.

Introduction to autophagy

One of the most conserved survival mechanisms in eukaryotic cells is autophagy. Autophagy refers to a survival mechanism that cells use to degrade damaged or useless organelles, proteins, and infectious agents to maintain homeostasis, allowing cells to respond to injuries, like starvation, hypoxia, energy depletion, and others [132,133]. There are three types of autophagy: macroautophagy, chaperone-mediated autophagy, and microautophagy. Among them, macroautophagy is the most intensively studied, and it is referred to as "autophagy" in general.

Autophagy starts with the recruitment of damaged organelles and proteins by phagophores, a double-membrane structure, which seems to originate from different sources, including plasma membrane, endoplasmic reticulum (ER), and Golgi complex [134]. Then, vesicles undergo elongation and form double-membraned vesicles, called autophagosomes, with the cytoplasmic components enclosed, thus fusing with lysosomes for degradation. These final structures, named autophagolysosomes, permit the degradation of the vesicular content by lysosomal hydrolases. At the end, degradation products are recycled in the cytoplasm to generate new macromolecules.

Regulation of autophagy machinery is complex. The mammalian target of rapamycin (mTOR) complex 1 (mTORC1) regulates the activation of autophagy machinery, acting as a sensor of energy levels. In presence of growth factors and amino acids, mTORC1 represses autophagy. On the contrary, in starvation conditions, the dissociation of mTORC1 from the induction complex triggers autophagy. Moreover, among the most important proteins involved in phagophores elongation, there is the class III phosphatidylinositol 3-kinase (PI3K-III) complex containing Beclin-1 and ATG14-like protein (ATG14L). Furthermore, two ubiquitin-like conjugation systems, ATG12–ATG5–ATG16L and microtubule-associated protein 1 light-chain 3 (LC3)–phosphatidylethanolamine (PE), mediate the expansion and closure of the autophagosomes [135]. The first system regulates the curvature of the growing membrane, and participates to the association of LC3 to PE. LC3 is cleaved by the cysteine protease ATG4 to produce the cytosolic form LC3-I, which, after being activated by ATG7, is transferred to ATG3 in order to be changed in the conjugate form with PE, named LC3-II. LC3-II is the most commonly used marker to test autophagic activity, remaining stably associated with the autophagosomes in maturation. P62 (sequestosome 1), on the other hand, is considered a marker of autophagosomes turnover, since its accumulation permits the removal of these vesicles from cytoplasm, linking LC3 with ubiquitinated proteins [136]. Among the drugs used to test autophagy, rapamycin is an autophagy-inducer, since it inhibits the initial repressor mTORC1.

Autophagy machinery deregulation in chronic inflammatory arthritis

Alterations in autophagy mechanisms have been enlisted among the most important pathogenic events in the natural history of different rheumatic conditions, including chronic inflammatory arthritis [134].

Autophagy in RA

In RA, large genome-wide association (GWAS) and large-scale cohorts studies have allowed to recognize an association between several genes polymorphisms, mainly human leukocyte antigens (HLA) alleles, and the risk of RA development [137]. Among non-HLA genes, autophagy related (ATG)5 and ATG7 genes associate with RA predisposition [138,139]. After sequencing RA cases and healthy relatives from 9 multiplex families which carried HLA-DRB1 risk alleles, a new variant in SUPT20H, a gene belonging to macro-autophagy pathway, was associated to RA [140]. Moreover, ATG7 gene was found to be co-expressed with relevant NF-κB protein family genes in synovial tissues from healthy controls, while this network was disrupted in RA synovitis, suggesting a deregulation in the connectivity between autophagic and NF-κB-dependent pro-inflammatory pathways [138].

One the earliest protein modifications related to RA development and autoantibodies production is citrullination of peptides [141]. This process, being dependent on genetic and environmental factors, such as smoking habits or periodontitis, is a chemical conversion of an arginine in citrulline by peptidyl-arginine deiminase (PAD). It is well-known that the presence of anti-citrullinated peptides autoantibodies (ACPAs) is a relevant poor prognostic factor in RA [142]. Recently, Sugawara et al. [143] have proposed that autophagy is essential for citrullination of intracellular vimentin in RA FLS. In this study, the authors detected an intracellular autoantigen by western blotting (WB) using $ACPA^{pos}$ RA patients' serum as primary antibody, and, after immunoprecipitation, this antigen was demonstrated to be a citrullinated vimentin. Production of citrullinated vimentin in RA FLS was enhanced after serum-free starvation (autophagy induction), while autophagy inhibitor 3-methyladenine (3-MA) inhibited this effect. Moreover, citrullinated vimentin interacted with major histocompatibility complex (MHC) class II after autophagy induction or treatment with IFN-γ, suggesting a role for FLS as antigen presenting cells (APCs) induced by autophagy and pro-inflammatory cytokines. These data are in line with previous results showing that PAD activity increased in RA FLS treated *in vitro* with the autophagy-inducer rapamycin [144], while classical APCs exploit autophagy to present citrullinated proteins [145], highlighting another important role for autophagy in RA, which is linked to immune tolerance break and autoantigens presentation.

The role of autophagy in RA lymphocytes homeostasis was clarified in 2016 by van Loosdregt et al. [146]. The authors demonstrated that the number of autophagosomes, the autophagic flux and the intracellular levels of LC3-II were increased in CD4 and CD8 T cells from RA patients with respect to healthy controls, while apoptosis was reduced. Activation of T cells increased the autophagic flux, while autophagy inhibition

reduced apoptosis, suggesting a role for autophagy in apoptosis resistance in RA, allowing lymphocytes to survive. Not only circulating lymphocytes, but also monocytes and granulocytes displayed higher autophagy machinery activation in RA versus healthy controls, with a correlation with disease activity [147]. However, the majority of autophagy studies were retrieved in mice models, and studies in humans present contradictions, claiming for further research. As an example, Yang et al. [148] have shown that naive CD4 T cells from RA patients were autophagy-deficient and more prone to apoptosis and senescence.

Apoptosis resistance is considered one of the key features of proliferating FLS in the context of active RA synovitis, and this behaviour confers to synovial pannus a tumour-like phenotype [149–151]. mRNA and protein levels of autophagy markers beclin1, ATG5, and LC3 were increased in RA with respect to osteoarthritis (OA) synovial tissue [152]. Moreover, a lower apoptosis activity in RA versus OA synovial tissue was highlighted using terminal deoxynucleotidyl transferase-mediated dUTP nick end labeling (TUNEL) assay, remarked by WB analysis of PolyADP-ribose polymerase (PARP)-p85, with an inverse correlation to LC3-II levels [153]. These preliminary results suggest autophagy plays a role in conferring apoptosis resistance to RA FLS, and this relationship increases in FLS in presence of pro-inflammatory stimuli, such as TNF or IL-17A [154–157]. Moreover, recent studies have suggested that autophagy plays a dual role in regulating cell death. After severe ER stress in RA-FLS, mediated by thapsigargin, cell death was enhanced through the formation of autophagic vacuoles, but this kind of death was mostly independent of caspase-3 [158]. When the proteasome inhibitor MG132 was added, autophagic flux was induced as well, but cell death became dependent of caspase-3, suggesting apoptosis activation. Autophagy inhibitor 3-MA significantly reduced ER stress-induced cell death, while it amplified MG132-dependent apoptosis. Again, recent data suggest insights in the interplay between mitochondrial function and RA-FLS properties. Dynamin 1-like protein (DNM1L), a key regulator of mitochondrial fission, is increased in RA synovial tissue with respect to OA [159]. Silencing DNM1L with a specific small interfering RNA (siRNA) reduced LC3-dependent autophagy, while a specific DNM1L inhibitor increased FLS apoptosis. Indeed, the multifaceted aspects of autophagy machineries regulation become evident when considering mTORC1, which has a recognized role as cell-type-specific inhibitor of autophagy. RA synovial tissue and FLS display increased mTORC1 activity [160]. This datum, along with the inhibitory effect of rapamycin, a well-known autophagy activator, on FLS invasivity [161] suggested multiple effects for mTOR in response to environmental and nutritional stimuli, without an exclusive effect on autophagic activity in RA-FLS, but also on invasive properties and pro-inflammatory cytokines and chemokines release [162].

Finally, autophagy participates in regulation of different bone health-related mechanisms, including osteoclast-mediated bone resorption and FLS secretion of RANKL, playing a key role in structural damage observed in RA. Recent data by Lee et al. [163] have shown that optineurin, which promotes the degradation of poly-ubiquitinated substrates and acts as autophagy adaptor, is able to reduce RANKL production by RA-

FLS. Again, when optineurin was silenced using a specific siRNA in co-cultures of RA-FLS and monocytes, the ratio of conversion to osteoclasts (tartrate-resistant acid phosphatase – TRAP - positive multinucleated cells) significantly increased. Similar results in a monocytic cell line (RAW264.7) confirmed the role of autophagy modulation on osteoclasts generation from cellular precursors [164].

In conclusion, autophagy appears involved in different crucial moments of RA pathogenesis, since its pre-clinical development through modification of proteins and immunological tolerance break, to activation and survival of key cellular elements in peripheral circulation and joints, and to structural damage and bone loss.

Autophagy in psoriasis, psoriatic arthritis and spondyloarthropathies

The role of autophagic mechanisms in psoriasis and spondyloarthropathies (SpA) pathogenesis is more debated. In skin psoriasis, IL-17A is able to stimulate keratinocytes to activate mTORC1 signalling, inhibiting autophagy [165]. Moreover, autophagic punctae in lesional tissues were found reduced compared to non-lesional areas [165], p62 levels on IHC were increased in psoriatic skin lesions compared to normal skin or atopic dermatitis [166], and mTORC1 mRNA levels were increased [167]. When autophagy was inhibited with 3-MA in keratinocytes, enhanced inflammatory responses and increased cells proliferation were observed [166]. These findings suggest a reduced autophagic activity in keratinocytes, which might be exploited by immune system to guarantee altered responses to bacteria and to perpetuate immune tolerance escape, as well as to accrue damaged proteins, leading to cell death, tissue damage, and chronic inflammation. A reduction in autophagy in psoriatic skin lesions is documented even in Langerhans cells: beta-blocker drugs, which are able to induce or exacerbate psoriatic lesions, increase IL-23A production from human monocyte-derived Langerhans-like cells *in vitro*, with inhibition of autophagic flux [168]. However, these results are not univocally accepted. Recent data documented increased expression of beclin-1, ATG5 and LC3-II in psoriatic skin lesions, suggesting activated autophagic activity in keratinocytes, in particular when keratinocytes were stimulated with the five most important cytokines in psoriatic skin (TNF, IL-1A, IL-17A, IL-22 and OSM) [169]. Again, polymorphisms in ATG16L1 gene (crucial for the formation of autophagosomes) contribute to psoriasis occurrence [170], underlining a role for a genetic background of altered autophagic activity in the development of skin disease.

Few studies have tried to unravel the role of autophagic mechanisms deregulation in PsA. In a previous report by Weninck et al. [171], the authors have demonstrated that patients with PsA displayed higher mRNA levels of the essential autophagy product ATG16L1 in peripheral blood-derived dendritic cells (DCs) with respect to healthy controls, and these levels were higher in PsA than in patients with RA or skin psoriasis. One of the most debated points regarding the role of autophagy in SpA pathogenesis refers to the “ER stress” hypothesis. It is known that HLA-B27 confers a strong susceptibility to clinical occurrence of SpA; misfolded HLA-B27 accumulates in the ER before its expression on cell membranes, inducing a stress response that

leads to unfolded proteins response and autophagy induction [172,173]. Specifically, autophagy might have different roles depending on the tissue of interest. Ciccia et al. [174], in fact, have demonstrated a relationship between the expression of ATG16L1 with the levels of IL-23p19 mRNA in the biopsies of chronic inflamed ileum of patients with ankylosing spondylitis (AS), and autophagy inhibition with 3-MA reduced the number of IL-23p19-positive lamina propria mononuclear cells, suggesting an increased autophagic activity in the gut of AS subjects. Misfolded MHC class I heavy chains were detected intracellularly in the gut of AS patients. On the other hand, ATG16L1, ATG5, beclin1, LC3 mRNA levels were reduced in PBMCs from SA compared to RA patients ant healthy controls [175,176], while the levels in the synovium did not differ substantially from RA and controls [175]. Recently, the mTORC1 inhibitor rapamycin was tested *in vitro* on anti-CD3-stimulated PBMCs from peripheral SpA patients, resulting in a reduction of TNF and IL-17A release [177]. Moreover, rapamycin reduced FLS osteogenic differentiation, suggesting an effect on bony changes typical of SpA.

In conclusion, since SpA and psoriasis are complex diseases characterized by protean involvement of organs and tissues, it is reasonable that autophagy machinery dysfunctions could change across different cells and tissues, and this aspect should be bear in mind when considering pharmacological approaches addressing autophagy.

JAK inhibitors and autophagy

In the context of diseases other than arthritis and in different cellular populations, JAK inhibitors have shown some effects on autophagy regulation. It was demonstrated that the JAK2 inhibitor TG101209 acted against acute lymphoblastic leukaemia T cells, reducing autophagy and inducing apoptosis [178], while, in Hutchinson-Gilford progeria syndrome fibroblasts cultures, the JAK1/2 inhibitor baricitinib enhanced autophagy levels, as measured assessing autophagic vacuoles intensity [179]. More recently, an animal model of a lipodystrophic autoimmune disease was exploited to investigate the effect of JAK/STAT interference with autophagy mechanisms [180]. Specifically, in a Clec16a tamoxifen inducible, ubiquitous knockout, mouse model, the CLEC16A gene was silenced (Clec16a$^{\Delta UBC}$ mouse model). This gene associates with susceptibility to several autoimmune diseases, including type 1 diabetes, multiple sclerosis, RA, and others. Clec16a$^{\Delta UBC}$ mice displayed glucose tolerance with a lipodystrophic phenotype, with visceral white adipose tissue depots remarkably reduced or absent, despite no decrease in food intake. This reduction involved several areas, including gonadal, inguinal, mesenteric, retroperitoneal, perineal, and pericardial regions. Moreover, elevated autoantibodies levels were found, including anti-nuclear antibodies (ANA), suggesting an overlying systemic autoimmune disease. A significant increase in phosphorylation of STAT1 and STAT3 in white adipose tissue was remarked, in presence of ER stress and defective autophagic flux. *Ex vivo* treatment with tofacitinib improved survival of Clec16a$^{\Delta UBC}$ mice, partially restored the lipodystrophic phenotype, and reduced cytokines release. Moreover, tofacitinib reduced p62 levels in adipose tissue of

mice, while LC3-II levels were not affected, thus suggesting an increase in autophagy. The authors hypothesized that autophagy activation by JAK inhibition was able to revert, at least partially, the pro-inflammatory cascade in adipose tissue and, confirming this, the autophagy-inducer rapamycin provided beneficial effects on mice, similarly to tofacitinib.

Despite it is established that JAK proteins have pleiotropic effects in arthritis perpetuation, data regarding an effect of JAK inhibitors on autophagy machinery in the context of chronic inflammatory arthritis are scant. To the best of our knowledge, only one conference abstract reported an effect of tofacitinib on spontaneous autophagic activity of RA FLS [181]. In this work, the authors cultured FLS in presence of the autophagy-inducer rapamycin, highlighting an increase in LC3-II levels in FLS homogenates; tofacitinib, conversely, reduced LC3-II levels with respect to the vehicle control. No effect on FLS apoptosis was documented. This study was performed in line with similar studies in the context of RA. Vomero et al. [154] investigated how the TNF inhibitor etanercept interacted with spontaneous autophagy levels of RA FLS. Eight patients were enrolled, and FLS were obtained after total knee replacement surgery. Autophagy and apoptosis increased after *in vitro* TNF administration, while etanercept reduced LC3-II levels and apoptotic annexin-V^{pos} cells. Similar data were provided by other groups [182], suggesting that, in RA inflamed synovium, autophagy is linked with apoptosis resistance of FLS, and agents able to revert the pro-inflammatory microenvironment are able to reduce autophagy, as well. PsA synovitis, however, is much different from RA one, and different mechanisms might take place. In conclusion, there remains a knowledge gap regarding the role of JAK inhibitors on spontaneous autophagic activity of PsA FLS and PsA synovial tissue, and how much this could impact the well-documented anti-inflammatory and anti-invasive properties of this class of drugs remains unexplained.

Aims

This *in vitro* study is nested into the PROFILE-PsA program, a clinical research study of biomarkers discovery, which compares cellular and molecular biomarkers of pro-inflammatory activity in the presence of monoclonal antibodies (TNFis, anti-IL-17A agents) or targeted synthetic drugs targeting JAK/STAT pathway, administered *in vitro.* The general objective of the PROFILE-PsA program is to test different drugs with different modes of action after *in vitro* cultures of different cells (PBMCs, FLS, and synovial explants) obtained from active PsA patients, in order to identify biomarkers of response to different treatments, differentiating clinical responders from non-responders. An exploratory objective of the PROFILE-PsA program is to evaluate novel mechanisms of action of different b- and tsDMARDs at synovial level.

Therefore, we took advantage of the PROFILE-PsA program, with the primary objective to evaluate the effect of tofacitinib on spontaneous autophagic activity in PsA FLS. Secondary objectives were (i) to confirm the effect of tofacitinib on mitochondrial function of FLS obtained from PsA patients; (ii) to evaluate if such interference drives anti-inflammatory and anti-invasive changes in PsA FLS and in synovial explants. Exploratory objective was to confirm the safety and clinical tolerability of US-guided synovial biopsy procedures in the context of a tertiary-referral outpatient-clinic.

Materials and Methods

Ethics approval and consent to participate

The study protocol was approved by the Ethics Committee of Area Vasta Emilia Centro - Regione Emilia-Romagna (CE-AVEC) (279/2019/Sper/AOUFe, approval 14/05/2019). All procedures followed were in accordance with the ethical standards of the responsible committee on human experimentation and with the Declaration of Helsinki. All subjects provided signed informed consent.

Study Population

Patients with a diagnosis of PsA according to an expert physician and fulfilling the Classification Criteria for Psoriatic Arthritis (CASPAR) criteria for PsA [183], attending the Rheumatology Unit, Department of Medical Sciences, University of Ferrara and Azienda Ospedaliero - Universitaria S.Anna, Cona (FE), were evaluated for recruitment in this study.

Study design and Setting

This is an *in vitro* study. This study is nested into a prospective, 26-week, open label, single arm, interventional, single-centre, pilot study (PROFILE-PsA study) comparing cellular/molecular synovial biomarkers (obtained before starting treatment with a new cs/b/tsDMARD approved for the treatment of PsA) with or without *in vitro* administration of etanercept, secukinumab, and tofacitinib.

Here, we provide methods and data regarding the *in vitro* effect of tofacitinib on FLS, PBMCs, and synovial explants cultures obtained from active PsA patients.

Inclusion criteria were the following:

- patients of 18 years or older;
- with an established diagnosis of PsA, according to an expert physician and fulfilling the CASPAR criteria for PsA [183];
- with active disease; one of the involved joints had to be appropriate for US-guided synovial biopsy;
- concomitant use of NSAIDs and oral prednisone at doses of 10 mg/day or less, provided dosage was stable for at least four weeks before the study; concomitant background use of csDMARDs, at stable dosage, when clinically indicated; patients previously treated with bDMARDs could have been enrolled in the study provided they have been off therapy for more than or equal to one month; chronic use of low-dose aspirin was allowed, however at least 24 hours of wash out (before US-guided synovial biopsy) was suggested;
- clinical indication to the start of a new cs/b/tsDMARD for the management of active PsA;

- clinical indication to synovial biopsy.

Exclusion criteria were:

- patients treated with intra-articular steroids within the previous month;
- previous treatment with tsDMARDs;
- active or recent infections, included chronic infections, a history of infection with HIV or not-treated tuberculosis, hepatitis B or C;
- pre-existing (less than five years from study enrolment) malignancies;
- pregnancy or breast-feeding;
- severe medical or psychiatric conditions or laboratory abnormalities;
- patients unable to tolerate synovial biopsy;
- contraindications to US-guided biopsy procedure, such as anticoagulant use, decompensated haemostatic disorders, allergies to local anaesthetics or tranexamic acid;
- refusal of giving written informed consent for US-guided synovial biopsy procedure or for the whole study.

After written informed consent acquisition, patients meeting eligibility criteria underwent baseline US-guided synovial biopsy of the most inflamed accessible joint within two weeks of receiving new treatment with designed cs/b/tsDMARD for active PsA (baseline evaluation, T-2). Ultrasound (US)-guided synovial biopsy was performed at the Rheumatology Unit, Department of Medical Sciences, University of Ferrara and Azienda Ospedaliero - Unversitaria S.Anna, Cona (FE), as part of a comprehensive clinical assessment of active PsA patients ('Refractory Arthritis Clinic'), encompassing clinical evaluation, articular US assessment, joint radiographic assessment, and synovial histopathological evaluation, scored according to Krenn's score for chronic synovitis [184–187] (Table 2). Blood samples were collected at baseline, as well. Designed treatment with cs/b/tsDMARD for active PsA was decided according to available treatment recommendations [9,10], according to local regulations and to good clinical practice, after clinical consensus among specialists of the Rheumatology Unit, independently from the *in vitro* experiments results. The subsequent visit was performed after 2 weeks (T0) from the US-guided procedure and, in absence of local or systemic complications, the designed treatment was started (Table 3).

Clinical variables

Data captured at baseline visit included:

1. Demographic variables: gender, date of birth, ethnicity;
2. Smoking habits, alcohol use, physical activity, body mass index (BMI);
3. Date of PsA diagnosis;
4. Concomitant psoriasis, familiarity for psoriasis or PsA;
5. Extra-articular manifestations, type of articular involvement according to Moll and Wright classification [188];
6. Main comorbidities;
7. Clinimetrics: Health Assessment Questionnaire–Disability Index (HAQ-DI) [189], patient global activity (PGA) (0-100), global pain (0-100), physician global assessment (PhGA) (0-100), 66/68 joint count, erythrocytes sedimentation rate (ESR), CRP, Disease activity in psoriatic arthritis (DAPSA) score [190], Leeds Enthesitis Index (LEI) [191], number of tender entheseal points [192,193], Body Surface Area (BSA) [194], patients' pain, stiffness and swelling of the joint to be biopsied (0-100);
8. 66/68 joint count assessment;
9. Joint US examination [195–198];
10. Ongoing PsA treatment, previous treatment history.

Data captured at T0 visit included patients' pain, stiffness and swelling of the biopsied joint (0-100); adverse events; joint US examination; ongoing PsA treatment and new treatment started.

Data were recorded using a secure electronic data capture database for PsA patients (https://www.redcap.ospfe.it) [199], hosted at the University Hospital of Ferrara.

US assessment

US examination was performed by experienced rheumatologists and musculoskeletal (MSK) ultrasonographers (CS, ES), using a commercially available real-time scanner (6-18 MHz, Esaote Mylab70). A comprehensive US assessment was performed at baseline evaluation (T-2), on the same day of clinical assessment, after the clinical decision to change the patient's treatment. Global MSK-US assessment was performed considering different joints, and scored according to PsASon22 score [195] – data not shown. The US assessment of the joint suitable for US-guided synovial biopsy was scored according to Global OMERACT–EULAR Synovitis Score (GLOESS) score for synovitis [200,201], considering effusion, synovial hypertrophy and Power Doppler signal.

For all US examinations, the procedures were performed at room temperature. Smoking or use of nicotine substitutions 12 hours prior to the examination were not permitted. Effusion and synovitis were identified and distinguished according to available OMERACT (Outcomes Measures for RheumAtology Clinical Trials) definitions [197].

Specifically, synovial effusion was defined as hypoechoic or anechoic compressible intra-articular material, within synovial recesses (grade 0: no effusion; grade 1: minimal amount of joint effusion; grade 2: moderate amount of joint effusion with little distension of the joint capsule; grade 3: extensive amount of joint effusion with high distension of the joint capsule).

Synovial hypertrophy was defined as echogenic non-compressible intraarticular tissue, within synovial recesses (grade 0: no hypoechoic synovial hyperplasia; grade 1: minimal hypoechoic synovial hyperplasia, filling the angle between the periarticular bones, without bulging over the line linking tops of the bones; grade 2: hypoechoic synovial hyperplasia bulging over the line linking tops of the periarticular bones but without extension along the bone diaphysis; grade 3: hypoechoic synovial hyperplasia bulging over the line linking tops of the periarticular bones and with extension to at least one of the bone diaphysis).

Power-Doppler (PD) variables were adjusted to the lowest permissible pulse repetition frequency to maximize the sensitivity; low wall filters was used; the colour gain was set just below the level at which colour noise appeared in underlying bone (no flow should have been visualized at the bony surface). For semiquantitative PD assessment, grade 0 was defined as no flow in the hypoechoic synovial hyperplasia; grade 1 as up to three single spots signals or up to two confluent spots or one confluent spot plus up to two single spots; grade 2 as vessel signals in less than half of the area of the synovium (≤50%); grade 3 as vessel signals in more than half of the area of the synovium (>50%).

US-guided synovial biopsy

US evaluation of the joint to be biopsied (knee joint in all patients) was performed before each examination. All US-guided biopsies were performed with a 14G guillotine-type biopsy-needle (Precisa 1410-HS or Precisa 1415-HS, Hospital Service Spa), according to recommended procedures [92,187,202,203]. Briefly, US-guided technique allows indirect visualization of the inflamed synovium [204–207], permitting to select the most suitable biopsy site based on synovial proliferation and vascularisation. All patients lied down on their back and the whole procedure was undertaken under sterile conditions. After skin disinfection with iodine or chlorhexidine, starting from the point of needle entrance up to 25 cm proximally and distally, the patient was covered with sterile draping. Under US visualization (the US probe was covered in a sterile sheath), arthrocentesis was performed, and injection with local anaesthetic (10 ml lidocaine 2%) was performed via the same needle. Then, synovial tissue was obtained percutaneously using a semi-automatic guillotine-type biopsy needle, introducing the 14G needle inside the joint under US guidance. During the procedure, 6 to 8

synovial tissue samples were collected for each laboratory technique (standard histology analysis and immunohistochemistry (IHC), *in vitro* cultures) [124]. Synovial samples were placed on a non-woven, wet gauze. Subsequent procedures for samples handling are described in detail in following sections, depending on the laboratory/pathological technique performed. At the end of the procedure, 5 ml of tranexamic acid were injected inside the joint. After the completion of the procedure, the skin was cleaned with alcohol and sterile gauze dressing was laid over the incisional wounds. An elastic stocking was placed around the knee, which was removed after one hour. Instructions were given about restrictions in daily activities (abstain from strenuous physical activity; returning to non-strenuous activity or working activity is the norm) and suspicion of complications.

Histology analysis and immunohistochemistry

Histological and immunohistochemistry (IHC) examinations of synovial tissue were performed at Pathology Division, Department of Translational Medicine, University of Ferrara. For histology analysis and IHC, tissue samples were fixed in formalin for 24h, embedded in paraffin. Four-micrometer-thick sections were cut from formalin-fixed paraffin embedded blocks. Two sections for each block were routinely stained with haematoxylin/eosin (H&E) for histological examination: sections were deparaffinized in xylene and rehydrated in a series of graded ethanol, stained in hematoxylin, and counterstained in eosin/phloxine. Finally, sections were dehydrated, cleared in xylene, and mounted with Bio Mount (Bio-Optica). Histopathological evaluation was performed according to pathologist's experience and scored according to Krenn's synovitis score [185] (Table 2). The pathologist (GL) was unaware of the patients' clinical and immunologic characteristics. Krenn's synovitis score evaluates three different features (synovial lining layer enlargement, stromal cell density, and inflammatory infiltrates), each ranked on a scale (0-3). At least two sequential sections for each patient were evaluated, and the highest score obtained was recorded. Globally, the sum of the values for each parameter were summarized as follows: a score of 0–1 (no synovitis), 2–4 (low-grade synovitis), and 5–9 (high-grade synovitis). Figure 3 shows representative images for each parameter of the Krenn's synovitis score obtained from patients with PsA enrolled in the present study.

Detection of B cells (CD20), T cells (CD3), and macrophages (CD68) was performed using a BenchMark XT automated immunostainer, in accordance to product data sheet. Staining was semi-quantitatively quantified using an Olympus AX60 microscope at 20x magnification. Immunohistochemical results were scored using a modified scoring system derived from Canete et al. [96], analysing the density of cells type on a semi-quantitative 0–4 scale, as follows: 0 = no reactive cells, 1 = 1–10 positive cells, 2 = 10–25 positive cells, 3 = 25–50 positive cells, and 4 = >50 positive cells.

Samples handling and cells cultures

Tests on blood and synovial tissue samples were carried out at the Signal Transduction Lab (Professor Paolo Pinton's Lab), Department of Medical Sciences, University of Ferrara.

For primary *FLS culture*, synovial tissue samples were collected and transported to local laboratories in medium (complete Dulbecco's modified Eagle's medium (DMEM) enriched with 3% penicillin and streptomycin P/S (Axenia BioLogix, Dixon, CA, USA) and Fungizone 250 ng/ml), maintained for 24h at 4°C to avoid contamination of samples. Samples were cut into small pieces and directly placed in culture medium (complete DMEM). Complete DMEM was enriched with foetal bovine serum (FBS) (Axenia BioLogix, Dixon, CA, USA) in percentages ranging from 30 to 50% every three days. Cells were allowed to grow out of the tissue lump, and trypsinized at confluence [208,209]. Synovial cells were then cultured at 37°C in humidified atmosphere 5% CO2 incubator, and FLS were used for experiments between 3rd and 8th passages, according to literature [122].

For *synovial explants cultures*, synovial tissue samples were collected and transported to local laboratories in medium, processed immediately at arrival, cut into small pieces and digested with Liberase Research Grade TM, in RPMI (Roswell Park Memorial Institute, 150 mcg/ml, Roche) with rotation in 37°C for 1.5 h. Digested tissue were passed through a 100 mm tissue-strainer and washed once with Phosphate Buffered Saline (PBS)/2%FBS/2mM EDTA. Cells were centrifuged and suspended in growth medium complete DMEM at 0.2x10^6 cells in 96-well plates [210], treated *in vitro* with dimethyl sulfoxide (DMSO) vehicle control or tofacitinib 1 μM, and maintained at 37°C in humidified atmosphere 5% CO2 incubator for 24h.

Peripheral blood mononuclear cells (PBMCs) were isolated from venous blood by Ficoll-Paque density centrifugation. After dilution of blood sample in a Falcon 15mL Conical Centrifuge Tubes with PBS (until a final volume of 10 ml), a new Falcon Conical Centrifuge Tube was prepared stratifying 5 ml of diluted blood sample carefully onto Ficoll-Paque media (4 ml). Centrifugation for 20 minutes, 2100 revolutions per minute (rpm) was performed. PBMCs were transferred to a sterile centrifuge tube using a sterile pipette, diluted with PBS until a final volume of 15 ml, and centrifuged for 10 minutes, 1600 RPM. Cellular pellet was re-suspended in PBS 10 ml, and centrifuged for 10 minutes, 1400 RPM. Red Blood Cells Lysis Buffer was added to cellular pellet for 5 minutes, and soon after re-suspended in PBS for final centrifugation (10 minutes, 1100 RPM). Cellular pellet was re-suspended in complete RPMI 1640 (Invitrogen, UK) (RPMI supplemented with 10% FBS, 2 mM L-glutamine, 100 U/mL P/S). After Burker chamber cell count, a total of 1,000,000 cells was placed for culture in a 24-well plate (1 ml per well of complete RPMI) for 24h at 37°C in humidified atmosphere 5% CO2 incubator. *In vitro* treatment with DMSO or tofacitinib 1 μM for 24 hours was performed accordingly.

Figure 4 is an exemplification of biological samples handling and cellular cultures performed.

In vitro experiments in FLS cultures

For *in vitro* treatment tests with tofacitinib, FLS were seeded at $150*10^3$ cells/well in 6-well plate with 2 ml of complete DMEM and treated according to available procedures with tofacitinib 1 µM (Sigma-Aldrich) [122,124] or DMSO vehicle control for 24 hours. Supernatants were collected and analysed by enzyme-linked immunosorbent assay (ELISA). Protein lysates were prepared and supernatants/cellular pellets collected for relevant autophagic markers analysis through Western Blot.

For specific autophagy tests, ammonium chloride (NH_4Cl) 10 µM for 6 hours or bafilomycin A1 100 nM (Sigma-Aldrich) for 2 hours were used before the end of the culture to test autophagy flux blockade, while rapamycin 1 µM for 12 hours was utilized as an autophagy inducer. To test reactive oxygen species (ROS) reduction, the antioxidant N-Acetyl-L-Cysteine (NAC, Merck Life Science S.r.l.) at 1-3-5 mM for 48 hours was used, according to literature data [130,211]. To evaluate the effect of tofacitinib at different exposure times, preliminary experiments were replicated at 24 and 72 hours.

Western Blot analysis

FLS and synovial explants were trypsinized and collected prior to cell lysis. Total cell lysates were prepared in RIPA buffer (50 mM Tris-HCl pH 7.8, 150 mM NaCl, 1% IGEPAL CA-630, 0.5% sodium deoxycholate, 0.1% SDS, 1 mM DTT) supplemented with proteases and phosphatases inhibitors. Proteins were quantified by the Lowry method and 10 µg of proteins, denatured for 5 min at 100°C in LDS sample buffer (Thermo Fisher Scientific) and Sample Reducing Agent (Thermo Fisher Scientific), were loaded on a Novex NuPage Bis-Tris 4–12% precast gel (Thermo Fisher Scientific). After electrophoretic separation, proteins were transferred onto nytrocellulose membranes. To saturate unspecific binding sites, the membranes were incubated with TBS–Tween-20 (0.05%) supplemented with 5% non-fat powdered milk for 1 hour at room temperature, and then incubated overnight with primary antibodies. Membranes were incubated with the following primary antibodies: anti- phospho (p)STAT3 (Tyr705, Cell-Signaling Technology, UK), anti-p62 (Sigma-Aldrich), anti-ATG7 (Cell-Signaling Technology, UK), anti-LC3-II (microtubule-associated protein light chain 3; Sigma-Aldrich, Merck), anti p-mTOR (Ser2448, Cell-Signaling Technology, UK) diluted in 5% non-fat milk containing 0.1% Tween 20 at 4°C overnight. GAPDH (Cell-Signaling Technology, UK) was used as a loading control. The revelation was assessed by specific horseradish peroxidase-labeled secondary antibodies (Thermo Fisher Scientific), followed by detection by chemiluminescence (Thermo Fisher Scientific), using ImageQuant LAS 4000 (GE Healthcare).

LC3 vacuoles count

Analysis of autophagy was also performed by fluorescence microscopy using GFP-LC3. 100,000 FLS were seeded on 24 mm coverslips and cultured overnight in complete DMEM. Next, cells were co-transfected with the Jet-Pei plasmid in combination with GFP-LC3 vector for 6 h using the Turbofect reagent (Thermo Fisher Scientific) in DMEM 0.4% FBS and cultured for further 24 hours in complete DMEM with DMSO or tofacitinib

1 µM. After transfection, cells were washed twice in PBS buffer, fixed at room temperature in 4% paraformaldehyde for 15 min. Next, cells were washed twice with PBS buffer, treated for 10 min with a Dapi solution and washed three more times. Images were acquired at 63x magnification using a Zeiss Axiovert 200 fluorescence microscope equipped with a back-illuminated CCD camera (Roper Scientific, Tucson, AZ) and processed by ImageJ software [212].

Cytokines quantification (ELISA)

Cytokines TNF-alfa, IL-17A, IL-6, and chemokine MCP-1 (CCL-2), were quantified by ELLA (Bio-Techne s.r.l.), according to manufacturer's instructions. Absorbance was measured in a microtiter plate spectrophometer. The autophagic marker ATG5 (MBS7209535) (My Biosource, San Diego, California, USA) was quantified by ELISA (R&D Systems, Abingdon, UK) according to manufacturer's instructions. Absorbance was measured in a microtiter plate spectrophometer (SPECTROstar Nano Microplate Reader, BMG LABTECH).

Migration analysis

FLS migration was evaluated using Culture-Insert 2 Well in µ-Dish 35 mm (Ibidi). After confluence (100,000 cells/well), the culture-insert was removed and migration of FLS was assessed in presence or absence of DMSO or tofacitinib 1 µM, as well as using rapamycin 1 µM or NAC 5 mM. Acquisitions were performed at 0, 24, 48 and 72 hours (Figure 5). Data analysis was performed using an in-house developed semi-automated algorithm to measure the percentage of cells open area (ImageJ software) [212].

Analysis of mRNA expression

Total RNA was extracted from FLS using RNeasy Mini Kit (Qiagen). The synthesis of cDNA was performed by using the Quantinova Reverse Transcription Kit (Qiagen). The expression of p62 was evaluated by Real Time RT-PCR using GAPDH cDNA for sample normalization (endogenous control). Quantitative PCR was carried out using Quantinova Sybr Green PCR Kit (Qiagen) with the Rotor-Gene Q Real time PCR cycler (Qiagen, Milan, Italy). The levels of p62 (target) were obtained by using the ΔCT method, which uses the threshold cycle (CT) number at which the emitted fluorescence of the sample passes a fixed threshold above the baseline. The abundance of the GAPDH cDNA was used as endogenous control RNA for sample normalization (reference). Primer sequences adopted (5'—>3'): p62 Reverse – CTGTAGACGGGTCCACTTCTT; p62 Forward – AGCAGATGAGGAAGATCGCC; GAPDH Reverse – TCTTCCTCTTGTGCTCTTGC; GAPDH Forward – CTTTGTCAAGCTCATTTCCTGG.

Quantification of intracellular reactive oxygen species (ROS) production

To determine cellular ROS release from FLS, 100,000 cells/well were allowed to grow to 80% confluence and treated *in vitro* in the presence of tofacitinib 1 µM or DMSO vehicle control for 24 hours, as well as NAC 1-3-5 mM for 48 hours. Then, cells were washed in PBS buffer, and MitoSOX™ Red Mitochondrial Superoxide

Indicator 5 µM was added for 30 minutes. Images were acquired at 63x magnification using a Zeiss Axiovert 200 fluorescence microscope equipped with a back-illuminated CCD camera (Roper Scientific, Tucson, AZ) and processed by ImageJ software [212].

To determine the most suitable concentration of NAC to be used for further experiments, FLS seeded in 12-well plates in duplicates were treated with NAC 1-3-5 mM for 48 hours and, then, stained with MitoSOX™ Red Mitochondrial Superoxide Indicator 5 µM for 30 minutes. Next, cells were centrifuged, washed with PBS, and counted using a Tali image-based cytometer (Life Technologies).

Cell Survival Assay

Cells seeded in 12-well plates were allowed to grow to 80% confluence and were treated with NAC 1-3-5 mM for 48 hours. Then, the cells were washed with PBS, fixed in 4% paraformaldehyde, and stained with 0.1% crystal violet. Crystal violet was dissolved with 1 mol/l acetic acid, and absorbance at 595 nm was measured (SPECTROstar Nano Microplate Reader, BMG LABTECH).

Measurement of mitochondrial membrane potential

A JC-1 Assay (Abcam) was used to determine the mitochondrial membrane potential in the presence of tofacitinib 1 µM or DMSO vehicle control for 24 hours. FLS were seeded into 6-well plates (100,000 cells/well) and were allowed to grow to 80% confluence. Cells were washed with PBS and stained with 200 nM JC-1 for 20 minutes at 37°C and 5% CO2. Images were acquired at 63x magnification using a Zeiss Axiovert 200 fluorescence microscope equipped with a back-illuminated CCD camera (Roper Scientific, Tucson, AZ) and processed by ImageJ software [212].

Cellular bio-energetic function analysis

Oxygen consumption rate (OCR), reflecting oxidative phosphorylation, was measured using the Agilent Seahorse XF Cell Mito Stress Test Kit, Agilent Technologies. The OCR is indicative of mitochondrial respiration, and it can be employed as an indicator of mitochondrial respiratory capacity and energy production to reveal defects in mitochondrial bioenergetics mechanisms. The consecutive addition of specific mitochondrial inhibitors to the cells allows the measurements of distinct modules of oxygen consumption related to different mitochondrial processes. The OCR was measured before and after treatment with the ATP synthase inhibitor oligomycin (1 µM; Agilent Seahorse XF Cell Mito Stress Test Kit, Agilent Technologies), the mitochondrial uncoupler carbonyl cyanide-4-(trifluoromethoxy) phenylhydrazone (FCCP) (1 µM; Agilent Seahorse XF Cell Mito Stress Test Kit, Agilent Technologies), and the complex I/III inhibitors rotenone / antimycin A (1 µM; Agilent Seahorse XF Cell Mito Stress Test Kit, Agilent Technologies) using an XF24 analyzer (Agilent Seahorse XF Cell Mito Stress Test Kit, Agilent Technologies) [213]. FLS were seeded at 20,000 cells per well in a 24-well cell culture XF microplate (Seahorse Biosciences) and were allowed to adhere for 24

hours. Following this, cells were cultured with tofacitinib 1 µM or DMSO for 24 hours. Cells were then washed with assay medium (unbuffered Dulbecco's modified Eagle's medium supplemented with 10 mM glucose, pH 7.4) before incubation with assay medium for 30 minutes at 37°C in a non-CO2 incubator. Basal oxidative phosphorylation was calculated by the average of 3 baseline measurements of OCR, obtained during 15 minutes before injection of specific metabolic inhibitors. The addition of oligomycin inhibits ATP synthase (complex V of the respiratory chain) causing a decrease in OCR that correlates with the amount of oxygen consumption linked to mitochondrial ATP production (OCR-ATP, determined by subtracting from baseline OCR the amount of respiration left after oligomycin injection). The maximal ATP output of mitochondria can be determined by addition of FCCP, an uncoupling agent that collapses the proton gradient and disrupts the mitochondrial membrane potential, inducing maximal oxygen consumption and substrate oxidation by complex IV (OCR-MRC, maximal respiratory capacity, determined by subtracting baseline OCR from FCCP-induced OCR, average of 3 measurements following injection). Finally, the complex I/III inhibitors rotenone / antimycin A shut down mitochondrial respiration. To determine the number of vital cells, FLS were washed with PBS, fixed in 4% paraformaldehyde, and stained with 0.1% crystal violet. Crystal violet was dissolved with 1 mol/l acetic acid, and absorbance at 595 nm was measured (SPECTROstar Nano Microplate Reader, BMG LABTECH).

Cellular mitophagy assessment

Mitophagy is a selective form of autophagy, which permits the removal of damaged mitochondria [214]. A MitoTracker™ Green FM / LysoTracker™ Red DND-99 assay (Invitrogen™) was used to determine the co-localization of mitochondria and lysosomes in the presence of tofacitinib 1 µM or DMSO vehicle control for 24 hours. FLS were seeded into 6-well plates (100,000 cells/well) and were allowed to grow to 80% confluence. Cells were washed with PBS and stained with 0.5 µM MitoTracker™ Green FM for 15 minutes at 37°C and 5% CO2. Then, the cells were washed twice with complete DMEM, and stained with 0.5 µM LysoTracker™ Red DND-99 for 15 minutes at 37°C and 5% CO2. Images were acquired at 63x magnification using a Zeiss Axiovert 200 fluorescence microscope equipped with a back-illuminated CCD camera (Roper Scientific, Tucson, AZ) and processed by ImageJ software [212]. Mander's overlap coefficients (M1 and M2) were used to quantify the degree of co-localization between fluorophores.

Statistical analysis

Descriptive analysis of demographic, clinical, US, and pathological data were performed assessing mean (standard deviation, SD) values. Categorical variables were described as counts and percentages.

Primary and secondary analyses: differences in biomarkers variations with and without *in vitro* tofacitinib administration were determined adopting the non-parametric Wilcoxon signed rank test. For western blot data, variations following *in vitro* tofacitinib administration were compared with the respective paired DMSO

administration. Data are displayed as mean ± standard error of the mean, s.e.m. A p value <0.05 was considered statistically significant. The standardised mean difference of tofacitinib effect over DMSO was generated to compare the effects of the drug on spontaneous cytokines release in cultures supernatants.

Exploratory analysis: Changes in the clinimetric scores between T-2 and T0 visits were performed using the non-parametric Wilcoxon signed rank test.

Analyses were performed using the Stata14 software (STATA Corporation, College Station, Texas, USA) and Prism® (GraphPad Software Inc.).

Sample size calculation

Given the pilot design of the study, sample size calculation was based on feasibility. A study population of 15-20 patients was judged sufficient for both practical and ethical reasons.

Results

Patients enrolled and clinical-pathological evaluations

Demographic and clinical data

16 patients with active PsA satisfying inclusion criteria were enrolled between 20th June 2019 and 24th June 2021. Table 4 enlists baseline demographic, clinical and treatment-related data of included patients. Mean (SD) age was 59.8 (7.9), and female were 5 (31.3%); all patients were Caucasian. Mean (SD) disease duration was 9.7 years (7.9), with 14 out of 16 patients suffering from skin psoriasis. The most common comorbidity recorded was hypertension (N=9, 56.3%), followed by obesity (N=6, 37.5%). Concomitant musculoskeletal (MSK) comorbidities were checked for, as well: fibromyalgia (N=4, 25.0%), osteoarthritis (3, 18.8%), and crystal-induced arthropathies (2, 12.5%) were only marginally present.

Clinimetrics

Enrolled patients had moderate disease activity. In particular, mean (SD) ESR and CRP were 28.9 mm (24.8) and 1.5 mg/dl (2.0), respectively. Mean (SD) tender and swollen joints were 6.6 (5.4) and 3.4 (1.9). DAPSA (25.6, 6.8) assessment depicted a moderately active peripheral joints disease, while cutaneous involvement was less important (mean BSA 1.3%). A certain degree of functional impairment was evident among patients (mean, SD HAQ 0.9, 0.5), and global pain component approximated 70% on a 0-100 scale.

Ultrasound data

Mean grey scale synovitis score (0-3) in the joint to be biopsied was 1.9 (0.8); effusion reached 1.4 (0.7), and Power Doppler 0.5 (0.6). These data suggest that the biopsied joint was effectively affected by the disease, since a moderately-active synovitis was retrieved on baseline US examination.

Treatment-related data

Patients enrolled had previous csDMARDs treatment in 13 out of 16 cases (81.3%), with 6 patients having experienced at least one course of bDMARD treatment, mostly with TNFis. Only 2/16 patients had previously received treatment with IL-17A inhibitor secukinumab, and no patients had been treated with ixekizumab or ustekinumab. 8 patients were on background treatment with NSAIDs (at occurrence) at baseline visit, while only two of them were stably receiving a low dosage of GCs.

Safety and clinical acceptability of US-guided synovial biopsy

In 13 cases the biopsied joint was the left knee, while in the remaining cases the right knee was biopsied. Our study confirms the safety of the procedure, as only one patient experienced a non-serious adverse event (knee swelling necessitating joint arthrocentesis after 7 days). No serious adverse events were recorded. Globally, patients experienced no increase in pain, stiffness and swelling components of the biopsied joint.

Indeed, mean pain, stiffness and swelling of the biopsied joint significantly reduced between T-2 and T0 visits (Figure 6), with no worsening of the US components recorded (joint effusion, grey scale synovitis, Power Doppler signal).

Histopathological and IHC evaluation of synovial tissue

Table 5 shows baseline histopathological and IHC data of synovial tissues from included patients. Mean (SD) Krenn's synovitis score was 4.4 (1.9), suggesting a grade of chronic synovitis transitioning between moderate- and high-grade synovitis. The most represented sub-parameter of the score was the inflammatory infiltrate (mean value, SD: 1.8, 0.9), followed by the lining cell layer enlargement (1.4, 0.8) and resident cells density (1.3, 0.7). A semiquantitative scoring system was applied to evaluate the number of $CD3^{pos}$, $CD20^{pos}$ and $CD68^{pos}$ cells in the tissue (Fig. 7). The mean (SD) IHC semiquantitative score was 1.9 (1.0) for $CD3^{pos}$, 1.6 (1.1) for $CD20^{pos}$ and 1.8 (0.9) for $CD68^{pos}$ cells.

In vitro study

Tofacitinib increases spontaneous autophagy levels in PsA FLS

To determine the effect of tofacitinib on spontaneous autophagic activity of PsA FLS, we performed cells cultures for 24h in presence of the vehicle control DMSO or tofacitinib 1 μM, and analysed protein levels in cellular homogenates by western blot. As compared to vehicle control, tofacitinib significantly increased LC3-II (N=16, p=0.0002) and ATG7 (N=14, p=0.0001) levels, suggesting an increase in autophagy activity. A non-significant increase in p62 levels was enhanced (N=16, p=0.0654). Figure 8A shows autophagy activation following tofacitinib administration by western blot. We confirmed data by counting autophagic vesicles visualized by using a fluorescence microscope at 40x magnification in FLS transfected with a recombinant plasmid expressing LC3 protein linked to GFP. We evaluated FLS obtained from two different patients (mean number of cells evaluated for each condition: 49), confirming a significant increase in LC3-autophagic vesicles after tofacitinib treatment ($p<0.0001$ and $p=0.0002$, respectively) (Fig. 8B-C).

We next sought to investigate if the concentrations and timings of tofacitinib adopted for *in vitro* experiments, mutually derived from literature [122,124], permitted the correct functioning of the drug. Tofacitinib is a pan-JAK inhibitor, with a preferential activity over JAK1 and JAK3 [18,19]. Since JAK1 is theoretically expressed on all nucleated cells, its activation by pro-inflammatory cytokines permits the phosphorylation of different STAT proteins, in particular STAT3. Therefore, we performed FLS cultures for 24h in presence of the vehicle control DMSO or tofacitinib 1 μM, and analysed protein levels in cellular homogenates by western blot to quantify the levels of pSTAT3. In our conditions, tofacitinib reduced pSTAT3 levels after 24h (N=7, p=0.0313) (Fig. 9A). This effect was lost after 72h (N=7, p=1.0000) (Fig. 9B). Moreover, the increase in LC3-II levels obtained at 24h following *in vitro* tofacitinib administration was no more evident

if the experiment was prolonged to 72h (N=11, p=0.5195) (Fig. 9C). Therefore, we confirmed tofacitinib dosages and timings for *in vitro* experiments at 1 μM for 24h.

Afterwards, we decided to evaluate if this modulatory effect of tofacitinib on autophagy was evident in other cellular populations, as well. We performed PBMCs and digested biopsy cultures (synovial explants) for 24h in presence of DMSO or tofacitinib. Protein levels were analysed by western blot. Tofacitinib was not able to significantly influence spontaneous autophagy levels neither in PBMCs (Fig. 10A), nor in synovial explants cultures (Fig. 10B). In conclusion, the effect of tofacitinib on spontaneous autophagy was selective on FLS.

Tofacitinib does not alter autophagic flux in PsA FLS

Given the increase in LC3-II and ATG7 levels following *in vitro* tofacitinib treatment, we tried to investigate if the drug produced an autophagy flux blockade. NH_4Cl 10 μM for 6 hours was used before the end of the FLS culture with DMSO or tofacitinib. In presence of NH_4Cl, we highlighted a significant increase in LC3-II levels (N=10, p=0.0020), both following DMSO and tofacitinib administration (Fig. 11A). A non-significant increase in ATG7 and p62 levels was enhanced, as well. These data confirms there was no autophagy flux blockade in presence of tofacitinib. We confirmed our results using bafilomycin A1 100 nM (Sigma-Aldrich) for 2 hours. Figure 11B shows a representative western blot image: similarly to NH_4Cl, after bafilomycin A1 administration we highlighted an increase in p62 and LC3-II levels.

To understand the effect of *in vitro* tofacitinib administration on autophagy, we analysed p62 mRNA expression, confirming no significant increase in p62 levels (N=6, p= 0.8148) (Fig. 12A). Also the autophagy marker ATG5, measured using ELISA in FLS culture supernatants, was found not significantly increased following tofacitinib administration (N=15, p=0.5995) (Fig. 12B).

Rapamycin stimulates autophagy in PsA FLS

To investigate the effect of an autophagy inducer on FLS cultures, we used rapamycin 1 μM for 12 hours before the end of the FLS culture with DMSO or tofacitinib. In presence of rapamycin, we confirmed a significant increase in LC3-II levels, both following DMSO and tofacitinib administration (N=10, p= 0.0273 and p=0.0371, respectively) (Fig. 11C). To test if the concentration and timing of rapamycin permitted the correct functioning of the drug, we evaluated the effect of rapamycin over p-mTOR protein levels by western blot. Rapamycin administration resulted in a reduction of p-mTOR levels, while tofacitinib did not interfere with them (Fig. 11D).

Tofacitinib and rapamycin reduce pro-invasive properties of PsA FLS

To investigate if tofacitinib was able to reduce pro-invasive properties of PsA FLS, we evaluated FLS migration. After cells confluence, migration was assessed in presence or absence of DMSO or tofacitinib 1 μM, and the percentage of the cells open area was compared at 0, 24, 48 and 72h (Figure 13A-B-C). In line with our

hypothesis, tofacitinib significantly reduced the percentage of cells open area at 24h, confirming a deceleration in FLS migration (N=13, p=0.0024), with a tendency towards lower migration enhanced also at 48h and 72h. To confirm if this effect was mediated by autophagy modulation, we added rapamycin 1 µM 12h before T24 acquisition. Rapamycin clarified a tendency towards reduction of FLS migration at 24h with respect to DMSO (N=5) (Fig. 13D-E). We hypothesized that autophagy increase by tofacitinib might have had a positive effect on FLS, reducing cellular pro-invasive properties.

Tofacitinib reduces cytokines and chemokines release into cultures supernatants

The anti-inflammatory effect of tofacitinib was tested using ELISA to quantify cytokines and chemokines release into cultures supernatants. FLS cultures were not enriched in IL-17A and TNF; however, we demonstrated a spontaneous release of MCP-1 and IL-6 into supernatants. Tofacitinib reduced MCP-1 and IL-6 levels in FLS supernatants (N=15, p=0.0007 and p=0.0022, respectively) (Fig. 14A), and this effect was more evident on MCP-1 rather than IL-6 (Table 6). In fact, the standardised mean difference of tofacitinib effect over DMSO was -1.28 (p=0.0002) for MCP-1 and -0.88 (p=0.0042) for IL-6. Therefore, we selected the MCP-1 release into FLS cultures supernatants to test if this reduction was mediated by autophagy induction. Following tofacitinib plus rapamycin *in vitro* administration, a slight not-significant decrease in MCP-1 levels with respect to DMSO vehicle control was demonstrated (N=8, p= 0.1953) (Fig. 15).

A significant effect of tofacitinib on MCP-1 and IL-6 release reduction was confirmed also in synovial explants cultures (Fig. 14B), but not in PMBCs cultures (Fig. 14C). A slight effect directed towards reduction of spontaneous IL-17A levels into synovial explants culture supernatants following tofacitinib administration was documented, as well, however the protein levels were very low.

Tofacitinib improves mitochondrial function of PsA FLS and increases mitophagy

Therefore, we wanted to confirm if, in our conditions, tofacitinib was able to improve mitochondrial function in PsA-FLS, similarly to other studies [123,124]. To test our hypothesis, MitoSOX™ Red Mitochondrial Superoxide Indicator was used to document the effect of tofacitinib over DMSO on intracellular ROS production. Tofacitinib significantly reduced the production of intracellular ROS (N=7, p=0.0180) (Fig. 16A-B). No effect was retrieved on mitochondrial potential following JC-1 staining (N=8, p=0.2626) (Fig. 16C-D-E-F), while we documented that tofacitinib was able to increase basal OCR in FLS (N=7, p=0.0280), as well as ATP production (N=7, p=0.0280) and MRC (N=7, p=0.0180) (Fig. 16G-H). These data confirmed that, in our conditions, a modification in cellular bio-energetics have taken place following *in vitro* tofacitinib administration. Finally, to verify if an accelerated clearance of mitochondria was present, we tested mitophagy, which permits the removal of damaged mitochondria. We determined the co-localization of mitochondria and lysosomes in the presence of tofacitinib 1 µM or DMSO vehicle control. Mander's overlap coefficients (M1 and M2) were used to quantify the co-localization of mitochondria inside lysosomes and

lysosomes inside mitochondria, respectively. M1 coefficient significantly increased following tofacitinib administration with respect to DMSO (N= 7, p=0.0156) (Fig. 16I), suggesting an increase in mitophagy.

Anti-oxidant agent NAC reduces pro-invasive properties of PsA FLS

We next wanted to explore if the decrease in ROS production could have a positive effect on pro-invasive properties of FLS. First, we selected the proper dosage of anti-oxidant agent NAC to use for further experiments. As shown in figure 17A, a concentration of 5 mM of NAC for 48h was able to reduce intracellular ROS production by FLS with respect to vehicle control, as documented by counting MitoSOX™ Red Mitochondrial Superoxide Indicator-stained cells using a Tali image-based cytometer. This concentration of NAC did not affect cell viability, as demonstrated by a cell survival assay (Fig. 17B). Then, we confirmed a significant reduction in intracellular ROS following NAC 5 mM in 3 independent experiments using MitoSOX™ Red Mitochondrial Superoxide Indicator and acquiring images at 63x magnification using a Zeiss Axiovert 200 fluorescence microscope (Fig. 17C-D). Finally, we performed migration analysis in presence of vehicle control, tofacitinib or NAC 5 mM for 48h. The experiment was replicated four times. Both tofacitinib and NAC reduced FLS migration with respect to the vehicle control (Fig. 17E-F-G). This effect was already evident after 24h (data not shown).

Discussion

This *in vitro* study demonstrates that the JAK inhibitor tofacitinib is able to increase spontaneous autophagy activity in FLS obtained from active PsA patients, showing anti-invasive and anti-inflammatory properties, and improving mitochondrial function. Our hypothesis is that induction of autophagy/mitophagy by tofacitinib in PsA FLS permits the removal of damaged mitochondria and a better functioning of the remaining ones. To the best of our knowledge, this is the first study evaluating *in vitro* autophagy modulation in PsA FLS, and one of the first dissecting the effect of tofacitinib on spontaneous autophagic activity of FLS obtained from chronic inflammatory arthritis patients.

First, we decided to select a patients' population with active disease in order to study the *in vitro* effect of tofacitinib. Patients enrolled in this study displayed a moderately active disease, well-documented by validated composite scores and clinimetric indexes in PsA management [189–191,194]. Patients were enrolled before starting/changing the systemic treatment for PsA, permitting to couple experimental with clinical information, at least for descriptive purposes, on a time-point in the disease history deemed clinically relevant for both patients and clinicians. Moreover, we confirmed a moderately active synovitis by performing standardized US evaluation of the joint to be biopsied at baseline, before performing synovial biopsy. Again, patients enrolled were well-representative of the disease spectrum, since we enrolled csDMARDs-naïve patients, csDMARDs-experienced patients, as well as bDMARDs-experienced ones. Patients already treated with biologics were less than half of the total, and only two of them have already received an anti-IL17A inhibitor. This permits a discrete stratification of patients enrolled, pertaining to time-points in disease history relevant to clinical JAK inhibitors application, and providing a balanced set of synovial biopsy-derived tissues to test for *in vitro* experiments. Despite, for the purposes of these analyses, we did not have the scope to provide information regarding clinical effectiveness of the drug, we wanted to select a population as close as possible to its clinical application window. Our approach, in line with relevant literature in the field [123], partially differs from the one adopted by other researchers, purchasing cells by companies [182,215], or focusing on larger amounts of tissue derived from total knee replacement surgery [154], which typically does not relate to early patients or to clinically-active disease.

The application of the Krenn's synovitis score depicted a chronic synovitis transitioning from moderate- to high-grade synovitis, with a mean Krenn's score of 4.4. The integration of a synovitis score, paired with IHC staining, in the evaluation of biopsies was performed according to the OMERACT consensus statement on synovial biopsies analyses in translational research [187]. According to OMERACT, in fact, a synovitis score should always be performed by pathologists in translational research studies on synovial biopsies, and IHC staining should be performed, as well [216]. Standardization of synovial biopsy procedures is important to increase comparability across studies in the field, as well to guarantee homogenization of assessments and reported results in eventual multicentre studies, and this awareness is expected to increase in the near future

[48,217,218]. Furthermore, we confirmed that US-guided synovial biopsy is a relatively safe procedure, with a minimally invasive profile [92,207,219], which permits to collect adequate quantity of tissue for *in vitro* experiments. In our study, only one adverse event was reported, with no serious adverse events. Moreover, patients' referred pain, swelling and stiffness of the biopsied joint reduced after two weeks from the procedure, with no signs of worsening of the US examination. In US-guided procedures, in fact, no new relevant safety concerns were demonstrated as compared to the most commonly used arthroscopic-guided synovial biopsy, with few serious adverse events reported in literature [206,207,220,221]. According to a SLR, only one major complication (erysipelas) was reported (0.4%) in 250 US-guided synovial biopsies [220]. No difference in pain, swelling or stiffness of the biopsied joint were reported, before and after the procedure, in a series of 93 biopsies [206], with 80% of patients being either 'very likely' or 'somewhat likely' to repeat the procedure. To sum-up, US-guided synovial biopsy is a minimally-invasive procedure, whose adoption is expected to increase exponentially for either clinical and translational research purposes [187,207,222].

Regarding *in vitro* experiments, it must be underlined that we have exploited unstimulated FLS cultures, differentiating from other studies on JAK inhibitors involving the addition of exogenous cytokines or pro-inflammatory mediators into cultures supernatants [123,208,223,224]. We confirmed that, in our conditions, FLS derived from synovial joints isolated by outgrowth from synovial tissue fragments are able to constitutively release cytokines and chemokines into supernatants [209,225–227], providing a mechanistic rationale for *in vitro* administration of JAK inhibitors, in line with other works [122]. Regarding synovial explants cultures, even if we were not able to replicate the experiments by other groups investigating the effect of tofacitinib on synovial tissue pieces directly placed in culture [122,124], we adopted a different approach by digesting synovial tissue and culturing it immediately after processing, in order to minimize the progressive time-dependent reduction in mediators release; this was in line with several similar approaches in the field [210,228]. We selected a concentration of tofacitinib for *in vitro* experiments borrowed by literature [122], and we adopted an almost univocal timing for cells cultures, proving effectiveness of the drug by showing a reduction in pSTAT3 levels after its *in vitro* administration. In line with this, inhomogeneity in dosages of drugs used for *in vitro* experiments, as well as variable exposure times for cells cultures, represent a relevant limitation to the comparability of results across literature [122,124,154,229].

In our conditions, tofacitinib raised autophagy in PsA FLS, increasing the levels of LC3-II and ATG7 in cellular homogenates. This effect was not dependent on autophagy flux blockade, and it was further potentiated by the autophagy-inducer rapamycin. Since autophagy in PsA has not been well characterized so far, an effect of tofacitinib on spontaneous autophagy activity of FLS has not been reported yet. In other diseases with different experimental conditions, another JAK inhibitor, baricitinib, displayed a pro-autophagic role, inducing autophagy in progeria cells [179]. These authors cultured fibroblasts from patients with progeria in presence or absence of baricitinib, showing an enhancement in autophagy, which persisted over time.

Moreover, similarly to our results, baricitinib reduced intracellular ROS and increased intracellular ATP levels, with a coherent decrease in pro-inflammatory cytokines genes expression. A similar finding was reported by Pandey et al. in the experimental model of a lipodystrophic autoimmune disease [180], in which tofacitinib administered *ex vivo* to knock-out mice induced an increase in autophagy, coupled with a clinical amelioration of the disease phenotype. Despite the obvious limitations that prevent formal comparisons between animal and human studies, as well as studies in fibroblasts obtained from different tissues and diseases, these works were fore-runner in highlighting a possible connection between JAK inhibition and autophagy modulation, and between autophagy modulation and mitochondrial function improvements.

So far, we were able to confirm that tofacitinib reduces pro-invasive and pro-inflammatory properties of PsA FLS when administered *in vitro*. Regarding invasivity, even if we did not focus on specific invasion assays or networks formation tests, we adopted migration assays to confirm our hypothesis. For inflammation, we have chosen to measure the levels of cytokines and chemokines in culture supernatants, demonstrating a reduction of MCP-1 and IL-6 after tofacitinib administration both in FLS and in synovial explants cultures. Moreover, the autophagy-inducer rapamycin exhibited an effect that was similar to that of tofacitinib, slowing down FLS migration attitude. On the other hand, the effect of rapamycin on MCP-1 release was less evident. To this end, the effect of rapamycin in spondyloarthritis FLS has been investigated with particular regard to the ability of this drug to reduce the osteoblastic differentiation rate of human FLS [177]. In presence of osteogenic media, and even after the addition of IL-17A or TNF, the percentage of alkaline phosphatase (ALP) and alizarin red staining, measures of FLS-derived osteogenesis, significantly reduced following rapamycin administration. Moreover, downstream targets of mTOR were found co-localized with $CD3^{pos}$ cells in SpA synovial tissue, suggesting that rapamycin downstream effectors participate to inflammation perpetuation. And this was confirmed in an animal model of spondyloarthritis, in which the *ex vivo* treatment of rats with rapamycin significantly diminished arthritis and spondylitis severity. Similar improvements were found in mice models of psoriasis [230]. However, the exact mechanism by which rapamycin exerts its activity in PsA might be not only related to autophagy induction. In fact, mTOR complexes integrate signals from a multitude of signaling pathways, not only related to starvation, and these include Wnt, IGF, Notch, BMP, mechanical stress, and others, with possible co-occurrence of several downstream effects [231–233].

It must be underlined that the pro-autophagic effect we documented was selective on FLS, while we did not show any influence neither in synovial explants cultures, nor in PBMCs cultures. The complicated physiology of heterogeneous cellular populations might explain, at least partially, this evidence, in line with lessons learned in another complex disease, like systemic lupus erythematosus (SLE) [234,235], in which the focus of research is, as an example, on lymphocytes subpopulations rather than on PBMCs as a whole. This might

suggest that, in order to clearly establish how tofacitinib works on autophagy properties in synovial tissue, cells sorting or single-cells technologies need to be applied [134].

In parallel with a similar work in RA [124], we demonstrated that tofacitinib improves mitochondrial function in PsA FLS, in particular reducing ROS production and increasing oxidative phosphorylation, with no significant effect on mitochondrial potential. Differing from the work by McGarry et al. [124], in which ROS and mitochondrial potential experiments were performed until 3h, we set all experiments at 24h, and this might explain the absence of effect for tofacitinib on mitochondrial potential. Nevertheless, we confirmed, in unstimulated conditions, that JAK inhibitors have a positive effect on mitochondrial respiration, increasing basal OCR, ATP and MRC. Mitochondria from tofacitinib-treated FLS appeared to display a more quiescent phenotype, with a change in FLS bio-energetic profile. This confirms that regulation of the metabolic pathways in FLS is strongly linked with resolution of inflammation in the inflamed joint, and our work contributes to this growing knowledge, arising not only in RA but even in PsA synovitis [123,128,130]. Moreover, we hypothesized that these beneficial effects of tofacitinib on PsA FLS could be mediated by mitophagy modulation. Mitophagy is a selective form of autophagy, which ensures the preservation of healthy mitochondria through the removal of damaged or superfluous ones, by mediating lysosomal degradation [214,236]. Specifically, mitophagy neutralizes the excess of mitochondrial ROS and damaged mitochondrial DNA relevant for inflammation [237]. Our experiments proved that the co-localization of mitochondria and lysosomes was significantly different between tofacitinib-treated FLS and those treated with the vehicle control, suggesting an active process of internalization of defective mitochondria inside autophagolysosomes.

Finally, to confirm the beneficial effect of anti-oxidant agents on FLS physiology, we highlighted a trend towards reduction in migration properties of FLS following NAC administration, thus underlining that intracellular ROS down-titration has positive effects on pro-invasive properties of these cells. The *in vitro* effects of NAC in FLS range from reduction in mitochondrial mutations, mitochondrial potential and ROS [130], to more complex regulation of cellular differentiations [211,238]. It is not surprising that literature regarding a possible effect of pharmacological anti-oxidant agents in the systemic management of chronic inflammatory arthritis is steadily increasing [131], and strategies aimed at controlling excessive oxidative stress within mitochondria are spreading not only to chronic inflammatory arthritis but also to other systemic autoimmune diseases [129].

Our study has some limitations that need to be mentioned. First, even if we set up FLS cultures according to literature [122,123,208,209], FLS is a heterogeneous population [239], and dissecting the effect of tofacitinib on relevant FLS sub-populations was out of the scope of our work. Second, as previously said, we decided to focus on unstimulated cellular populations for experiments. Despite *in vitro* stimulation with cytokines or other mediators could have amplified the synovial effects of tofacitinib [123,208,223,224], these additions

remain an exogenous manipulation that could limit the interpretation of results. Third, patients enrolled were not all treatment-naïve, and this could have generated a heterogeneous cellular population for *in vitro* studies, since previous treatments could have influenced the features of synovial inflammation. However, our results were consistent across different patients, even if a certain grade oh heterogeneity throughout experiments was recorded. Moreover, we did not provide information about the pathotype (i.e., myeloid, lymphoid, pauci-immune), since we did not include tissue mRNA expression analyses [12,240–242]. However, pathotypes definition in PsA is less validated than in RA, and, again, we performed at least IHC staining. Finally, we did not include controls in our analysis, since investigating the effect of tofacitinib on OA FLS was out of our scopes, and collecting synovial tissues from healthy adults was not possible for ethical reasons. Notwithstanding these limitations, the strengths of this study refer to the well-characterized clinical population at study entry, the adherence to OMERACT consensus statement regarding synovial tissue handling and reporting [187], as well as the innovation of the matter, with the possibility to provide data regarding the fascinating and actually unsolved correlation between JAK inhibition at synovial level and mitochondrial function improvement.

Conclusions

Tofacitinib enhances autophagy activity and improves mitochondrial function in PsA FLS, reducing their pro-invasive and pro-inflammatory properties. Induction of autophagy/mitophagy by tofacitinib in PsA FLS might permit the removal of damaged mitochondria and a better functioning of the remaining ones. This reinforce the significance of the beneficial effects of JAK inhibitors at synovial level, expanding the rationale for the use of these drugs in the systemic management of PsA patients.

Tables

Table 1. b/tsDMARDs that have been approved or are in different phases of development for the systemic management of PsA.

bDMARDs	Mechanism of action	EMA/FDA approval or phase of development
Etanercept	TNFi	RA; PsA; PsO; JIA; AS/nrAS
Adalimumab	TNFi	RA; PsA; PsO; JIA; AS/nrAS; SH; CD/UC; Chronic uveitis
Infliximab	TNFi	RA; PsA; PsO; AS; CD/UC
Golimumab	TNFi	RA; PsA; JIA; AS/nrAS; UC
Certolizumab pegol	TNFi	RA; PsA; PsO; AS/nrAS
Ustekinumab	p40 common subunit (IL-12, IL-23) inhibitor	PsA; PsO; CD/UC
Secukinumab	IL-17A inhibitor	PsA; PsO; AS/nrAS
Ixekizumab	IL-17A inhibitor	PsA; PsO; AS/nrAS
Abatacept	CD80/CD86-mediated costimulation inhibitor	RA; PsA; JIA
Risankizumab	p19 subunit (IL-23) inhibitor	PsO *PsA (phase II trial completed, phase III trials ongoing)*
Tildrakizumab	p19 subunit (IL-23) inhibitor	PsO *PsA (phase II trial completed, phase III trials ongoing)*
Guselkumab	p19 subunit (IL-23) inhibitor	PsO PsA
Brodalumab	IL-17RA inhibitor	PsO *PsA (phase III trials completed)*
Bimekizumab	IL-17A and IL-17F bispecific antibody	PsO *PsA (phase IIb trial completed, phase III trials ongoing)*
tsDMARDs	**Mechanism of action**	**EMA/FDA approval or phase of development**
Apremilast	PDE4 inhibitor	PsA; PsO; BD

Tofacitinib	JAK1/3 inhibitor	RA; PsA; UC
Upadacitinib	JAK1 inhibitor	RA; PsA; AS; AD
Filgotinib	JAK1 inhibitor	RA; UC *PsA (phase II completed, phase III trials ongoing)*

Abbreviations: b/tsDMARDs, biological/targeted synthetic disease-modifying antirheumatic drugs; PsA, psoriatic arthritis; EMA, European Medicines Agency; FDA, U.S. Food and Drug Administration; TNFi, tumor necrosis factor-alpha inhibitor; RA, rheumatoid arthritis; PsO, psoriasis; JIA, juvenile idiopathic arthritis; AS/nrAS, ankylosing spondylitis/nonradiographic axial spondylarthritis; SH, suppurative hidradenitis; CD, Crohn's disease; UC, ulcerative colitis; IL, interleukin; IL-17RA, IL-17 Receptor A; PDE4, phosphodiesterase-4; BD, Behcet's disease; JAK, Janus Kinase; AD, atopic dermatitis.

Table 2. Histopathological Krenn's synovitis score [185,186].

Score	Definition
Enlargement of the synovial lining cell layer	
0 points	The lining cells form one layer.
1 point	The lining cells form 2–3 layers.
2 points	The lining cells form 4–5 layers, few multinucleated cells might occur.
3 points	The lining cells form more than 5 layers, the lining might be ulcerated and multinucleated cells might occur.
Density of the resident cells	
0 points	The synovial stroma shows normal cellularity.
1 point	The cellularity is slightly increased.
2 points	The cellularity is moderately increased, multinucleated cells might occur.
3 points	The cellularity is greatly increased, multinucleated giant cells, pannus formation and rheumatoid granulomas might occur.
Inflammatory infiltrate	
0 points	No inflammatory infiltrate.
1 point	Few mostly perivascular situated lymphocytes or plasma-cells.
2 points	Numerous lymphocytes or plasma-cells, sometimes forming follicle-like aggregates.
3 points	Dense band-like inflammatory infiltrate or numerous large follicle-like aggregates.
Cumulative score	
0-1 points	No synovitis
2-4 points	Low-grade synovitis
5-9 points	High-grade synovitis

Table 3. Outline of the study and scheduled patients' visits.

Procedures	T-2	T0
Informed consent	X	
Inclusion/Exclusion Criteria	X	
US-guided synovial biopsy	X	
Socio-demographic data and medical history	X	
Clinical examination	X	X
US assessment	X	X
Clinimetric assessment	X	X
PROs	X	X
Blood samples collection	X	
Adverse events		X
Start of designed cs/b/tsDMARD treatment		X

Abbreviations: US, ultrasound; PROs, patient reported outcomes; cs, conventional synthetic; b, biological; ts, targeted synthetic; DMARD, disease modifying anti-rheumatic drug.

Table 4. Baseline demographic, clinical, US and treatment-related data of included patients (N=16).

Demographic variables	Frequency
Age (years), mean (SD)	59.8 (7.9)
Female, N (%)	5 (31.3%)
Caucasian ethnicity, N (%)	16 (100%)
Height (cm), mean (SD)	171.5 (8.3)
Weight (kg), mean (SD)	82.9 (11.4)
BMI (kg/m^2), mean (SD)	28.3 (4.3)
Actual smokers, N (%)	2 (12.5%)
Actual alcohol users, N (%)	6 (37.5%)
Regular physical activity, N (%)	2/15 (13.33%)
Clinical variables	**Frequency**
Disease duration (years), mean (SD)	9.7 (7.9)
Skin psoriasis, N (%)	14 (87.5%)
First-degree relative with psoriasis, N (%)	7 (43.8%)
Nail psoriasis, N (%)	4 (25.0%)
Inflammatory bowel disease (IBD), N (%)	0 (0.0%)
Previous uveitis, N (%)	1 (6.25%)
Hypertension, N %)	9 (56.3%)
Obesity, N (%)	6 (37.5%)
Diabetes, N (%)	2 (12.5%)
Dyslipidaemia, N (%)	5 (31.3%)
Anxiety/depression, N (%)	1 (6.3%)
NAFLD, N (%)	3 (18.8%)
Osteoporosis, N (%)	1 (6.3%)
Ischaemic cardiomyopathy, N (%)	0 (0.0%)
Cerebrovascular disease, N (%)	1 (6.3%)
COPD, N (%)	1 (6.3%)
Moderate-to-severe CKD, N (%)	0 (0.0%)
Mild liver disease, N (%)	2 (12.5%)
Moderate-to-severe liver disease, N (%)	0 (0.0%)
Solid tumours, N (%)	1 (6.3%)
Leukemia/lymphoma, N (%)	0 (0.0%)
Thyroid disease, N (%)	1 (6.3%)

Concomitant fibromyalgia, N (%)	4 (25.0%)
Concomitant osteoarthritis, N (%)	3 (18.8%)
Concomitant crystal-induced arthropathy, N (%)	2 (12.5%)
Moll and Wright criteria, symmetric arthritis, N (%)	7 (43.8%)
Moll and Wright criteria, asymmetric oligoarthritis, N (%)	8 (50.0%)
Moll and Wright criteria, arthritis mutilans, N (%)	1 (6.3%)
Moll and Wright criteria, IFD arthritis, N (%)	0 (0.0%)
ESR (mm), mean (SD)	28.9 (24.8)
CRP (mg/dl), mean (SD)	1.5 (2.0)
Clinimetrics	Frequency
Pain joint to be biopsied (0-100), mean (SD)	57.8 (28.8)
Stiffness joint to be biopsied (0-100), mean (SD)	53.1 (28.3)
Swelling joint to be biopsied (0-100), mean (SD)	58.4 (32.8)
Patient Global Pain (0-100), mean (SD)	67.4 (22.6)
Patient Global Activity (0-100), mean (SD)	73.4 (16.9)
Physician Global Activity (0-100), mean (SD)	56.3 (18.1)
Tender joint count (0-68), mean (SD)	6.6 (5.4)
Swollen joint count (0-66), mean (SD)	3.4 (1.9)
DAPSA, mean (SD)	25.6 (6.8)
BSA, mean (SD)	1.3 (1.8)
LEI, mean (SD)	0.4 (0.5)
Mean number of painful entheseal points, mean (SD)	0.8 (0.3)
HAQ (0-3), mean (SD)	0.9 (0.5)
US variables	Frequency
Grey scale synovitis joint to be biopsied (0-3), mean (SD)	1.9 (0.8)
Joint effusion joint to be biopsied (0-3), mean (SD)	1.4 (0.7)
Power Doppler joint to be biopsied (0-3), mean (SD)	0.5 (0.6)
Treatment-related variables	Frequency
Previous csDMARDs treatment, N (%)	13 (81.3%)
Previous bDMARDs treatment, N (%)	6 (37.5%)
Actual NSAIDs treatment, N (%)	8 (50.0%)
Actual GCs treatment, N (%)	2 (12.5%)
Actual GC dosage (mg of prednisone equivalent, N=2), mean (SD)	5 (0)

Abbreviations: US; ultrasound; SD, standard deviation; BMI, body mass index; NAFLD, non-alcoholic Fatty Liver Disease; COPD, chronic obstructive pulmonary disease; CKD, chronic kidney disease; ESR, erythrocyte sedimentation rate; CRP, C reactive protein; DAPSA, Disease Activity Index for Psoriatic Arthritis; BSA, body surface area; LEI, Leeds Enthesitis Index; HAQ, Health Assessment Questionnaire; csDMARD, conventional synthetic disease modifying antirheumatic drugs; bDMARD, biological disease modifying antirheumatic drugs; NSAIDs, Non-steroidal anti-inflammatory drugs; GCs, glucocorticoids.

Table 5. Baseline histopathological and IHC data (N=16).

Variable	Frequency
Biopsied joint: right knee, N (%)	3 (18.8%)
Biopsied joint: left knee, N (%)	13 (81.2%)
Krenn's synovitis score (0-9), mean (SD)	4.4 (1.9)
Krenn's lining layer enlargement (0-3), mean (SD)	1.4 (0.8)
Krenn's resident cells density (0-3), mean (SD)	1.3 (0.7)
Krenn's inflammatory infiltrate (0-3), mean (SD)	1.8 (0.9)
$CD3^{pos}$ semiquantitative score (0-4), mean (SD)	1.9 (1.0)
$CD20^{pos}$ semiquantitative score (0-4), mean (SD)	1.6 (1.1)
$CD68^{pos}$ semiquantitative score (0-4), mean (SD)	1.8 (0.9)

Abbreviations: IHC, immunohistochemistry; SD, standard deviation. Krenn's synovitis score was derived from Krenn et al. [185]. Semiquantitative IHC score was modified from Canete et al. [96].

Table 6. Standardised mean difference comparison of tofacitinib effect over DMSO on spontaneous chemokines/cytokines release in cultures supernatants.

Type of cell culture	Measured chemokine/cytokine	Standardised mean difference	p
FLS	MCP-1	-1.28	0.0002
	IL-6	-0.88	0.0042
Synovial explants	MCP-1	-0.97	0.0423
	IL-6	-0.52	0.2615
	IL-17A	-1.19	0.0564
	TNF	0.62	0.1501
PBMCs	MCP-1	-0.43	0.2374
	IL-6	0.28	0.4255
	IL-17A	-0.05	0.9077
	TNF	-0.43	0.2357

Abbreviations: DMSO, dimethyl Sulfoxide; FLS, fibroblast-like synoviocytes; MCP-1, monocyte chemoattractant protein-1; IL, interleukin; TNF, tumour necrosis factor alpha.

Figures

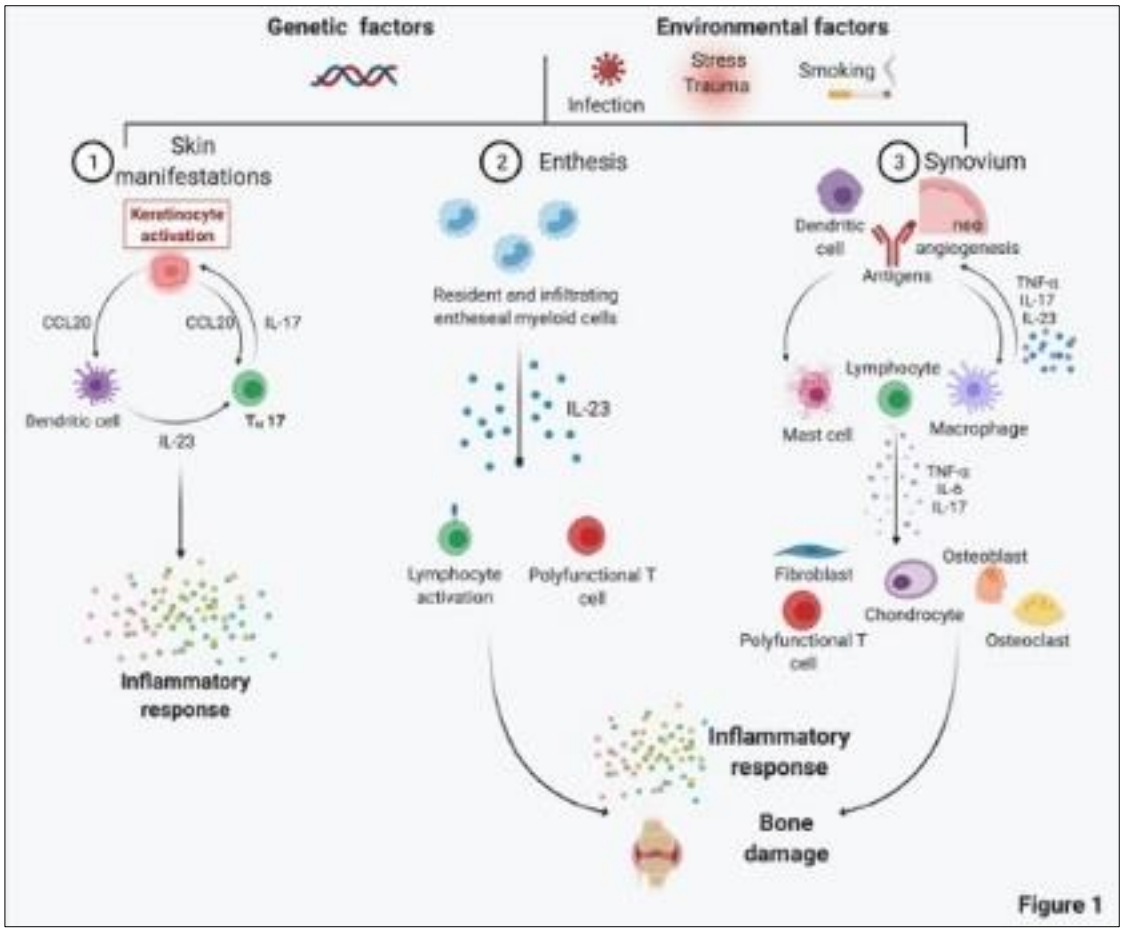

Figure 1. Schematic representation of the main pathogenic processes driving PsA development and chronicity.

From: Silvagni E. et al. From Bed to Bench and Back: TNF-α, IL-23/IL-17A, and JAK-Dependent Inflammation in the Pathogenesis of Psoriatic Synovitis. Front Pharmacol. 2021 Jun 15;12:672515 [7]. PsA is a heterogeneous chronic disease, with skin, entheseal and synovial tissue involvement occurring in different proportions across patients under genetic and environmental triggers. For skin manifestations, activated dendritic cells secrete predominantly IL-23, which in turn induces the differentiation of naïve T cells into Th17 cells. IL-17 is responsible for keratinocyte activation and subsequent perpetuation of skin inflammation. At the entheseal level, resident and infiltrating entheseal myeloid cells produce IL-23, which is responsible for lymphocyte activation and the inflammatory response, as well as bone damage. Psoriatic synovitis, on the other hand, is characterized by tortuous and immature neoangiogenesis, with antigen presentation by dendritic cells and macrophages leading to lymphocyte activation. As a result, the synovial inflammatory infiltrate is rich in activated lymphocytes, mast cells and macrophages. Polyfunctional T cells are responsible for the production of several types of proinflammatory cytokines (e.g., TNF-α, IL-17A, GM-CSF, and IFN-γ) in

the synovial membrane and synovial fluid. The proinflammatory cytokine milieu further activates fibroblast-like synoviocytes, chondrocytes, osteoblasts, and osteoclasts, resulting in bone damage.

Abbreviations: PsA, psoriatic arthritis; IL, interleukin; Th, T helper cells; TNF-α, tumor necrosis factor-alpha; GM-CSF, Granulocyte-Macrophage Colony-Stimulating Factor; IFN-γ, interferon gamma. This image was created with © BioRender 2021.

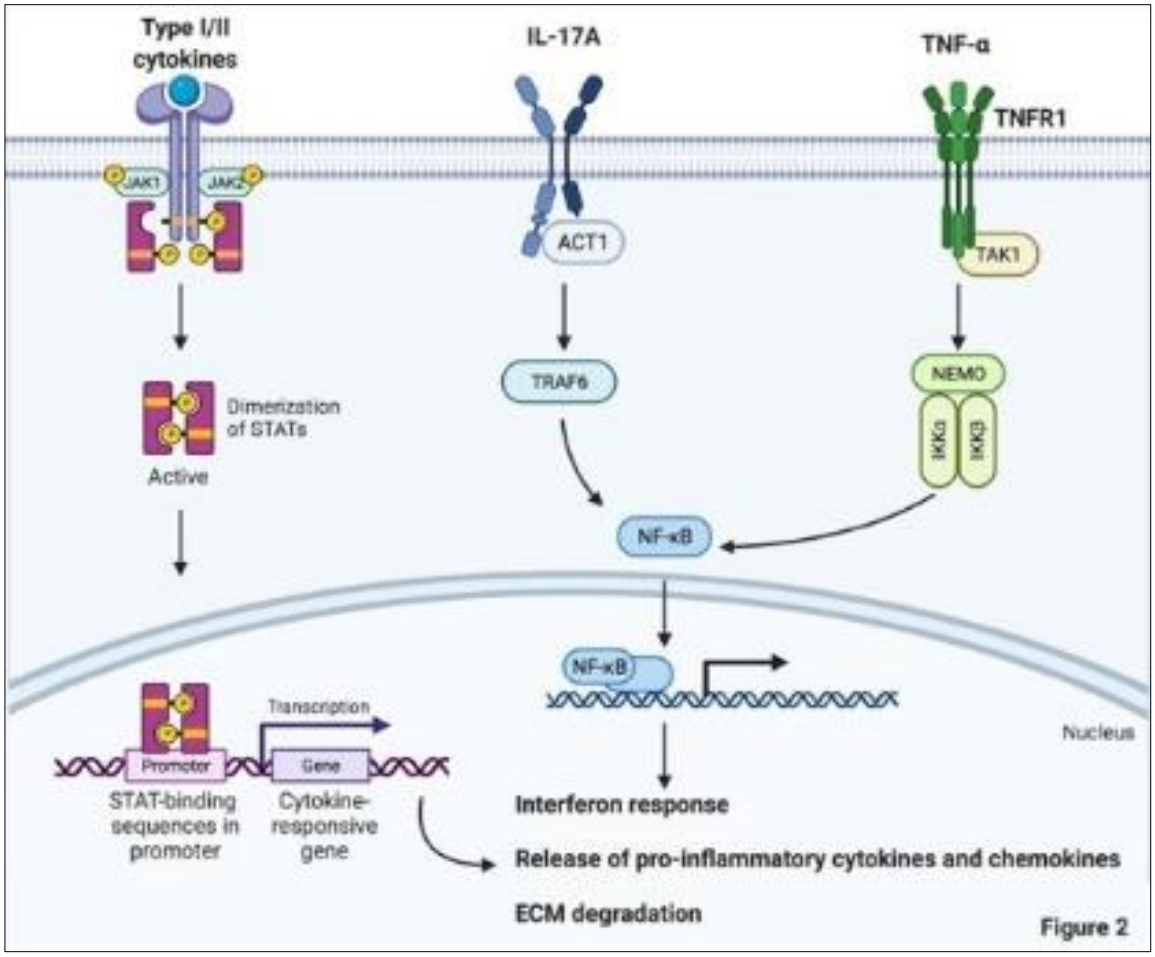

Figure 2. Downstream signal transduction mechanisms following TNF-α, IL-17A or JAK/STAT-coupled receptor activation.

From: Silvagni E. et al. From Bed to Bench and Back: TNF-α, IL-23/IL-17A, and JAK-Dependent Inflammation in the Pathogenesis of Psoriatic Synovitis. Front Pharmacol. 2021 Jun 15;12:672515 [7]. Type I and II cytokines (e.g., IL-23, IL-22, IL-6, and type I, II and III IFNs) bind JAK/STAT-associated receptors. JAK proteins are associated with the cytoplasmic domain of these receptors, and when cytokines bind to the receptor, JAKs undergo autophosphorylation and phosphorylate other JAKs. STATs recognize JAKs, bind their cognate receptors and become phosphorylated by JAKs. STATs then translocate to the nucleus, bind DNA and activate the transcription of target genes for the interferon response, proinflammatory mediator production and ECM degradation. IL-17A binds IL-17R, a transmembrane heterodimer of IL17RA and IL-17RC. This binding induces Act-1 activation, which in turn activates TRAF6 and, accordingly, NF-kB. NF-kB migrates to the nucleus and induces target gene transcription. TNF-α, either in its soluble or transmembrane form, binds TNFR1 or TNFR2. After binding, in the classical proinflammatory axis induced by TNF-α-dependent cellular activation, TAK1 engages NEMO. NEMO activation results in the phosphorylation of specific serine residues in inhibitory proteins of NF-κB (IκBs) by IKK-1 and IKK-2, leading to IκB polyubiquitination and proteasome-dependent degradation. This process releases NF-κB proteins, which translocate to the nucleus and induce target gene

transcription. Taken together, these mechanisms result in an interferon response, proinflammatory chemokine and cytokine release, and extracellular matrix degradation.

Abbreviations: TNF-α, tumor necrosis factor-alpha; IL, interleukin; JAK/STAT, Janus Kinase/signal transducer and activator of transcription; ECM, extracellular matrix; IL-17R, IL-17 Receptor; Act1, NF-kappaB activator 1; TRAF6, TNFR-associated factor 6; NF-kB, nuclear factor kappa-light-chain-enhancer of activated B cells; TNFR, tumor necrosis factor-alpha receptor; TAK1, Transforming growth factor-alpha-activated kinase 1; NEMO, NF-κB essential modulator; IKK, inhibitor of IκB kinase; IκBs, inhibitory proteins of NF-κB. This image was created with © BioRender 2021.

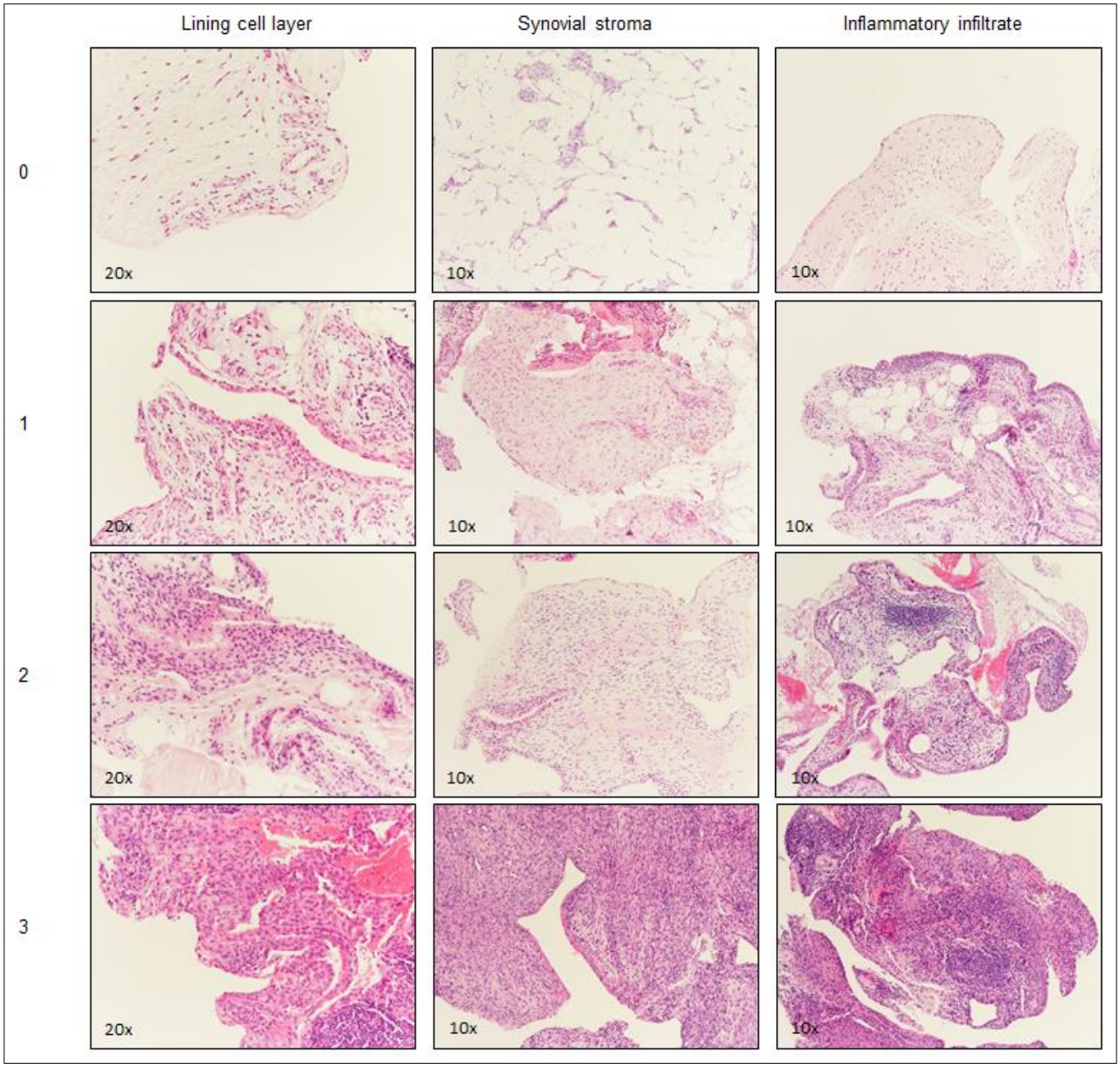

Figure 3. Krenn's synovitis score.

Representative images for each parameter and degree of the Krenn's synovitis score obtained from patients with PsA enrolled in the present study (enlargement of the synovial lining cell layer, density of the resident cells - synovial stroma, inflammatory infiltrate). Images were visualized by using a microscope at 20x magnification for synovial lining cell layer evaluation, and at 10x magnification for stroma and inflammatory infiltrate.

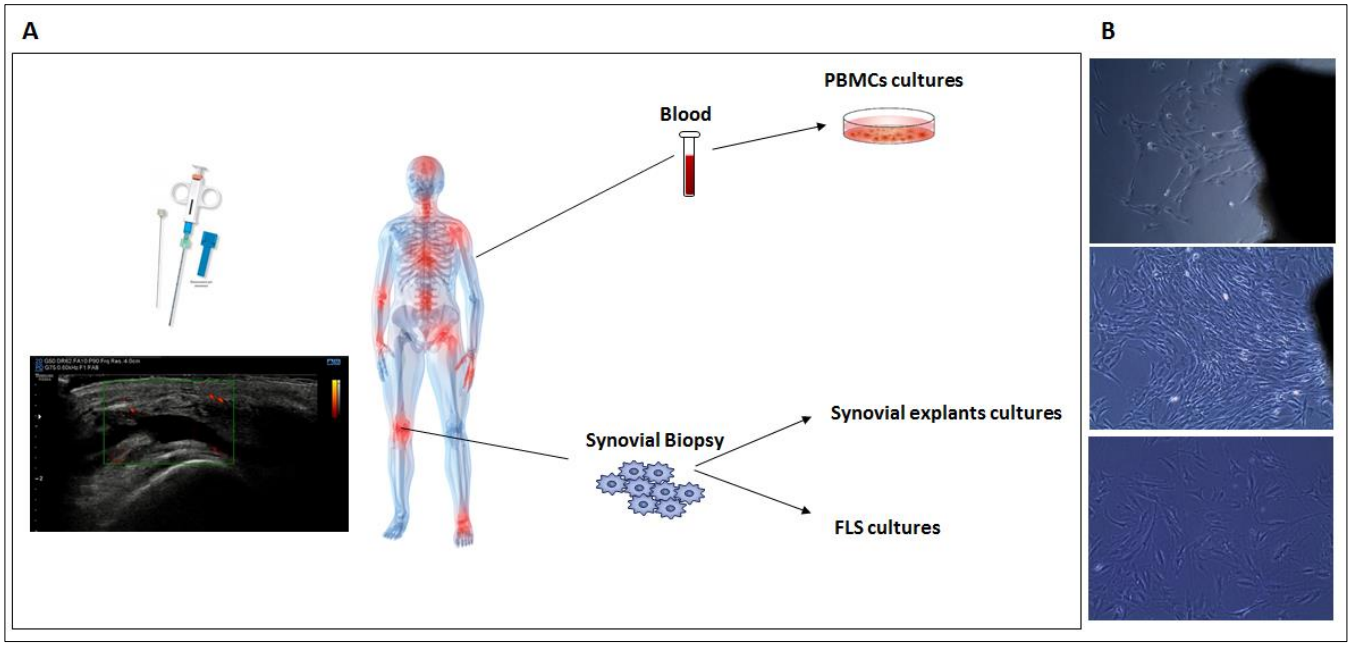

Figure 4. Schematic representation of biological samples handling and cellular cultures performed.

A: Patients with active PsA were recruited for participation in this study and, after signing informed consent, underwent synovial biopsy of an inflamed joint under US guidance. Synovial tissue was delivered to the laboratory for synovial explants cultures and FLS cultures. Blood samples were used for PBMCs cultures. B: FLS were allowed to grow out of the tissue lump, and trypsinized at confluence. Synovial cells were then cultured at 37°C in humidified atmosphere 5% CO2 incubator, and FLS were used for experiments between 3rd and 8th passages.

Abbreviations: PBMCs, peripheral blood mononuclear cells; FLS, fibroblast-like synoviocytes; PsA, psoriatic arthritis; US, ultrasound.

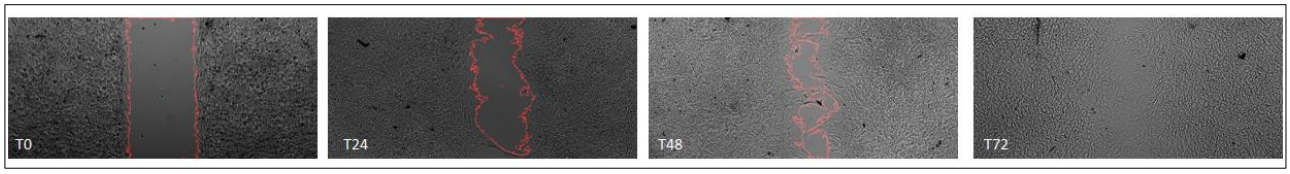

Figure 5. FLS migration analysis.

FLS migration was evaluated using Culture-Insert 2 Well in µ-Dish 35 mm (Ibidi). After confluence (100,000 cells/well), the culture-insert was removed and migration of FLS was assessed in presence or absence of DMSO or tofacitinib 1 µM. Acquisitions were performed at 0, 24, 48 and 72 hours. Data analysis was performed using an in-house developed semi-automated algorithm to measure the percentage of cells open area (ImageJ software). Images were visualized by using a microscope at 4x magnification.

Abbreviations: FLS, fibroblast-like synoviocytes; DMSO, dimethyl Sulfoxide.

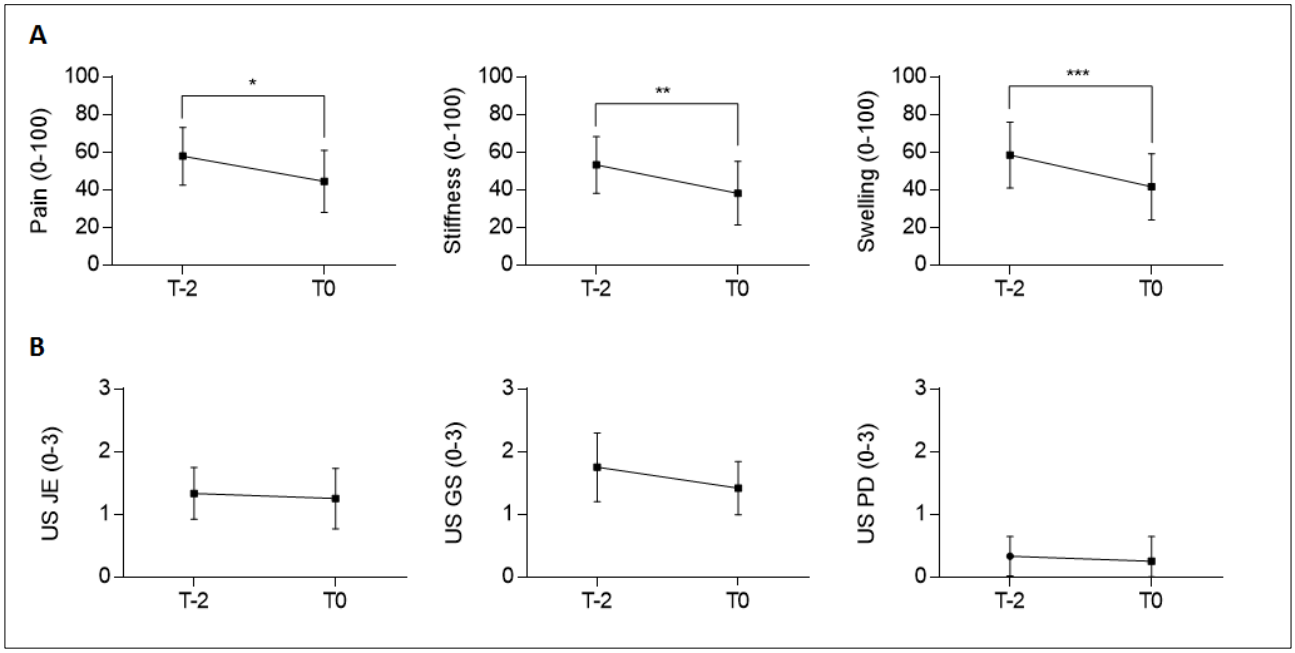

Figure 6. Clinimetric and US-related variables modification before and after US-guided synovial biopsy procedure.

A: Longitudinal evaluation of pain, stiffness and swelling of the biopsied joint between T-2 and T0 visits. Globally, mean pain, stiffness and swelling of the biopsied joint significantly reduced between T-2 and T0 visits (N=16). *: p=0.0215. **: p=0.0176. ***: p=0.0048. B: No significant worsening of the US components recorded (grey scale synovitis, joint effusion, power Doppler signal) (N=12). Graphs are representative of means and confidence intervals.

Abbreviations: US, ultrasound; JE, joint effusion; GS, grey scale; PD, Power Doppler.

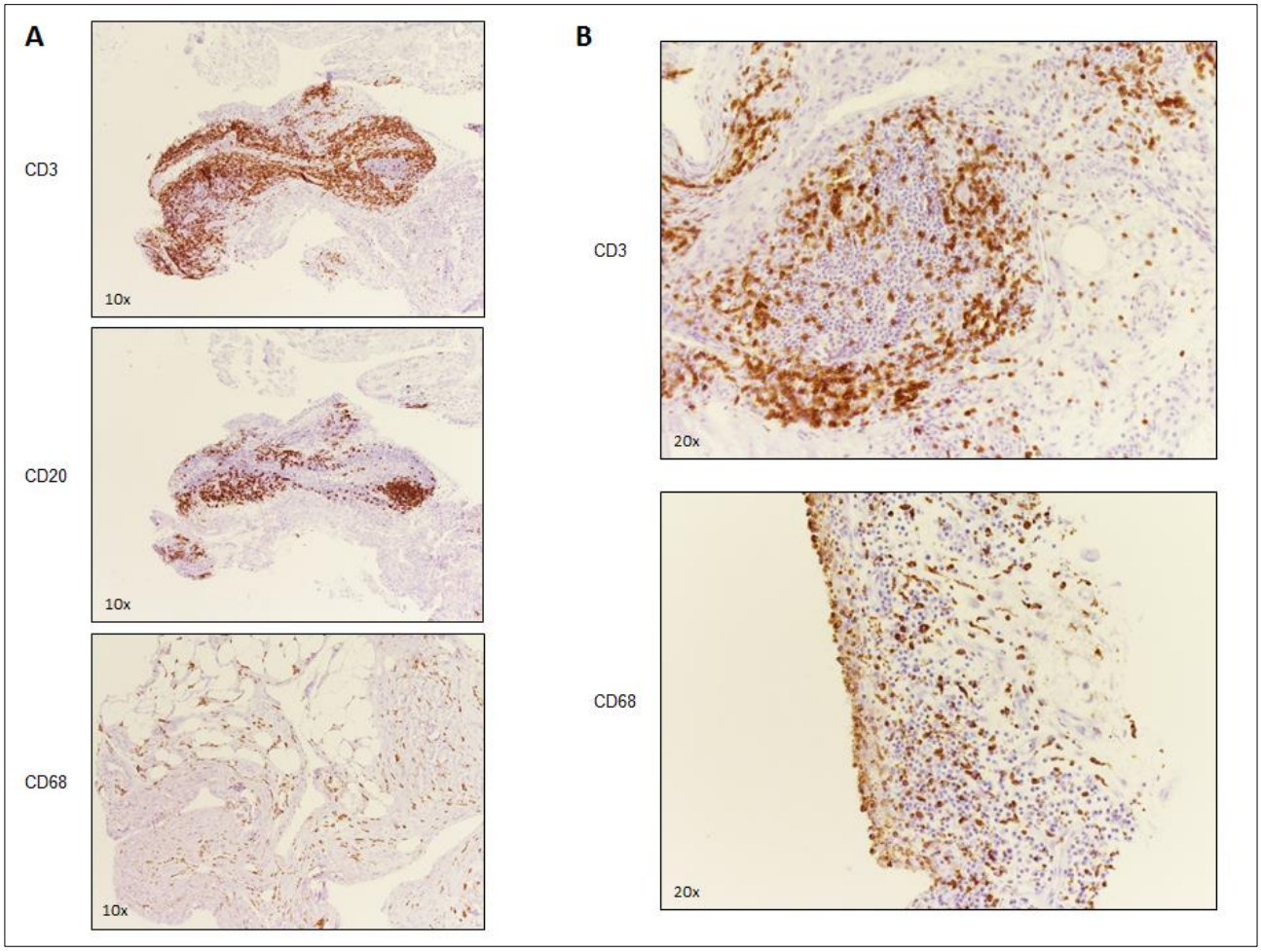

Figure 7. IHC evaluation of T cells ($CD3^{pos}$), B cells ($CD20^{pos}$) and macrophages ($CD68^{pos}$) in synovial tissue.

A: T cells (CD3), B cells (CD20), and macrophages (CD68) evaluated using an Olympus AX60 microscope at 10x magnification. B: T cells (CD3), and macrophages (CD68) evaluated using an Olympus AX60 microscope at 20x magnification.

Abbreviations: IHC, immunohistochemistry.

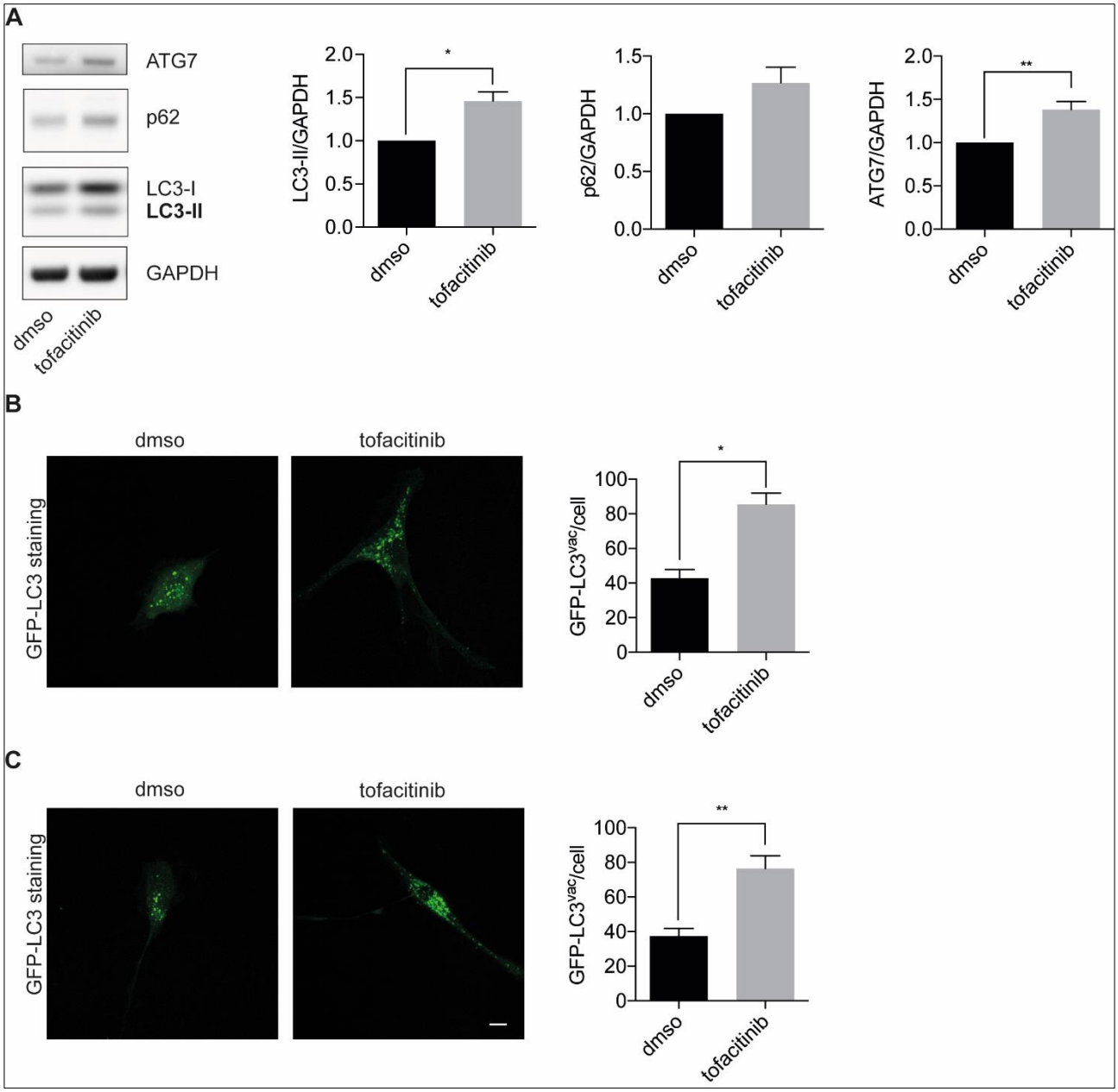

Figure 8. Tofacitinib increases spontaneous autophagic activity in PsA FLS.

A: FLS cultures were performed for 24h in presence of the vehicle control DMSO or tofacitinib 1 µM, and protein levels in cellular homogenates were analysed by western blot (representative western blot image and protein levels quantification). As compared to vehicle control, tofacitinib significantly increased mean ± s.e.m. LC3-II (DMSO: 1.000; tofacitinib: 1.460 ± 0.105, N=16, p=0.0002) and ATG7 (DMSO: 1.000; tofacitinib: 1.384 ± 0.092, N=14, p=0.0001) levels, suggesting an increase in autophagic activity. A non-significant increase in p62 levels was enhanced (DMSO: 1.000; tofacitinib: 1.269 ± 0.134, N=16, p=0.0654). Total cell lysates were resolved by NuPAGE LDS Sample Buffer (Thermo Fisher Scientific). Error bars indicate s.e.m. *: p=0.0002. ** p=0.0001. GAPDH was used as loading control. B-C: autophagic vesicles were visualized by using a fluorescence microscope at 40x magnification in FLS transfected with a recombinant plasmid expressing

LC3 protein linked to GFP (FLS obtained from two different patients - mean number of cells evaluated for each condition: 49). Results confirmed an increase in LC3-autophagic vesicles after tofacitinib treatment (PT1 DMSO: 42.81 ± 4.99; PT1 tofacitinib: 85.52 ± 6.50, $p<0.0001$; PT2 DMSO: 37.37 ± 4.35; PT2 tofacitinib: 76.52 ± 7.36. $p=0.0002$). Error bars indicate s.e.m. *: $p<0.0001$; **: $p=0.0002$.

Abbreviations: ATG7, Autophagy Related 7; LC3-II, Microtubule-associated protein light chain 3-II; GAPDH, Glyceraldehyde-3-Phosphate Dehydrogenase; DMSO, dimethyl Sulfoxide; GFP, Green Fluorescent Protein; PsA: psoriatic arthritis; FLS, fibroblast-like synoviocytes; s.e.m., standard error of the mean.

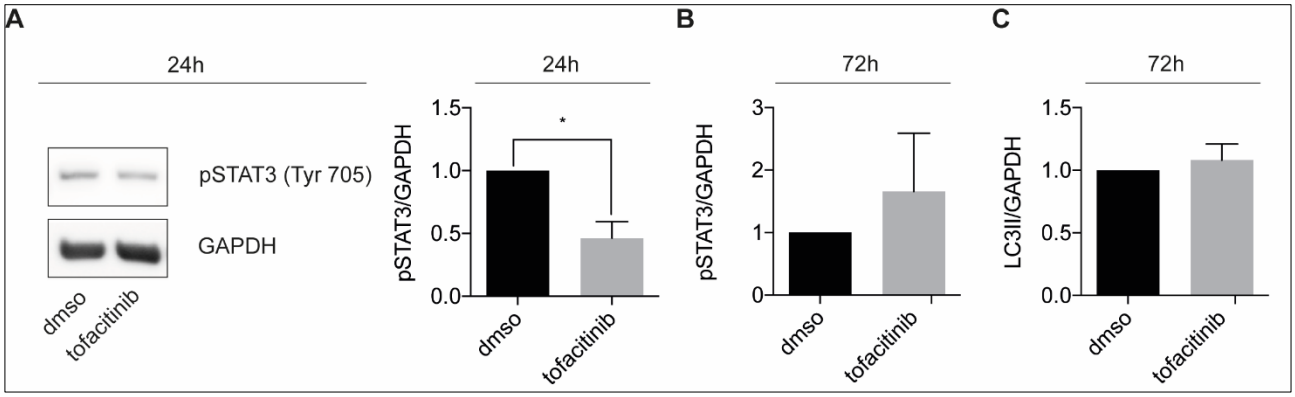

Figure 9. Tofacitinib reduces phospho-STAT3 levels in PsA FLS after 24h.

A: FLS cultures were performed for 24h in presence of the vehicle control DMSO or tofacitinib 1 µM, and protein levels in cellular homogenates were analysed by western blot (representative western blot image and protein levels quantification). Tofacitinib reduced pSTAT3 levels as compared to DMSO (DMSO: 1.000; tofacitinib: 0.463 ± 0.131, N=7, p=0.0313). Total cell lysates were resolved by NuPAGE LDS Sample Buffer (Thermo Fisher Scientific). Error bars indicate s.e.m. *: p=0.0313. GAPDH was used as loading control. B: FLS cultures performed for 72h in presence of the vehicle control DMSO or tofacitinib 1 µM, analysed by western blot (protein levels quantification). Tofacitinib had no significant effect on pSTAT3 levels (DMSO: 1.000; tofacitinib: 1.661 ± 0.929, N=7, p=1.0000). Total cell lysates were resolved by NuPAGE LDS Sample Buffer (Thermo Fisher Scientific). Error bars indicate s.e.m. C: FLS cultures performed for 72h in presence of the vehicle control DMSO or tofacitinib 1 µM, analysed by western blot (protein levels quantification). Tofacitinib had no significant effect on LC3-II levels (DMSO: 1.000; tofacitinib: 1.082 ± 0.128, N=11, p=0.5195). Total cell lysates were resolved by NuPAGE LDS Sample Buffer (Thermo Fisher Scientific). Error bars indicate s.e.m. GAPDH was used as loading control.

Abbreviations: pSTAT3, Phospho Signal Transducer And Activator Of Transcription 3; GAPDH, Glyceraldehyde-3-Phosphate Dehydrogenase; DMSO, dimethyl Sulfoxide; LC3-II, Microtubule-associated protein light chain 3-II; PsA: psoriatic arthritis; FLS, fibroblast-like synoviocytes; s.e.m., standard error of the mean.

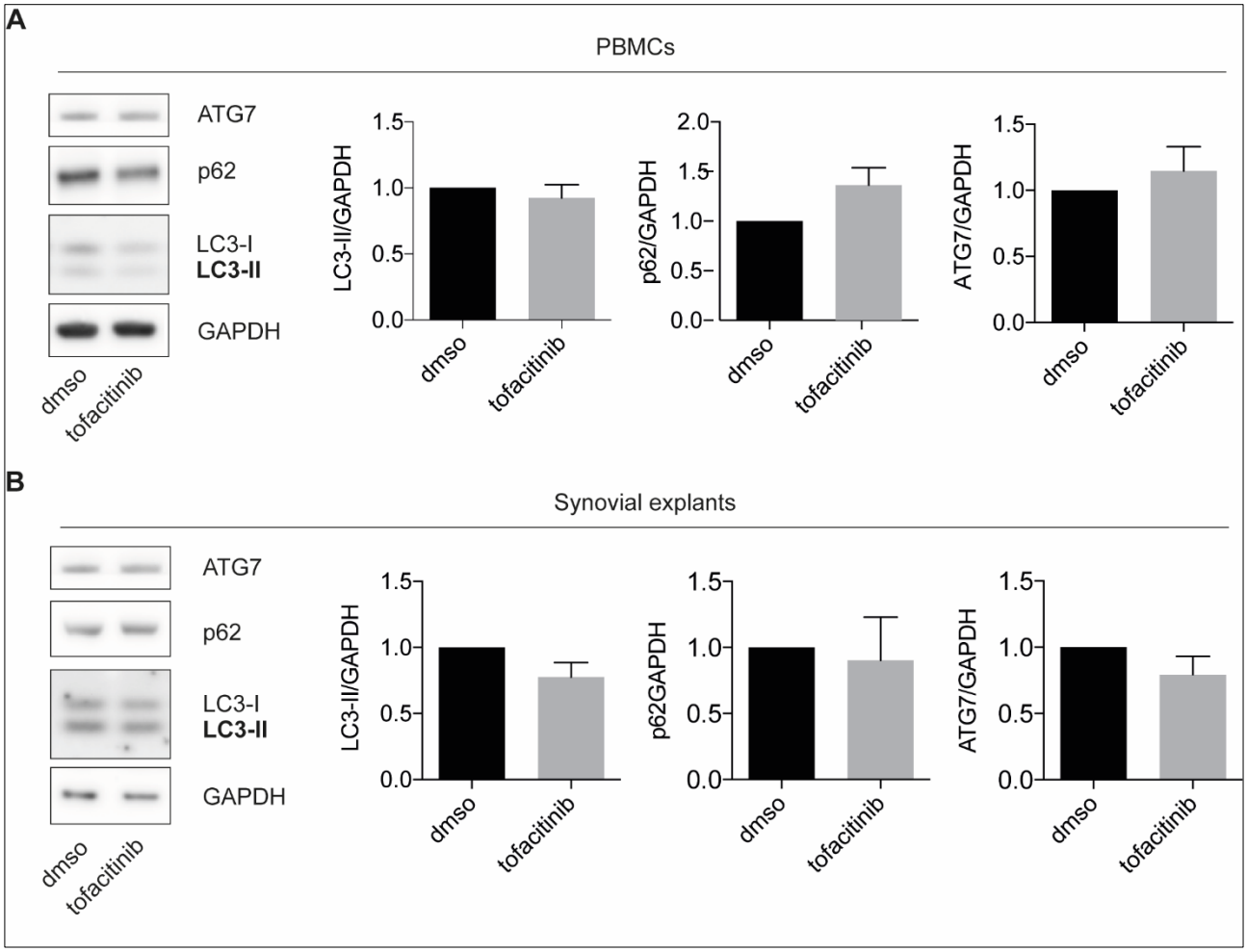

Figure 10. Tofacitinib has no effect on spontaneous autophagic activity in PBMCs cultures and synovial explants cultures.

A: PBMCs cultures were performed for 24h in presence of the vehicle control DMSO or tofacitinib 1 µM, and protein levels in cellular homogenates were analysed by western blot (representative western blot image and protein levels quantification). Tofacitinib did not have any significant effect over LC3-II levels as compared to DMSO (DMSO: 1.000; tofacitinib: 0.924 ± 0.100, N=10, p=0.4922). Similarly, tofacitinib did not significantly act on p62 (DMSO: 1.000; tofacitinib: 1.362 ± 0.175, N=8, p=0.1484), and ATG7 (DMSO: 1.000; tofacitinib: 1.147 ± 0.184, N=10, p=0.9219). Total cell lysates were resolved by NuPAGE LDS Sample Buffer (Thermo Fisher Scientific). Error bars indicate s.e.m. GAPDH was used as loading control. B: Digested synovial biopsy cultures (synovial explants) were performed for 24h in presence of the vehicle control DMSO or tofacitinib 1 µM, and protein levels in cellular homogenates were analysed by western blot (representative western blot image and protein levels quantification). Tofacitinib did not increase LC3-II levels as compared to DMSO (DMSO: 1.000; tofacitinib: 0.776 ± 0.109, N=5). A slight reduction of p62 (DMSO: 1.000; tofacitinib: 0.905 ± 0.326, N=2) and ATG7 (DMSO: 1.000; tofacitinib: 0.794 ± 0.137, N=3) levels was underlined, as well. Total cell lysates were resolved by NuPAGE LDS Sample Buffer (Thermo Fisher Scientific). Error bars indicate s.e.m. GAPDH was used as loading control.

Abbreviations: PBMCs, peripheral blood mononuclear cells; ATG7, Autophagy Related 7; LC3-II, Microtubule-associated protein light chain 3-II; GAPDH, Glyceraldehyde-3-Phosphate Dehydrogenase; DMSO, dimethyl Sulfoxide; s.e.m., standard error of the mean.

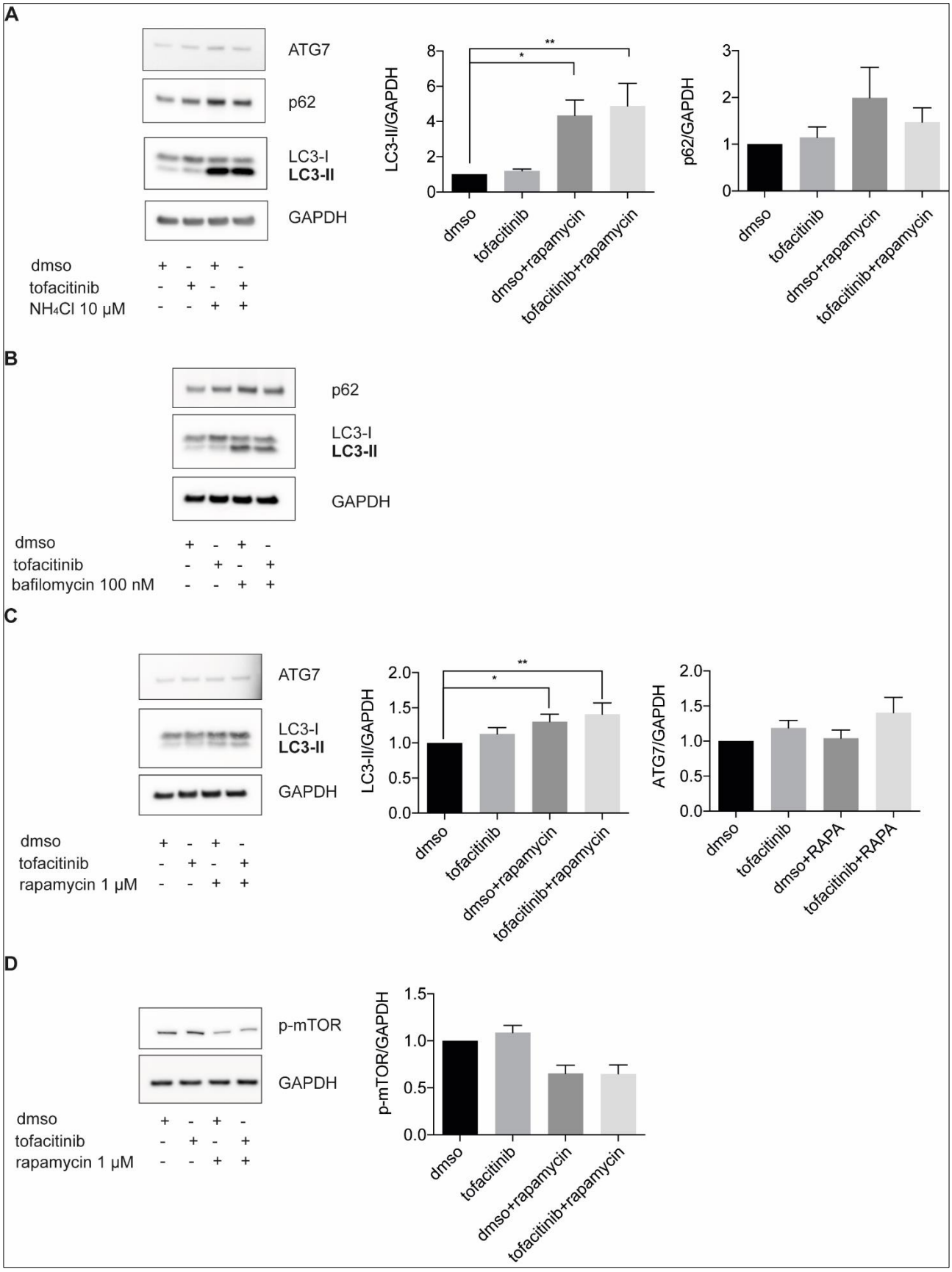

Figure 11. Tofacitinib does not alter autophagy flux in PsA FLS, while rapamycin acts as an autophagy inducer.

A: FLS cultures were performed for 24h in presence of the vehicle control DMSO or tofacitinib 1 µM, and NH_4Cl 10 µM was used for 6 hours before the end of the culture. Protein levels in cellular homogenates were analysed by western blot (representative western blot image and protein levels quantification). In presence of NH_4Cl, LC3-II levels significantly increased (DMSO: 1.000; DMSO+NH_4Cl: 4.35 ± 0.877, N=10, p=0.0020; tofacitinib+NH_4Cl: 4.886 ± 1.279, N=10, p=0.0020). A non-significant increase in ATG7 and p62 levels was enhanced, as well. Total cell lysates were resolved by NuPAGE LDS Sample Buffer (Thermo Fisher Scientific). Error bars indicate s.e.m. *: p=0.0020. **: p=0.0020. B: Representative western blot image of autophagy assessment following bafilomycin A1 100 nM (Sigma-Aldrich) for 2 hours. After bafilomycin A1, an increase in p62 and LC3-II levels was enhanced. Total cell lysates were resolved by NuPAGE LDS Sample Buffer (Thermo Fisher Scientific). C: FLS cultures were performed for 24h in presence of the vehicle control DMSO or tofacitinib 1 µM, and rapamycin 1 µM was added for 12 before the end of the culture. Protein levels in cellular homogenates were analysed by western blot (representative western blot image and protein levels quantification). In presence of rapamycin, a significant increase in LC3-II levels (DMSO: 1.000; DMSO+rapamycin: 1.303 ± 0.105, N=10, p= 0.0273; tofacitinib+ rapamycin: 1.409 ± 0.160, N=10, p=0.0371) was enhanced, as well as an increase in ATG7 levels. Total cell lysates were resolved by NuPAGE LDS Sample Buffer (Thermo Fisher Scientific). Error bars indicate s.e.m. *: p= 0.0273. **: p=0.0371. D: FLS cultures were performed for 24h in presence of the vehicle control DMSO or tofacitinib 1 µM, and rapamycin 1 µM was added for 12 before the end of the culture. Protein levels in cellular homogenates were analysed by western blot (representative western blot image and protein levels quantification). Rapamycin reduced p-mTOR levels (DMSO: 1.000; DMSO+rapamycin: 0.653 ± 0.088, N=5; tofacitinib+rapamycin: 0.650 ± 0.095, N=5). Total cell lysates were resolved by NuPAGE LDS Sample Buffer (Thermo Fisher Scientific). Error bars indicate s.e.m. GAPDH was used as loading control.

Abbreviations: PBMCs, peripheral blood mononuclear cells; ATG7, Autophagy Related 7; LC3-II, Microtubule-associated protein light chain 3-II; GAPDH, Glyceraldehyde-3-Phosphate Dehydrogenase; DMSO, dimethyl Sulfoxide; s.e.m., standard error of the mean; p-mTOR: phospho mammalian target of rapamycin.

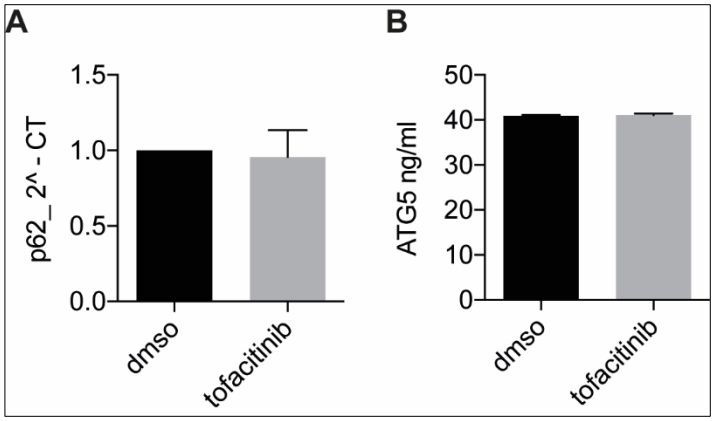

Figure 12. Tofacitinib does not increase p62 mRNA expression and ATG5 release in culture supernatants.

A: Total RNA was extracted from FLS treated with DMSO or tofacitinib using RNeasy Mini Kit (Qiagen). The expression of p62 was evaluated by Real Time RT-PCR using GAPDH cDNA for sample normalization (endogenous control). Quantitative PCR was carried out using Quantinova Sybr Green PCR Kit with the Rotor-Gene Q Real time PCR cycler. P62 mRNA levels were not significantly different between DMSO- and tofacitinib-treated FLS cultures (N=6, p= 0.8148). B: The autophagic marker ATG5 (MBS7209535) was quantified by ELISA in FLS cultures supernatants, following 24h of DMSO or tofacitinib treatment. Absorbance was measured in a microtiter plate spectrophometer. No significant increase was demonstrated following *in vitro* tofacitinib administration (DMSO: 972.2 ± 201.7; tofacitinib: 820.5 ± 178.4, N=15, p=0.5995). Results are expressed in ng/ml. Error bars indicate s.e.m.

Abbreviations: ATG5, Autophagy Related 5; FLS, fibroblast-like synoviocytes; DMSO, dimethyl Sulfoxide; GAPDH, Glyceraldehyde-3-Phosphate Dehydrogenase.

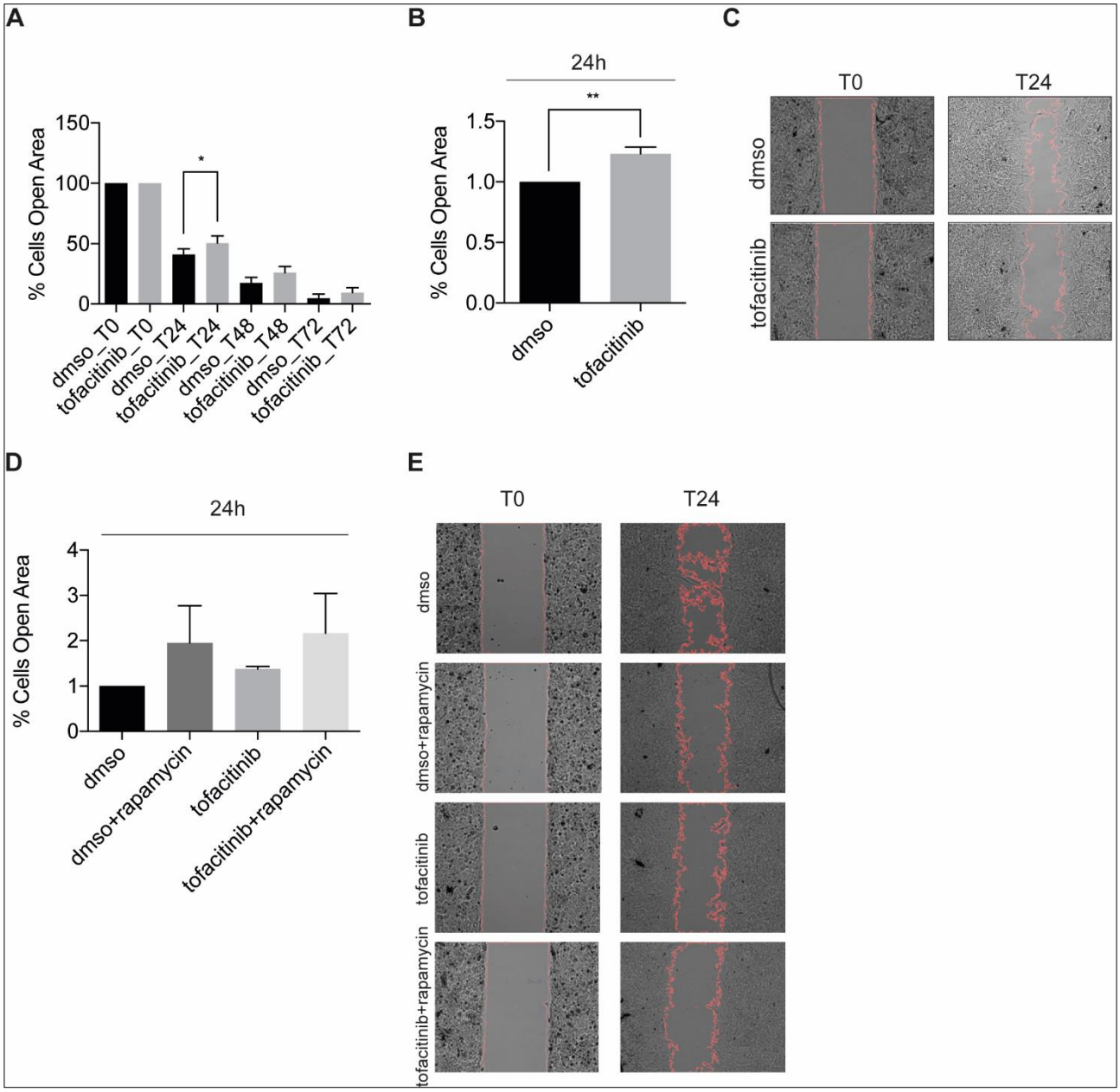

Figure 13. Tofacitinib reduces pro-invasive properties of PsA FLS.

A: Migration assay: After cells confluence, FLS migration was assessed in presence or absence of DMSO or tofacitinib 1 µM, and the percentage of the cells open area was compared at 0, 24, 48 and 72h. Tofacitinib significantly reduced the percentage of cells open area at 24h with respect to DMSO (DMSO: 40.990% ± 4.566; tofacitinib: 50.560% ± 5.897, N=13, p=0.0024), confirming a deceleration in FLS migration, with a tendency towards lower migration enhanced also at 48h and 72h. B: Schematic representation of the effect of tofacitinib on reduction of FLS migration at 24h with respect to DMSO (DMSO: 1.000; tofacitinib: 1.232 ± 0.055, N=13, p=0.0017). C: Representative images of FLS migration at T0 and T24 after *in vitro* DMSO or tofacitinib treatment. Images were visualized by using a microscope at 4x magnification. D: FLS migration assay in presence of DMSO, DMSO+rapamycin, tofacitinib, tofacitinib+rapamycin. A tendency towards

reduction in FLS migration at 24h was enhanced following *in vitro* rapamycin administration (DMSO: 1.000; DMSO+rapamycin: 1.951 ± 0.818; tofacitinib: 1.374 ± 0.060; tofacitinib+rapamycin: 2.167 ± 0.878, N=5). E: Representative images of FLS migration at T0 and T24 after *in vitro* DMSO, DMSO+rapamycin, tofacitinib, and tofacitinib+rapamycin treatment. Images were visualized by using a microscope at 4x magnification. Error bars indicate s.e.m.

Abbreviations: DMSO, dimethyl Sulfoxide; FLS, fibroblast-like synoviocytes.

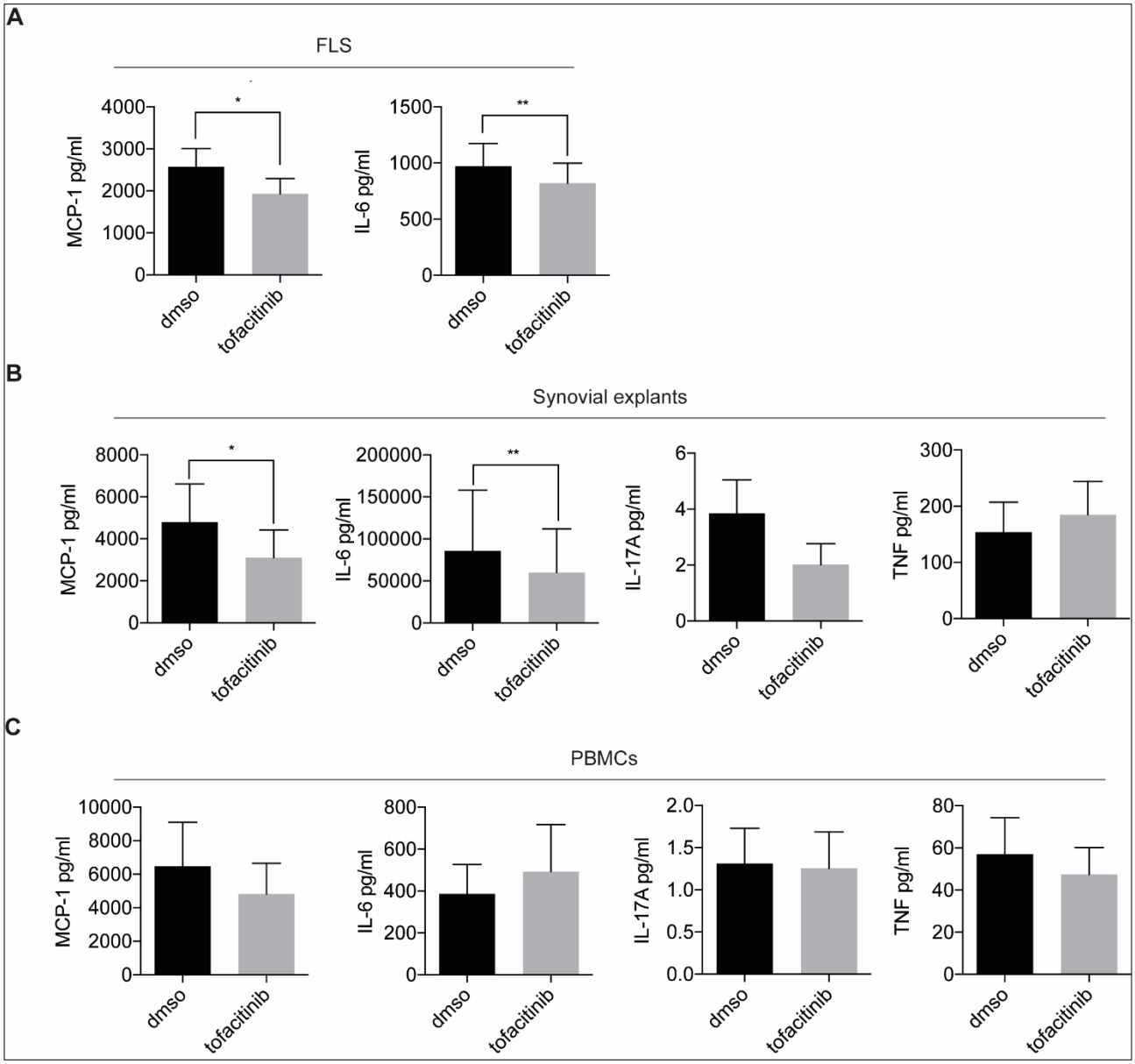

Figure 14. Tofacitinib reduces chemokines and cytokines release in cultures supernatants.

A: Production of MCP-1 and IL-6 in FLS cultures supernatants, as measured by ELISA. Tofacitinib reduced MCP-1 (DMSO: 2571 ± 439.0; tofacitinib: 1931 ± 366.7, N=15, p=0.0007) and IL-6 (DMSO: 972.2 ± 201.7; tofacitinib: 820.5 ± 178.4, N=15, p=0.0022) levels in FLS cultures. IL-17A and TNF were unremarkable. *:p=0.0007. **:p=0.0022. B: Production of MCP-1, IL-6, IL-17A and TNF in synovial explant cultures supernatants, as measured by ELISA. Tofacitinib reduced MCP-1 (DMSO: 4799 ± 1820; tofacitinib: 3113 ± 1313, N=7, p=0.0180), IL-6 (DMSO: 85844 ± 72319; tofacitinib: 59954 ± 51960, N=6, p=0.0277), and IL-17A (DMSO: 3.849 ± 1.200; tofacitinib: 2.016 ± 0.754, N=5) levels in synovial explants, with no significant effect on TNF production (DMSO: 153.9 ± 53.56; tofacitinib: 184.9 ± 59.19, N=7, p=0.0910). *:p=0.0180. **p=0.0277. C: Production of MCP-1, IL-6, IL-17A and TNF in PBMCs cultures supernatants, as measured by ELISA. Tofacitinib did not significantly affect MCP-1 (DMSO: 6483 ± 2624; tofacitinib: 4824 ± 1838, N=9,

p=0.1386), IL-6 (DMSO: 385.8 ± 141.8; tofacitinib: 492.4 ± 224.4,N=9, p=0.6784), IL_17A (DMSO: 1.312 ± 0.419; tofacitinib: 1.255 ± 0.433, N=6, p=0.9165), and TNF (DMSO: 57.00 ± 17.39; tofacitinib: 47.38 ± 12.77, N=9, p=0.2604) production levels in PBMCs cultures. Results are expressed in pg/ml. Error bars indicate s.e.m.

Abbreviations: FLS, fibroblast-like synoviocytes; MCP-1, Monocyte Chemoattractant Protein-1; IL, interleukin; DMSO, dimethyl Sulfoxide; TNF, tumour necrosis factor-alpha; PBMCs, peripheral blood mononuclear cells.

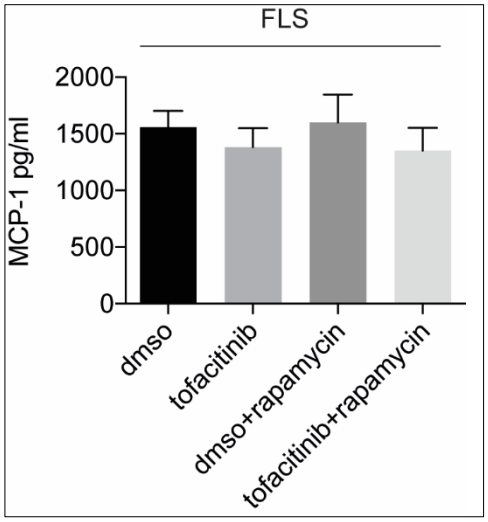

Figure 15. Rapamycin slightly reduces MCP-1 release in cultures supernatants.

Production of MCP-1 in FLS cultures supernatants, as measured by ELISA. Tofacitinib and tofacitinib+rapamycin slightly reduced MCP-1 production (DMSO: 1557 ± 144.6; tofacitinib: 1384 ± 164.4, p= 0.3125; DMSO+rapamycin: 1601 ± 245.8, p= 0.9453; tofacitinib+rapamycin: 1352 ± 201.0, p= 0.1953, N=8) in FLS cultures supernatants. Results are expressed in pg/ml. Error bars indicate s.e.m.

Abbreviations: FLS, fibroblast-like synoviocytes; MCP-1, Monocyte Chemoattractant Protein-1; DMSO, dimethyl Sulfoxide.

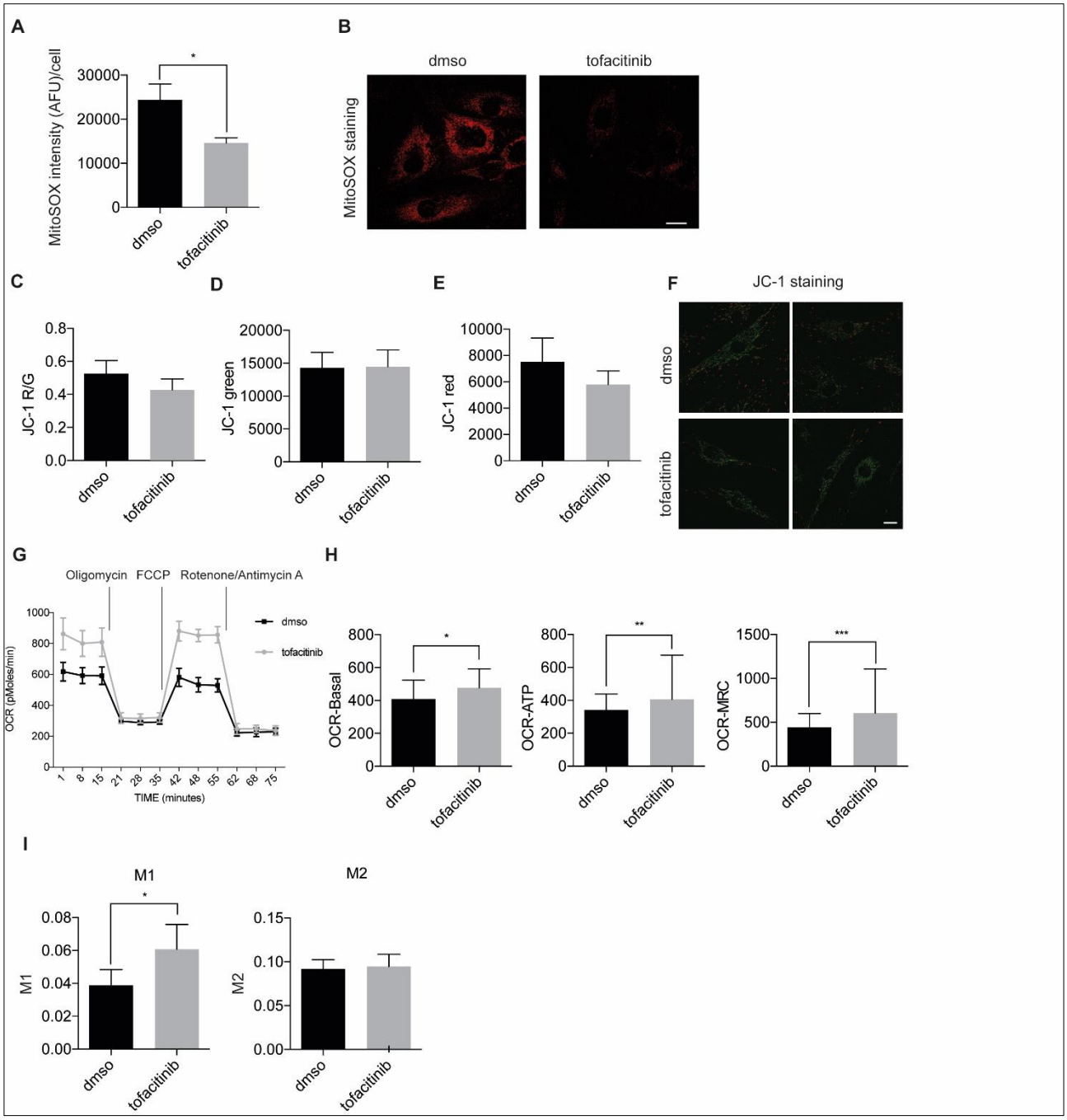

Figure 16. Tofacitinib improves mitochondrial function of PsA FLS and increases mitophagy.

A: MitoSOX™ Red Mitochondrial Superoxide Indicator was used to document the effect of tofacitinib over DMSO on intracellular ROS production. Tofacitinib significantly reduced the production of intracellular ROS (DMSO: 24384 ± 3583; tofacitinib: 14606 ± 1159, N=7, p=0.0180). Results are expressed in AFU/cell. *: p=0.0180. B: Representative images of FLS after MitoSOX staining, following DMSO and tofacitinib *in vitro* administration. C: A JC-1 staining was used to document the effect of tofacitinib over DMSO on mitochondrial potential (JC1 red/green). No effect of tofacitinib was retrieved on mitochondrial potential (DMSO: 0.527 ± 0.079; tofacitinib: 0.4271 ± 0.067, N=8, p=0.2626). D: JC-1 green. DMSO: 14278 ± 2362; tofacitinib: 14468 ± 2561, N=8, p=0.7794. E: JC-1 red. DMSO: 7525 ± 1801; tofacitinib: 5801 ± 1034, N=8, p=0.0929). F:

Representative images of FLS after JC-1 staining, following DMSO and tofacitinib *in vitro* administration. G: OCR, reflecting oxidative phosphorylation, was measured using the Agilent Seahorse XF Cell Mito Stress Test Kit, Agilent Technologies. The OCR was measured before and after treatment with the ATP synthase inhibitor oligomycin, the mitochondrial uncoupler FCCP, and the complex I/III inhibitors rotenone / antimycin A. Representative graph showing the effect of tofacitinib on FLS OCR. H: Quantification of OCR variations following DMSO or tofacitinib administration to PsA FLS. Tofacitinib increased basal OCR (DMSO: 409.7 ± 114.5; tofacitinib: 476.9 ± 115.4, N=7, p=0.0280), ATP production (DMSO: 342.7 ± 96.53; tofacitinib: 405.7 ± 101.7, N=7, p=0.0280) and MRC (DMSO: 442.2 ± 158.3; tofacitinib: 604.6 ± 190.8, N=7, p=0.0180). Results are expressed in pmoles/min. *: p=0.0280. **: p=0.0280. ***: p=0.0180. I: Co-localization of mitochondria and lysosomes in the presence of tofacitinib 1 µM or DMSO vehicle control. Mander's overlap coefficients (M1 and M2) were used to quantify the co-localization of mitochondria inside lysosomes and lysosomes inside mitochondria, respectively. M1 coefficient significantly increased following tofacitinib administration with respect to DMSO (DMSO: 0.0389 ± 0.0096; tofacitinib: 0.061 ± 0.015, N=7, p=0.0156). M2: DMSO: 0.092 ± 0,010; tofacitinib: 0.095 ± 0.014, N=7, p=0.8125. *: p=0.0156. A, B, C, images were acquired at 63x magnification using a Zeiss Axiovert 200 fluorescence microscope equipped with a back-illuminated CCD camera (Roper Scientific, Tucson, AZ) and processed by ImageJ software. Error bars indicate s.e.m.

Abbreviations: AFU, arbitrary fluorescence units; DMSO, dimethyl Sulfoxide; OCR: oxygen consumption rate; ROS: reactive oxygen species, FCCP: carbonyl cyanide-4-(trifluoromethoxy) phenylhydrazone.

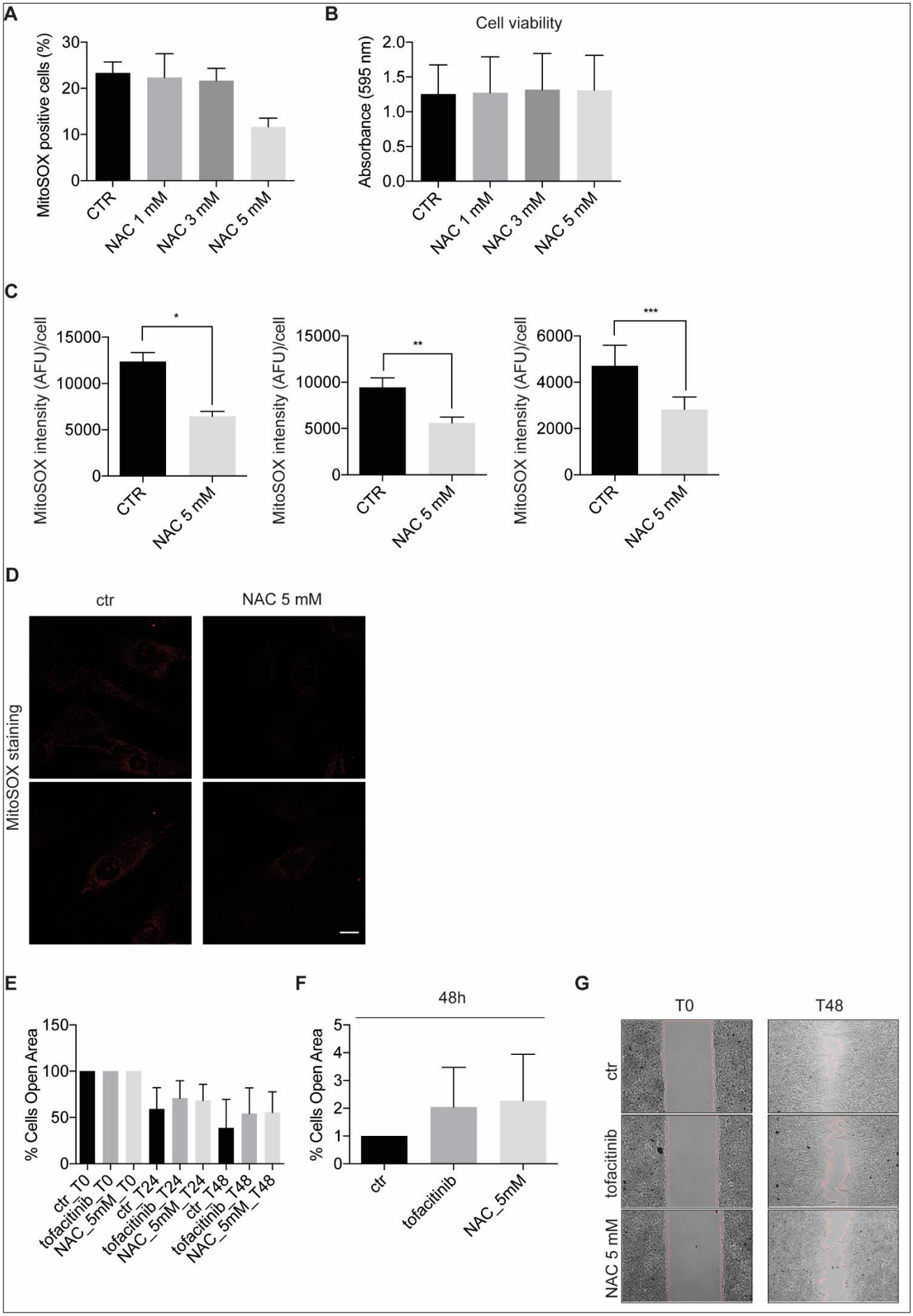
A
MitoSOX positive cells (%)
30
20
10
0
CTR
NAC 1 mM
NAC 3 mM
NAC 5 mM
B
Cell viability
Absorbance (595 nm)
2.0
1.5
1.0
0.5
0.0
CTR
NAC 1 mM
NAC 3 mM
NAC 5 mM
C
MitoSOX intensity (AFU)/cell
15000
10000
5000
0
*
CTR
NAC 5 mM
MitoSOX intensity (AFU)/cell
15000
10000
5000
0
**
CTR
NAC 5 mM
MitoSOX intensity (AFU)/cell
6000
4000
2000
0
***
CTR
NAC 5 mM
D
ctr
NAC 5 mM
MitoSOX staining
E
% Cells Open Area
150
100
50
0
ctr_T0
tofacitinib_T0
NAC_5mM_T0
ctr_T24
tofacitinib_T24
NAC_5mM_T24
ctr_T48
tofacitinib_T48
NAC_5mM_T48
F
48h
% Cells Open Area
5
4
3
2
1
0
ctr
tofacitinib
NAC_5mM
G
T0
T48
ctr
tofacitinib
NAC 5 mM

Figure 17. Antioxidant agent NAC reduces pro-invasive properties of PsA FLS.

A: Counting of MitoSOX™ Red Mitochondrial Superoxide Indicator-stained cells using a Tali image-based cytometer was used to select the proper dosage of the anti-oxidant agent NAC. A concentration of 5 mM of NAC for 48h was able to reduce intracellular ROS production by FLS with respect to vehicle control (N=3). Vehicle control: 23.33% ± 2.40. NAC 1 mM: 22.33% ± 5.18. NAC 3 mM: 21.67% ± 2.67. NAC 5 mM: 11.67% ± 1.86. B: To demonstrate if NAC determined an influence on cells viability, FLS seeded in 12-well plates were treated with NAC 1-3-5 mM for 48 hours. Then, the cells were washed with stained with 0.1% crystal violet. Crystal violet was dissolved with 1 mol/l acetic acid, and absorbance at 595 nm was measured (SPECTROstar Nano Microplate Reader, BMG LABTECH). No difference was highlighted among different dosages of NAC in terms of absorbance (N=3). Vehicle control: 1.254 ± 0.420. NAC 1 mM: 1.273 ± 0.516. NAC 3 mM: 1.319 ± 0.519. NAC 5 mM: 1.309 ± 0.503. C: MitoSOX™ Red Mitochondrial Superoxide Indicator-stained cells were acquired on a 63x magnification using a Zeiss Axiovert 200 fluorescence microscope. NAC 5 mM reduced intracellular ROS production in PsA FLS. The experiment was replicated 3 times (mean number of cells acquired: 24 for each condition). Results are expressed in AFU/cell. *: p<0.0001; **:p=0.0273; ***:p< 0.0001. E: Migration assay: After cells confluence, FLS migration was assessed in presence or absence of vehicle control, tofacitinib 1 µM, or NAC 5 mM, and the percentage of the cells open area was compared at 0, 24, and 48h. Tofacitinib and NAC reduced the percentage of cells open area at 48h with respect to vehicle control (vehicle control: 38.76 ± 15.38; tofacitinib: 54.22 ± 13.85; NAC: 55.39 ± 11.09, N=4), confirming a deceleration in FLS migration. B: Schematic representation of the effect of tofacitinib and NAC on reduction of FLS migration at 48h with respect to vehicle control (vehicle control: 1.000; tofacitinib: 2.048 ± 0.711; NAC: 2.273 ± 0.834, N=4). C: Representative images of FLS migration at T0 and T48 after *in vitro* vehicle control, tofacitinib or NAC treatment. Images were visualized by using a microscope at 4x magnification. Error bars indicate s.e.m.

Abbreviations: ROS: reactive oxygen species; CTR, vehicle control; NAC, N-Acetyl-L-Cysteine; AFU, arbitrary fluorescence units; PsA: psoriatic arthritis; FLS: fibroblast-like synoviocytes.

Bibliography

1 Scher JU, Ogdie A, Merola JF, *et al.* Preventing psoriatic arthritis: focusing on patients with psoriasis at increased risk of transition. *Nat Rev Rheumatol* Published Online First: 11 February 2019. doi:10.1038/s41584-019-0175-0

2 Zabotti A, Tinazzi I, Aydin SZ, *et al.* From Psoriasis to Psoriatic Arthritis: Insights from Imaging on the Transition to Psoriatic Arthritis and Implications for Arthritis Prevention. *Curr Rheumatol Rep* 2020;**22**. doi:10.1007/s11926-020-00891-x

3 Gladman D, Antoni C, Mease P, *et al.* Psoriatic arthritis: epidemiology, clinical features, course, and outcome. *Ann Rheum Dis* 2005;**64**:ii14–7. doi:10.1136/ard.2004.032482

4 Singh JA, Strand V. Health care utilization in patients with spondyloarthropathies. *Rheumatology (Oxford)* 2009;**48**:272–6. doi:10.1093/rheumatology/ken472

5 Veale DJ, Fearon U. The pathogenesis of psoriatic arthritis. *The Lancet* 2018;**391**:2273–84. doi:10.1016/S0140-6736(18)30830-4

6 Russell T, Bridgewood C, Rowe H, *et al.* Cytokine “fine tuning” of enthesis tissue homeostasis as a pointer to spondyloarthritis pathogenesis with a focus on relevant TNF and IL-17 targeted therapies. *Semin Immunopathol* Published Online First: 5 February 2021. doi:10.1007/s00281-021-00836-1

7 Silvagni E, Missiroli S, Perrone M, *et al.* From Bed to Bench and Back: TNF-α, IL-23/IL-17A, and JAK-Dependent Inflammation in the Pathogenesis of Psoriatic Synovitis. *Front Pharmacol* 2021;**12**:672515. doi:10.3389/fphar.2021.672515

8 Jadon DR, Stober C, Pennington SR, *et al.* Applying precision medicine to unmet clinical needs in psoriatic disease. *Nature Reviews Rheumatology* 2020;**16**:609–27. doi:10.1038/s41584-020-00507-9

9 Gossec L, Smolen JS, Ramiro S, *et al.* European League Against Rheumatism (EULAR) recommendations for the management of psoriatic arthritis with pharmacological therapies: 2015 update. *Annals of the Rheumatic Diseases* 2016;**75**:499–510. doi:10.1136/annrheumdis-2015-208337

10 Gossec L, Baraliakos X, Kerschbaumer A, *et al.* EULAR recommendations for the management of psoriatic arthritis with pharmacological therapies: 2019 update. *Annals of the Rheumatic Diseases* 2020;**79**:700–12. doi:10.1136/annrheumdis-2020-217159

11 Singh JA, Guyatt G, Ogdie A, *et al.* 2018 American College of Rheumatology/National Psoriasis Foundation Guideline for the Treatment of Psoriatic Arthritis. *Arthritis Care & Research* 2018;**0**. doi:10.1002/acr.23789

12 Humby F, Durez P, Buch MH, *et al.* Rituximab versus tocilizumab in anti-TNF inadequate responder patients with rheumatoid arthritis (R4RA): 16-week outcomes of a stratified, biopsy-driven, multicentre, open-label, phase 4 randomised controlled trial. *Lancet* 2021;**397**:305–17. doi:10.1016/S0140-6736(20)32341-2

13 Silvagni E, Sakellariou G, Bortoluzzi A, *et al.* One year in review 2021: novelties in the treatment of rheumatoid arthritis. *Clin Exp Rheumatol* 2021;**39**:705–20.

14 Kerschbaumer A, Smolen JS, Dougados M, *et al.* Pharmacological treatment of psoriatic arthritis: a systematic literature research for the 2019 update of the EULAR recommendations for the management of psoriatic arthritis. *Annals of the Rheumatic Diseases* 2020;**79**:778–86. doi:10.1136/annrheumdis-2020-217163

15 Coates LC, Kavanaugh A, Mease PJ, *et al.* Group for Research and Assessment of Psoriasis and Psoriatic Arthritis 2015 Treatment Recommendations for Psoriatic Arthritis. *Arthritis & Rheumatology* 2016;**68**:1060–71. doi:10.1002/art.39573

16 Deodhar A, Helliwell PS, Boehncke W-H, *et al.* Guselkumab in patients with active psoriatic arthritis who were biologic-naive or had previously received TNFα inhibitor treatment (DISCOVER-1): a double-blind, randomised, placebo-controlled phase 3 trial. *The Lancet* 2020;**395**:1115–25. doi:10.1016/S0140-6736(20)30265-8

17 Mease PJ, Rahman P, Gottlieb AB, *et al.* Guselkumab in biologic-naive patients with active psoriatic arthritis (DISCOVER-2): a double-blind, randomised, placebo-controlled phase 3 trial. *Lancet* 2020;**395**:1126–36. doi:10.1016/S0140-6736(20)30263-4

18 Gladman D, Rigby W, Azevedo VF, *et al.* Tofacitinib for Psoriatic Arthritis in Patients with an Inadequate Response to TNF Inhibitors. *New England Journal of Medicine* 2017;**377**:1525–36. doi:10.1056/NEJMoa1615977

19 Mease P, Hall S, FitzGerald O, *et al.* Tofacitinib or Adalimumab versus Placebo for Psoriatic Arthritis. *New England Journal of Medicine* 2017;**377**:1537–50. doi:10.1056/NEJMoa1615975

20 Mease PJ, Lertratanakul A, Anderson JK, *et al.* Upadacitinib for psoriatic arthritis refractory to biologics: SELECT-PsA 2. *Annals of the Rheumatic Diseases* 2021;**80**:312–20. doi:10.1136/annrheumdis-2020-218870

21 Clinical trial registration, KEEPsAKE 1. A Phase 3, Randomized, Double-Blind, Study Comparing Risankizumab to Placebo in Subjects With Active Psoriatic Arthritis (PsA) Who Have a History of Inadequate Response to or Intolerance to at Least One Disease Modifying Anti-Rheumatic Drug (DMARD) Therapy (KEEPsAKE 1). clinicaltrials.gov 2021. https://clinicaltrials.gov/ct2/show/NCT03675308 (accessed 18 Feb 2021).

22 Clinical trial registration, KEEPsAKE 2. A Phase 3, Randomized, Double-Blind Study Comparing Risankizumab to Placebo in Subjects With Active Psoriatic Arthritis Including Those Who Have a History of Inadequate Response or Intolerance to Biologic Therapy(Ies) (KEEPsAKE 2). clinicaltrials.gov 2021. https://clinicaltrials.gov/ct2/show/NCT03671148 (accessed 18 Feb 2021).

23 Östör A, Bosch FV den, Papp K, *et al.* Efficacy and safety of risankizumab for active psoriatic arthritis: 24-week results from the randomised, double-blind, phase 3 KEEPsAKE 2 trial. *Annals of the Rheumatic Diseases* Published Online First: 23 November 2021. doi:10.1136/annrheumdis-2021-221048

24 Clinical trial registration, INSPIRE 1. A Phase III, Randomized, Double-Blind, Single-Dose, Placebo-Controlled Study to Demonstrate the Efficacy and Safety of Tildrakizumab in Subjects With Active Psoriatic Arthritis I (INSPIRE 1). clinicaltrials.gov 2021. https://clinicaltrials.gov/ct2/show/NCT04314544 (accessed 18 Feb 2021).

25 Clinical trial registration, INSPIRE 2. A Phase III, Randomized, Double-Blind, Placebo-Controlled Study to Demonstrate the Efficacy and Safety of Tildrakizumab in Anti-TNF Naïve Subjects With Active Psoriatic Arthritis II (INSPIRE 2). clinicaltrials.gov 2021. https://clinicaltrials.gov/ct2/show/NCT04314531 (accessed 18 Feb 2021).

26 Mease PJ, Helliwell PS, Hjuler KF, *et al.* Brodalumab in psoriatic arthritis: results from the randomised phase III AMVISION-1 and AMVISION-2 trials. *Ann Rheum Dis* 2021;**80**:185–93. doi:10.1136/annrheumdis-2019-216835

27 Ritchlin CT, Kavanaugh A, Merola JF, *et al.* Bimekizumab in patients with active psoriatic arthritis: results from a 48-week, randomised, double-blind, placebo-controlled, dose-ranging phase 2b trial. *The Lancet* 2020;**395**:427–40. doi:10.1016/S0140-6736(19)33161-7

28 Clinical trial registration, PENGUIN 1. A Phase 3, Randomized, Double-blind, Placebo and Adalimumab-controlled Study to Evaluate the Efficacy and Safety of Filgotinib in Subjects With Active Psoriatic Arthritis Who Are Naive to Biologic DMARD Therapy. clinicaltrials.gov 2021. https://clinicaltrials.gov/ct2/show/NCT04115748 (accessed 18 Feb 2021).

29 Clinical trial registration, PENGUIN 2. A Phase 3, Randomized, Double-blind, Placebo-controlled Study to Evaluate the Efficacy and Safety of Filgotinib in Subjects With Active Psoriatic Arthritis Who Have an Inadequate Response or Are Intolerant to Biologic DMARD Therapy. clinicaltrials.gov 2021. https://clinicaltrials.gov/ct2/show/NCT04115839 (accessed 18 Feb 2021).

30 Silvagni E, Bortoluzzi A, Ciancio G, *et al.* Biological and synthetic target DMARDs in psoriatic arthritis. *Pharmacol Res* 2019;:104473. doi:10.1016/j.phrs.2019.104473

31 Chimenti MS, D'Antonio A, Conigliaro P, *et al.* An Update for the Clinician on Biologics for the Treatment of Psoriatic Arthritis. *Biologics* 2020;**14**:53–75. doi:10.2147/BTT.S260754

32 Haugeberg G, Michelsen B, Tengesdal S, *et al.* Ten years of follow-up data in psoriatic arthritis: results based on standardized monitoring of patients in an ordinary outpatient clinic in southern Norway. *Arthritis Research & Therapy* 2018;**20**. doi:10.1186/s13075-018-1659-z

33 Fagerli KM, Kearsley-Fleet L, Watson KD, *et al.* Long-term persistence of TNF-inhibitor treatment in patients with psoriatic arthritis. Data from the British Society for Rheumatology Biologics Register. *RMD Open* 2018;**4**. doi:10.1136/rmdopen-2017-000596

34 McInnes IB, Kavanaugh A, Gottlieb AB, *et al.* Efficacy and safety of ustekinumab in patients with active psoriatic arthritis: 1 year results of the phase 3, multicentre, double-blind, placebo-controlled PSUMMIT 1 trial. *Lancet* 2013;**382**:780–9.

35 Mease PJ, van der Heijde D, Ritchlin CT, *et al.* Ixekizumab, an interleukin-17A specific monoclonal antibody, for the treatment of biologic-naive patients with active psoriatic arthritis: results from the 24-week randomised, double-blind, placebo-controlled and active (adalimumab)-controlled period of the phase III trial SPIRIT-P1. *Ann Rheum Dis* 2017;**76**:79–87.

36 Ritchlin C, Rahman P, Kavanaugh A, *et al.* Efficacy and safety of the anti-IL-12/23 p40 monoclonal antibody, ustekinumab, in patients with active psoriatic arthritis despite conventional non-biological and biological anti-tumour necrosis factor therapy: 6-month and 1-year results of the phase 3, multicentre, double-blind, placebo-controlled, randomised PSUMMIT 2 trial. *Ann Rheum Dis* 2014;**73**:990–9. doi:10.1136/annrheumdis-2013-204655

37 Mease PJ, McInnes IB, Kirkham B, *et al.* Secukinumab Inhibition of Interleukin-17A in Patients with Psoriatic Arthritis. *N Engl J Med* 2015;**373**:1329–39. doi:10.1056/NEJMoa1412679

38 McInnes IB, Mease PJ, Kirkham B, *et al.* Secukinumab, a human anti-interleukin-17A monoclonal antibody, in patients with psoriatic arthritis (FUTURE 2): a randomised, double-blind, placebo-controlled, phase 3 trial. *The Lancet* 2015;**386**:1137–46. doi:10.1016/S0140-6736(15)61134-5

39 Nash P, Kirkham B, Okada M, *et al.* Ixekizumab for the treatment of patients with active psoriatic arthritis and an inadequate response to tumour necrosis factor inhibitors: results from the 24-week randomised, double-blind, placebo-controlled period of the SPIRIT-P2 phase 3 trial. *Lancet* 2017;**389**:2317–27.

40 Boutet M-A, Nerviani A, Gallo Afflitto G, *et al.* Role of the IL-23/IL-17 Axis in Psoriasis and Psoriatic Arthritis: The Clinical Importance of Its Divergence in Skin and Joints. *Int J Mol Sci* 2018;**19**. doi:10.3390/ijms19020530

41 Gladman DD, Orbai A-M, Gomez-Reino J, *et al.* Network Meta-Analysis of Tofacitinib, Biologic Disease-Modifying Antirheumatic Drugs, and Apremilast for the Treatment of Psoriatic Arthritis. *Curr Ther Res Clin Exp* 2020;**93**. doi:10.1016/j.curtheres.2020.100601

42 Ruyssen-Witrand A, Perry R, Watkins C, *et al.* Efficacy and safety of biologics in psoriatic arthritis: a systematic literature review and network meta-analysis. *RMD Open* 2020;**6**. doi:10.1136/rmdopen-2019-001117

43 McInnes IB, Behrens F, Mease PJ, *et al.* Secukinumab versus adalimumab for treatment of active psoriatic arthritis (EXCEED): a double-blind, parallel-group, randomised, active-controlled, phase 3b trial. *The Lancet* 2020;**395**:1496–505. doi:10.1016/S0140-6736(20)30564-X

44 Mease PJ, Smolen JS, Behrens F, *et al.* A head-to-head comparison of the efficacy and safety of ixekizumab and adalimumab in biological-naïve patients with active psoriatic arthritis: 24-week results of a randomised, open-label, blinded-assessor trial. *Annals of the Rheumatic Diseases* 2020;**79**:123–31. doi:10.1136/annrheumdis-2019-215386

45 Smolen JS, Mease P, Tahir H, *et al.* Multicentre, randomised, open-label, parallel-group study evaluating the efficacy and safety of ixekizumab versus adalimumab in patients with psoriatic arthritis naïve to biological disease-modifying antirheumatic drug: final results by week 52. *Annals of the Rheumatic Diseases* 2020;**79**:1310–9. doi:10.1136/annrheumdis-2020-217372

46 Coates LC, Kishimoto M, Gottlieb A, *et al.* Ixekizumab efficacy and safety with and without concomitant conventional disease-modifying antirheumatic drugs (cDMARDs) in biologic DMARD (bDMARD)-naïve patients with active psoriatic arthritis (PsA): results from SPIRIT-P1. *RMD Open* 2017;**3**. doi:10.1136/rmdopen-2017-000567

47 Ogdie A, Coates LC, Gladman DD. Treatment guidelines in psoriatic arthritis. *Rheumatology* 2020;**59**:i37–46. doi:10.1093/rheumatology/kez383

48 Ritchlin CT, Pennington SR, Reynolds NJ, *et al.* Moving Toward Precision Medicine in Psoriasis and Psoriatic Arthritis. *J Rheumatol Suppl* 2020;**96**:19–24. doi:10.3899/jrheum.200122

49 Miyagawa I, Nakayamada S, Nakano K, *et al.* Precision medicine using different biological DMARDs based on characteristic phenotypes of peripheral T helper cells in psoriatic arthritis. *Rheumatology* Published Online First: 2 April 2018. doi:10.1093/rheumatology/key069

50 Leijten EF, Radstake TR, McInnes IB, *et al.* Limits of traditional evidence-based medicine methodologies exemplified by the novel era in psoriatic arthritis drug development. *Expert Review of Clinical Immunology* 2019;**0**:null. doi:10.1080/1744666X.2019.1580144

51 Pitzalis C, Choy EHS, Buch MH. Transforming clinical trials in rheumatology: towards patient-centric precision medicine. *Nat Rev Rheumatol* Published Online First: 4 September 2020. doi:10.1038/s41584-020-0491-4

52 Generali E, Scirè CA, Favalli EG, *et al.* Biomarkers in psoriatic arthritis: a systematic literature review. *Expert Review of Clinical Immunology* 2016;**12**:651–60. doi:10.1586/1744666X.2016.1147954

53 Mahmood F, Coates LC, Helliwell PS. Current concepts and unmet needs in psoriatic arthritis. *Clin Rheumatol* 2018;**37**:297–305. doi:10.1007/s10067-017-3908-y

54 Mahendran S, Chandran V. Exploring the Psoriatic Arthritis Proteome in Search of Novel Biomarkers. *Proteomes* 2018;**6**:5. doi:10.3390/proteomes6010005

55 O'Rielly DD, Jani M, Rahman P, *et al.* The Genetics of Psoriasis and Psoriatic Arthritis. *J Rheumatol Suppl* 2019;**95**:46–50. doi:10.3899/jrheum.190119

56 Ovejero-Benito MC, Muñoz-Aceituno E, Reolid A, *et al.* Polymorphisms associated with anti-TNF drugs response in patients with psoriasis and psoriatic arthritis. *J Eur Acad Dermatol Venereol* 2019;**33**:e175–7. doi:10.1111/jdv.15431

57 Fabris M, Quartuccio L, Fabro C, *et al.* The -308 TNFα and the -174 IL-6 promoter polymorphisms associate with effective anti-TNFα treatment in seronegative spondyloarthritis. *Pharmacogenomics J* 2016;**16**:238–42. doi:10.1038/tpj.2015.49

58 Murdaca G, Gulli R, Spanò F, *et al.* TNF-α gene polymorphisms: association with disease susceptibility and response to anti-TNF-α treatment in psoriatic arthritis. *J Invest Dermatol* 2014;**134**:2503–9. doi:10.1038/jid.2014.123

59 Ovejero-Benito MC, Reolid A, Sánchez-Jiménez P, *et al.* Histone modifications associated with biological drug response in moderate-to-severe psoriasis. *Experimental Dermatology* 2018;**27**:1361–71. doi:10.1111/exd.13790

60 Dand N, Duckworth M, Baudry D, *et al.* HLA-C*06:02 genotype is a predictive biomarker of biologic treatment response in psoriasis. *J Allergy Clin Immunol* 2019;**143**:2120–30. doi:10.1016/j.jaci.2018.11.038

61 Londono J, Romero-Sanchez MC, Torres VG, *et al.* The association between serum levels of potential biomarkers with the presence of factors related to the clinical activity and poor prognosis in spondyloarthritis. *Rev Bras Reumatol* 2012;**52**:536–44.

62 Raychaudhuri SP, Raychaudhuri SK. Mechanistic rationales for targeting interleukin-17A in spondyloarthritis. *Arthritis Res Ther* 2017;**19**. doi:10.1186/s13075-017-1249-5

63 Muramatsu S, Kubo R, Nishida E, *et al.* Serum interleukin-6 levels in response to biologic treatment in patients with psoriasis. *Mod Rheumatol* 2017;**27**:137–41. doi:10.3109/14397595.2016.1174328

64 Chandran V, Shen H, Pollock RA, *et al.* Soluble biomarkers associated with response to treatment with tumor necrosis factor inhibitors in psoriatic arthritis. *J Rheumatol* 2013;**40**:866–71. doi:10.3899/jrheum.121162

65 Hellman U, Engström-Laurent A, Larsson A, *et al.* Hyaluronan concentration and molecular mass in psoriatic arthritis: biomarkers of disease severity, resistance to treatment, and outcome. *Scand J Rheumatol* 2019;**48**:284–93. doi:10.1080/03009742.2019.1577490

66 Chimenti MS, Perricone C, Graceffa D, *et al.* Complement system in psoriatic arthritis: a useful marker in response prediction and monitoring of anti-TNF treatment. *Clin Exp Rheumatol* 2012;**30**:23–30.

67 Gratacós J, Casado E, Real J, *et al.* Prediction of major clinical response (ACR50) to infliximab in psoriatic arthritis refractory to methotrexate. *Ann Rheum Dis* 2007;**66**:493–7. doi:10.1136/ard.2006.060079

68 Kristensen LE, Gülfe A, Saxne T, *et al.* Efficacy and tolerability of anti-tumour necrosis factor therapy in psoriatic arthritis patients: results from the South Swedish Arthritis Treatment Group register. *Ann Rheum Dis* 2008;**67**:364–9. doi:10.1136/ard.2007.073544

69 Scrivo R, Giardino AM, Salvarani C, *et al.* An observational prospective study on predictors of clinical response at six months in patients with active psoriatic arthritis treated with golimumab. *Clin Exp Rheumatol* 2020;**38**:107–14.

70 Pedersen SJ, Hetland ML, Sørensen IJ, *et al.* Circulating levels of interleukin-6, vascular endothelial growth factor, YKL-40, matrix metalloproteinase-3, and total aggrecan in spondyloarthritis patients during 3 years of treatment with TNFα inhibitors. *Clin Rheumatol* 2010;**29**:1301–9. doi:10.1007/s10067-010-1528-x

71 Wagner CL, Visvanathan S, Elashoff M, *et al.* Markers of inflammation and bone remodelling associated with improvement in clinical response measures in psoriatic arthritis patients treated with golimumab. *Ann Rheum Dis* 2013;**72**:83–8. doi:10.1136/annrheumdis-2012-201697

72 Leipe J, Grunke M, Dechant C, *et al.* Role of Th17 cells in human autoimmune arthritis. *Arthritis & Rheumatism* 2010;**62**:2876–85. doi:10.1002/art.27622

73 Dolcino M, Ottria A, Barbieri A, *et al.* Gene Expression Profiling in Peripheral Blood Cells and Synovial Membranes of Patients with Psoriatic Arthritis. *PLoS One* 2015;**10**. doi:10.1371/journal.pone.0128262

74 Raychaudhuri SP, Raychaudhuri SK, Genovese MC. IL-17 receptor and its functional significance in psoriatic arthritis. *Molecular and Cellular Biochemistry* 2012;**359**:419–29. doi:10.1007/s11010-011-1036-6

75 Menon B, Gullick NJ, Walter GJ, *et al.* Interleukin-17+CD8+ T Cells Are Enriched in the Joints of Patients With Psoriatic Arthritis and Correlate With Disease Activity and Joint Damage Progression. *Arthritis Rheumatol* 2014;**66**:1272–81. doi:10.1002/art.38376

76 van Kuijk AWR, Tak PP. Synovitis in Psoriatic Arthritis: Immunohistochemistry, Comparisons With Rheumatoid Arthritis, and Effects of Therapy. *Curr Rheumatol Rep* 2011;**13**:353–9. doi:10.1007/s11926-011-0181-y

77 Alivernini S, Tolusso B, Petricca L, *et al.* Synovial Predictors of Differentiation to Definite Arthritis in Patients With Seronegative Undifferentiated Peripheral Inflammatory Arthritis: microRNA Signature, Histological, and Ultrasound Features. *Front Med (Lausanne)* 2018;**5**. doi:10.3389/fmed.2018.00186

78 Kruithof E, Baeten D, De Rycke L, *et al.* Synovial histopathology of psoriatic arthritis, both oligo- and polyarticular, resembles spondyloarthropathy more than it does rheumatoid arthritis. *Arthritis Res Ther* 2005;**7**:R569–80. doi:10.1186/ar1698

79 Fromm S, Cunningham CC, Dunne MR, *et al.* Enhanced angiogenic function in response to fibroblasts from psoriatic arthritis synovium compared to rheumatoid arthritis. *Arthritis Res Ther* 2019;**21**:297. doi:10.1186/s13075-019-2088-3

80 Ambarus CA, Noordenbos T, de Hair MJ, *et al.* Intimal lining layer macrophages but not synovial sublining macrophages display an IL-10 polarized-like phenotype in chronic synovitis. *Arthritis Res Ther* 2012;**14**:R74. doi:10.1186/ar3796

81 Rycke LD, Baeten D, Foell D, *et al.* Differential expression and response to anti-TNFα treatment of infiltrating versus resident tissue macrophage subsets in autoimmune arthritis. *The Journal of Pathology* 2005;**206**:17–27. doi:10.1002/path.1758

82 Noordenbos T, Yeremenko N, Gofita I, *et al.* Interleukin-17-positive mast cells contribute to synovial inflammation in spondylarthritis. *Arthritis & Rheumatism* 2012;**64**:99–109. doi:10.1002/art.33396

83 Curran SA, FitzGerald OM, Costello PJ, *et al.* Nucleotide Sequencing of Psoriatic Arthritis Tissue before and during Methotrexate Administration Reveals a Complex Inflammatory T Cell Infiltrate with Very Few Clones Exhibiting Features That Suggest They Drive the Inflammatory Process by Recognizing Autoantigens. *The Journal of Immunology* 2004;**172**:1935–44. doi:10.4049/jimmunol.172.3.1935

84 Penkava F, Velasco-Herrera MDC, Young MD, *et al.* Single-cell sequencing reveals clonal expansions of pro-inflammatory synovial CD8 T cells expressing tissue-homing receptors in psoriatic arthritis. *Nat Commun* 2020;**11**:4767. doi:10.1038/s41467-020-18513-6

85 Alivernini S, Bruno D, Tolusso B, *et al.* Differential synovial tissue biomarkers among psoriatic arthritis and rheumatoid factor/anti-citrulline antibody-negative rheumatoid arthritis. *Arthritis Research & Therapy* 2019;**21**:116. doi:10.1186/s13075-019-1898-7

86 Nerviani A, Ribera GL, Boutet MA, *et al.* Op0113 Histological and Molecular Portrait of the Synovial Tissue in Early Treatment-Naïve Psoriatic Arthritis in Comparison with Rheumatoid Arthritis. *Annals of the Rheumatic Diseases* 2019;**78**:130–1. doi:10.1136/annrheumdis-2019-eular.3634

87 Frasca L, Palazzo R, Chimenti MS, *et al.* Anti-LL37 Antibodies Are Present in Psoriatic Arthritis (PsA) Patients: New Biomarkers in PsA. *Front Immunol* 2018;**9**. doi:10.3389/fimmu.2018.01936

88 Rahimi H, Ritchlin CT. Altered Bone Biology in Psoriatic Arthritis. *Current Rheumatology Reports* 2012;**14**:349–57. doi:10.1007/s11926-012-0259-1

89 van Tok MN, van Duivenvoorde LM, Kramer I, *et al.* IL-17A Inhibition Diminishes Inflammation and New Bone Formation In Experimental Spondyloarthritis. *Arthritis & Rheumatology* Published Online First: 2 November 2018. doi:10.1002/art.40770

90 Codullo V, McInnes IB. Synovial Tissue Response to Treatment in Psoriatic Arthritis. *Open Rheumatol J* 2011;**5**:133–7. doi:10.2174/1874312901105010133

91 Gerlag DM, Tak PP. Novel approaches for the treatment of rheumatoid arthritis: lessons from the evaluation of synovial biomarkers in clinical trials. *Best Practice & Research Clinical Rheumatology* 2008;**22**:311–23. doi:10.1016/j.berh.2008.02.002

92 Sande MGH van de, Gerlag DM, Lodde BM, *et al.* Evaluating antirheumatic treatments using synovial biopsy: a recommendation for standardisation to be used in clinical trials. *Annals of the Rheumatic Diseases* 2011;**70**:423–7. doi:10.1136/ard.2010.139550

93 Pontifex EK, Gerlag DM, Gogarty M, *et al.* Change in CD3 positive T-cell expression in psoriatic arthritis synovium correlates with change in DAS28 and magnetic resonance imaging synovitis scores following initiation of biologic therapy - a single centre, open-label study. *Arthritis Res Ther* 2011;**13**:R7. doi:10.1186/ar3228

94 Kruithof E, De Rycke L, Vandooren B, *et al.* Identification of synovial biomarkers of response to experimental treatment in early-phase clinical trials in spondylarthritis. *Arthritis & Rheumatism* 2006;**54**:1795–804. doi:10.1002/art.21914

95 Goedkoop A, Kraan M, Teunissen M, *et al.* Early effects of tumour necrosis factor α blockade on skin and synovial tissue in patients with active psoriasis and psoriatic arthritis. *Ann Rheum Dis* 2004;**63**:769–73. doi:10.1136/ard.2003.018085

96 Cañete JD, Pablos JL, Sanmartí R, *et al.* Antiangiogenic effects of anti–tumor necrosis factor α therapy with infliximab in psoriatic arthritis. *Arthritis & Rheumatism* 2004;**50**:1636–41. doi:10.1002/art.20181

97 van Kuijk AWR, Gerlag DM, Vos K, *et al.* A prospective, randomised, placebo-controlled study to identify biomarkers associated with active treatment in psoriatic arthritis: effects of adalimumab treatment on synovial tissue. *Ann Rheum Dis* 2008;**68**:1303–9. doi:10.1136/ard.2008.091389

98 Collins ES, Butt AQ, Gibson DS, *et al.* A clinically based protein discovery strategy to identify potential biomarkers of response to anti-TNF-α treatment of psoriatic arthritis. *PROTEOMICS - Clinical Applications* 2016;**10**:645–62. doi:10.1002/prca.201500051

99 Ademowo OS, Hernandez B, Collins E, *et al.* Discovery and confirmation of a protein biomarker panel with potential to predict response to biological therapy in psoriatic arthritis. *Annals of the Rheumatic Diseases* 2016;**75**:234–41. doi:10.1136/annrheumdis-2014-205417

100 Smeets TJM, Kraan MC, van Loon ME, *et al.* Tumor necrosis factor ? blockade reduces the synovial cell infiltrate early after initiation of treatment, but apparently not by induction of apoptosis in synovial tissue. *Arthritis & Rheumatism* 2003;**48**:2155–62. doi:10.1002/art.11098

101 Baeten D, Kruithof E, Van den Bosch F, *et al.* Immunomodulatory effects of anti–tumor necrosis factor α therapy on synovium in spondylarthropathy: Histologic findings in eight patients from an open-label pilot study. *Arthritis & Rheumatism* 2001;**44**:186–95. doi:10.1002/1529-0131(200101)44:1<186::AID-ANR25>3.0.CO;2-B

102 Kruithof E, Baeten D, Van den Bosch F, *et al.* Histological evidence that infliximab treatment leads to downregulation of inflammation and tissue remodelling of the synovial membrane in spondyloarthropathy. *Ann Rheum Dis* 2005;**64**:529–36. doi:10.1136/ard.2003.018549

103 Goedkoop AY, Kraan MC, Picavet DI, *et al.* Deactivation of endothelium and reduction in angiogenesis in psoriatic skin and synovium by low dose infliximab therapy in combination with stable methotrexate therapy: a prospective single-centre study. *Arthritis Res Ther* 2004;**6**:R326–34. doi:10.1186/ar1182

104 Mens LJJ, Sande MGH, Menegatti S, *et al.* Brief Report: Interleukin-17 Blockade With Secukinumab in Peripheral Spondyloarthritis Impacts Synovial Immunopathology Without Compromising Systemic Immune Responses. *Arthritis & Rheumatology* 2018;**70**:1994–2002. doi:10.1002/art.40581

105 Chen S, Noordenbos T, Blijdorp I, *et al.* Histologic evidence that mast cells contribute to local tissue inflammation in peripheral spondyloarthritis by regulating interleukin-17A content. *Rheumatology (Oxford)* doi:10.1093/rheumatology/key331

106 Frommer K, Rehart S, Müller-Ladner U, *et al.* Thu0028 Comparison of Il-17a and Tnf Induced Cytokine Secretion by Rheumatoid and Psoriatic Arthritis Synovial Fibroblasts and Their Inhibition by Biologics. *Annals of the Rheumatic Diseases* 2019;**78**:281–2. doi:10.1136/annrheumdis-2019-eular.3321

107 Nielsen MA, Lomholt S, Mellemkjær A, *et al.* Responses to Cytokine Inhibitors Associated with Cellular Composition in Models of Immune-Mediated Inflammatory Arthritis. *ACR Open Rheumatology* 2020;**2**:3–10. doi:10.1002/acr2.11094

108 Szentpetery A, Heffernan E, Gogarty M, *et al.* Abatacept reduces synovial regulatory T-cell expression in patients with psoriatic arthritis. *Arthritis Research & Therapy* 2017;**19**. doi:10.1186/s13075-017-1364-3

109 Fiechter RH, de Jong HM, van Mens LJJ, *et al.* IL-12p40/IL-23p40 Blockade With Ustekinumab Decreases the Synovial Inflammatory Infiltrate Through Modulation of Multiple Signaling Pathways Including MAPK-ERK and Wnt. *Frontiers in Immunology* 2021;**12**:504. doi:10.3389/fimmu.2021.611656

110 Humby FC, Al Balushi F, Lliso G, *et al.* Can Synovial Pathobiology Integrate with Current Clinical and Imaging Prediction Models to Achieve Personalized Health Care in Rheumatoid Arthritis? *Frontiers in Medicine* 2017;**4**. doi:10.3389/fmed.2017.00041

111 Palladino MA, Bahjat FR, Theodorakis EA, *et al.* Anti-TNF-α therapies: the next generation. *Nature Reviews Drug Discovery* 2003;**2**:736–46. doi:10.1038/nrd1175

112 Croft M, Siegel RM. Beyond TNF: TNF superfamily cytokines as targets for the treatment of rheumatic diseases. *Nat Rev Rheumatol* 2017;**13**:217–33. doi:10.1038/nrrheum.2017.22

113 Tracey D, Klareskog L, Sasso EH, *et al.* Tumor necrosis factor antagonist mechanisms of action: A comprehensive review. *Pharmacology & Therapeutics* 2008;**117**:244–79. doi:10.1016/j.pharmthera.2007.10.001

114 Higuchi M, Aggarwal BB. TNF induces internalization of the p60 receptor and shedding of the p80 receptor. *J Immunol* 1994;**152**:3550–8.

115 Kuwano K, Hara N. Signal transduction pathways of apoptosis and inflammation induced by the tumor necrosis factor receptor family. *Am J Respir Cell Mol Biol* 2000;**22**:147–9. doi:10.1165/ajrcmb.22.2.f178

116 Hayden MS, Ghosh S. Regulation of NF-κB by TNF Family Cytokines. *Semin Immunol* 2014;**26**:253–66. doi:10.1016/j.smim.2014.05.004

117 Sedger LM, McDermott MF. TNF and TNF-receptors: From mediators of cell death and inflammation to therapeutic giants – past, present and future. *Cytokine & Growth Factor Reviews* 2014;**25**:453–72. doi:10.1016/j.cytogfr.2014.07.016

118 Robert M, Miossec P. IL-17 in Rheumatoid Arthritis and Precision Medicine: From Synovitis Expression to Circulating Bioactive Levels. *Frontiers in Medicine* 2019;**5**. doi:10.3389/fmed.2018.00364

119 Doyle MS, Collins ES, FitzGerald OM, *et al.* New insight into the functions of the interleukin-17 receptor adaptor protein Act1 in psoriatic arthritis. *Arthritis Res Ther* 2012;**14**:226. doi:10.1186/ar4071

120 Blijdorp IC, Menegatti S, Van Mens LJ, *et al.* IL-22-and GM-CSF-expressing but not IL-17A-expressing group 3 innate lymphoid cells are expanded in the inflamed spondyloarthritis joint. *Arthritis & Rheumatology* 2018.

121 Schwartz DM, Bonelli M, Gadina M, *et al.* Type I/II cytokines, JAKs, and new strategies for treating autoimmune diseases. *Nat Rev Rheumatol* 2016;**12**:25–36. doi:10.1038/nrrheum.2015.167

122 Gao W, McGarry T, Orr C, *et al.* Tofacitinib regulates synovial inflammation in psoriatic arthritis, inhibiting STAT activation and induction of negative feedback inhibitors. *Ann Rheum Dis* 2016;**75**:311–5. doi:10.1136/annrheumdis-2014-207201

123 O'Brien A, Hanlon MM, Marzaioli V, *et al.* Targeting JAK-STAT Signalling Alters PsA Synovial Fibroblast Pro-Inflammatory and Metabolic Function. *Front Immunol* 2021;**12**:672461. doi:10.3389/fimmu.2021.672461

124 McGarry T, Orr C, Wade S, *et al.* JAK/STAT Blockade Alters Synovial Bioenergetics, Mitochondrial Function, and Proinflammatory Mediators in Rheumatoid Arthritis. *Arthritis & Rheumatology* 2018;**70**:1959–70. doi:10.1002/art.40569

125 Ahn JK, Kim S, Hwang J, *et al.* GC/TOF-MS-based metabolomic profiling in cultured fibroblast-like synoviocytes from rheumatoid arthritis. *Joint Bone Spine* 2016;**83**:707–13. doi:10.1016/j.jbspin.2015.11.009

126 Ng CT, Biniecka M, Kennedy A, *et al.* Synovial tissue hypoxia and inflammation in vivo. *Ann Rheum Dis* 2010;**69**:1389–95. doi:10.1136/ard.2009.119776

127 Biniecka M, Canavan M, McGarry T, *et al.* Dysregulated bioenergetics: a key regulator of joint inflammation. *Ann Rheum Dis* 2016;**75**:2192–200. doi:10.1136/annrheumdis-2015-208476

128 Harty LC, Biniecka M, O'Sullivan J, *et al.* Mitochondrial mutagenesis correlates with the local inflammatory environment in arthritis. *Annals of the Rheumatic Diseases* 2012;**71**:582–8. doi:10.1136/annrheumdis-2011-200245

129 Vaamonde-García C, López-Armada MJ. Role of mitochondrial dysfunction on rheumatic diseases. *Biochemical Pharmacology* 2019;**165**:181–95. doi:10.1016/j.bcp.2019.03.008

130 Biniecka M, Fox E, Gao W, *et al.* Hypoxia induces mitochondrial mutagenesis and dysfunction in inflammatory arthritis. *Arthritis & Rheumatism* 2011;**63**:2172–82. doi:10.1002/art.30395

131 Zeng L, Yu G, Yang K, *et al.* The Efficacy of Antioxidative Stress Therapy on Oxidative Stress Levels in Rheumatoid Arthritis: A Systematic Review and Meta-analysis of Randomized Controlled Trials. *Oxidative Medicine and Cellular Longevity* 2021;**2021**:1–30. doi:10.1155/2021/3302886

132 Giorgi C, Bouhamida E, Danese A, *et al.* Relevance of Autophagy and Mitophagy Dynamics and Markers in Neurodegenerative Diseases. *Biomedicines* 2021;**9**:149. doi:10.3390/biomedicines9020149

133 Missiroli S, Bonora M, Patergnani S, *et al.* PML at Mitochondria-Associated Membranes Is Critical for the Repression of Autophagy and Cancer Development. *Cell Rep* 2016;**16**:2415–27. doi:10.1016/j.celrep.2016.07.082

134 Vomero M, Barbati C, Colasanti T, *et al.* Autophagy and Rheumatoid Arthritis: Current Knowledges and Future Perspectives. *Frontiers in Immunology* 2018;**9**. doi:10.3389/fimmu.2018.01577

135 Yin H, Wu H, Chen Y, *et al.* The Therapeutic and Pathogenic Role of Autophagy in Autoimmune Diseases. *Front Immunol* 2018;**9**. doi:10.3389/fimmu.2018.01512

136 Klionsky DJ, Abdelmohsen K, Abe A, *et al.* Guidelines for the use and interpretation of assays for monitoring autophagy (3rd edition). *Autophagy* 2016;**12**:1–222. doi:10.1080/15548627.2015.1100356

137 Karami J, Aslani S, Jamshidi A, *et al.* Genetic implications in the pathogenesis of rheumatoid arthritis; an updated review. *Gene* 2019;**702**:8–16. doi:10.1016/j.gene.2019.03.033

138 Sabir JSM, El Omri A, Banaganapalli B, *et al.* Dissecting the Role of NF-κb Protein Family and Its Regulators in Rheumatoid Arthritis Using Weighted Gene Co-Expression Network. *Frontiers in Genetics* 2019;**10**. doi:10.3389/fgene.2019.01163

139 Messemaker TC, Huizinga TW, Kurreeman F. Immunogenetics of rheumatoid arthritis: Understanding functional implications. *J Autoimmun* 2015;**64**:74–81. doi:10.1016/j.jaut.2015.07.007

140 Veyssiere M, Perea J, Michou L, *et al.* A novel nonsense variant in SUPT20H gene associated with Rheumatoid Arthritis identified by Whole Exome Sequencing of multiplex families. *PLoS One* 2019;**14**:e0213387. doi:10.1371/journal.pone.0213387

141 Hafkenscheid L, de Moel E, Smolik I, *et al.* N-Linked Glycans in the Variable Domain of IgG Anti–Citrullinated Protein Antibodies Predict the Development of Rheumatoid Arthritis. *Arthritis Rheumatol* 2019;**71**:1626–33. doi:10.1002/art.40920

142 McInnes IB, Schett G. Pathogenetic insights from the treatment of rheumatoid arthritis. *The Lancet* 2017;**389**:2328–37.

143 Sugawara E, Kato M, Kudo Y, *et al.* Autophagy promotes citrullination of VIM (vimentin) and its interaction with major histocompatibility complex class II in synovial fibroblasts. *Autophagy* 2020;**16**:946–55. doi:10.1080/15548627.2019.1664144

144 Sorice M, Iannuccelli C, Manganelli V, *et al.* Autophagy generates citrullinated peptides in human synoviocytes: a possible trigger for anti-citrullinated peptide antibodies. *Rheumatology (Oxford)* 2016;**55**:1374–85. doi:10.1093/rheumatology/kew178

145 Ireland JM, Unanue ER. Autophagy in antigen-presenting cells results in presentation of citrullinated peptides to CD4 T cells. *J Exp Med* 2011;**208**:2625–32. doi:10.1084/jem.20110640

146 van Loosdregt J, Rossetti M, Spreafico R, *et al.* Increased autophagy in CD4 $^{+}$ T cells of rheumatoid arthritis patients results in T-cell hyperactivation and apoptosis resistance: Immunomodulation and Immune Therapies. *European Journal of Immunology* 2016;**46**:2862–70. doi:10.1002/eji.201646375

147 Chen Y-M, Chang C-Y, Chen H-H, *et al.* Association between autophagy and inflammation in patients with rheumatoid arthritis receiving biologic therapy. *Arthritis Research & Therapy* 2018;**20**. doi:10.1186/s13075-018-1763-0

148 Yang Z, Fujii H, Mohan SV, *et al.* Phosphofructokinase deficiency impairs ATP generation, autophagy, and redox balance in rheumatoid arthritis T cells. *J Exp Med* 2013;**210**:2119–34. doi:10.1084/jem.20130252

149 You S, Koh JH, Leng L, *et al.* Review: The Tumor-Like Phenotype of Rheumatoid Synovium: Molecular Profiling and Prospects for Precision Medicine. *Arthritis & Rheumatology* 2018;**70**:637–52. doi:10.1002/art.40406

150 Fearon U, Hanlon MM, Wade SM, *et al.* Altered metabolic pathways regulate synovial inflammation in rheumatoid arthritis. *Clinical and Experimental Immunology* 2019;**197**:170–80. doi:10.1111/cei.13228

151 Nygaard G, Firestein GS. Restoring synovial homeostasis in rheumatoid arthritis by targeting fibroblast-like synoviocytes. *Nature Reviews Rheumatology* Published Online First: 2020. doi:10.1038/s41584-020-0413-5

152 Zhu L, Wang H, Wu Y, *et al.* The Autophagy Level Is Increased in the Synovial Tissues of Patients with Active Rheumatoid Arthritis and Is Correlated with Disease Severity. *Mediators Inflamm* 2017;**2017**. doi:10.1155/2017/7623145

153 Xu K, Xu P, Yao J-F, *et al.* Reduced apoptosis correlates with enhanced autophagy in synovial tissues of rheumatoid arthritis. *Inflammation Research* 2013;**62**:229–37. doi:10.1007/s00011-012-0572-1

154 Vomero M, Manganelli V, Barbati C, *et al.* Reduction of autophagy and increase in apoptosis correlates with a favorable clinical outcome in patients with rheumatoid arthritis treated with anti-TNF drugs. *Arthritis Res Ther* 2019;**21**. doi:10.1186/s13075-019-1818-x

155 Chang L, Feng X, Gao W. Proliferation of Rheumatoid Arthritis Fibroblast-Like Synoviocytes Is Enhanced by IL-17-mediated Autophagy Through STAT3 Activation. *Connect Tissue Res* 2019;**60**:358–66. doi:10.1080/03008207.2018.1552266

156 Kim EK, Kwon J-E, Lee S-Y, *et al.* IL-17-mediated mitochondrial dysfunction impairs apoptosis in rheumatoid arthritis synovial fibroblasts through activation of autophagy. *Cell Death & Disease* 2018;**8**:e2565–e2565. doi:10.1038/cddis.2016.490

157 Connor AM, Mahomed N, Gandhi R, *et al.* TNFα modulates protein degradation pathways in rheumatoid arthritis synovial fibroblasts. *Arthritis Res Ther* 2012;**14**:R62. doi:10.1186/ar3778

158 Kato M, Ospelt C, Gay RE, *et al.* Dual Role of Autophagy in Stress-Induced Cell Death in Rheumatoid Arthritis Synovial Fibroblasts. *Arthritis & Rheumatology* 2014;**66**:40–8. doi:10.1002/art.38190

159 Wang X, Chen Z, Fan X, *et al.* Inhibition of DNM1L and mitochondrial fission attenuates inflammatory response in fibroblast-like synoviocytes of rheumatoid arthritis. *J Cell Mol Med* 2020;**24**:1516–28. doi:10.1111/jcmm.14837

160 Karonitsch T, Kandasamy RK, Kartnig F, *et al.* mTOR Senses Environmental Cues to Shape the Fibroblast-like Synoviocyte Response to Inflammation. *Cell Rep* 2018;**23**:2157–67. doi:10.1016/j.celrep.2018.04.044

161 Laragione T, Gulko PS. mTOR Regulates the Invasive Properties of Synovial Fibroblasts in Rheumatoid Arthritis. *Mol Med* 2010;**16**:352–8. doi:10.2119/molmed.2010.00049

162 Perl A. Activation of mTOR (mechanistic target of rapamycin) in rheumatic diseases. *Nature reviews Rheumatology* 2016;**12**:169. doi:10.1038/nrrheum.2015.172

163 Lee WS, Kato M, Sugawara E, *et al.* Optineurin in Synovial Fibroblasts Plays a Protective Role against Joint Destructions in Rheumatoid Arthritis. *Arthritis Rheumatol* Published Online First: 20 April 2020. doi:10.1002/art.41290

164 Laha D, Deb M, Das H. KLF2 (kruppel-like factor 2 [lung]) regulates osteoclastogenesis by modulating autophagy. *Autophagy* 2019;**15**:2063–75. doi:10.1080/15548627.2019.1596491

165 Varshney P, Saini N. PI3K/AKT/mTOR activation and autophagy inhibition plays a key role in increased cholesterol during IL-17A mediated inflammatory response in psoriasis. *Biochimica et Biophysica Acta (BBA) - Molecular Basis of Disease* 2018;**1864**:1795–803. doi:10.1016/j.bbadis.2018.02.003

166 Lee H-M, Shin D-M, Yuk J-M, *et al.* Autophagy Negatively Regulates Keratinocyte Inflammatory Responses via Scaffolding Protein p62/SQSTM1. *The Journal of Immunology* 2011;**186**:1248–58. doi:10.4049/jimmunol.1001954

167 Bocheńska K, Moskot M, Malinowska M, *et al.* Lysosome alterations in the human epithelial cell line hacat and skin specimens: Relevance to psoriasis. *International Journal of Molecular Sciences* 2019;**20**. doi:10.3390/ijms20092255

168 Müller G, Lübow C, Weindl G. Lysosomotropic beta blockers induce oxidative stress and IL23A production in Langerhans cells. *Autophagy* 2019;:1–16. doi:10.1080/15548627.2019.1686728

169 Wang Z, Zhou H, Zheng H, *et al.* Autophagy-based unconventional secretion of HMGB1 by keratinocytes plays a pivotal role in psoriatic skin inflammation. *Autophagy* 2020;:1–24. doi:10.1080/15548627.2020.1725381

170 Douroudis K, Kingo K, Traks T, *et al.* Polymorphisms in the ATG16L1 gene are associated with psoriasis vulgaris. *Acta Derm Venereol* 2012;**92**:85–7. doi:10.2340/00015555-1183

171 Wenink MH, Santegoets KCM, Butcher J, *et al.* Impaired dendritic cell proinflammatory cytokine production in psoriatic arthritis. *Arthritis & Rheumatism* 2011;**63**:3313–22. doi:10.1002/art.30577

172 Pedersen SJ, Maksymowych WP. The Pathogenesis of Ankylosing Spondylitis: an Update. *Curr Rheumatol Rep* 2019;**21**:58. doi:10.1007/s11926-019-0856-3

173 Romero-López JP, Domínguez-López ML, Burgos-Vargas R, *et al.* Stress proteins in the pathogenesis of spondyloarthritis. *Rheumatology International* 2019;**39**:595–604. doi:10.1007/s00296-018-4070-9

174 Ciccia F, Accardo-Palumbo A, Rizzo A, *et al.* Evidence that autophagy, but not the unfolded protein response, regulates the expression of IL-23 in the gut of patients with Ankylosing Spondylitis and subclinical gut inflammation. *Ann Rheum Dis* 2014;**73**:1566–74. doi:10.1136/annrheumdis-2012-202925

175 Neerinckx B, Carter S, Lories R. IL-23 expression and activation of autophagy in synovium and PBMCs of HLA-B27 positive patients with ankylosing spondylitis. Response to: 'Evidence that autophagy, but not the unfolded protein response, regulates the expression of IL-23 in the gut of patients with ankylosing spondylitis and subclinical gut inflammation' by Ciccia et al. *Annals of the Rheumatic Diseases* 2014;**73**:e68–e68. doi:10.1136/annrheumdis-2014-206277

176 Wang Y, Luo J, Wang X, *et al.* MicroRNA-199a-5p Induced Autophagy and Inhibits the Pathogenesis of Ankylosing Spondylitis by Modulating the mTOR Signaling ***via*** Directly Targeting Ras Homolog Enriched in Brain (Rheb). *Cellular Physiology and Biochemistry* 2017;**42**:2481–91. doi:10.1159/000480211

177 Chen S, van Tok MN, Knaup VL, *et al.* mTOR Blockade by Rapamycin in Spondyloarthritis: Impact on Inflammation and New Bone Formation in vitro and in vivo. *Frontiers in Immunology* 2020;**10**. doi:10.3389/fimmu.2019.02344

178 Cheng Z, Yi Y, Xie S, *et al.* The effect of the JAK2 inhibitor TG101209 against T cell acute lymphoblastic leukemia (T-ALL) is mediated by inhibition of JAK-STAT signaling and activation of the crosstalk between apoptosis and autophagy signaling. *Oncotarget* 2017;**8**:106753–63. doi:10.18632/oncotarget.22053

179 Liu C, Arnold R, Henriques G, *et al.* Inhibition of JAK-STAT Signaling with Baricitinib Reduces Inflammation and Improves Cellular Homeostasis in Progeria Cells. *Cells* 2019;**8**. doi:10.3390/cells8101276

180 Pandey R, Bakay M, Strenkowski BP, *et al.* JAK/STAT inhibitor therapy partially rescues the lipodystrophic autoimmune phenotype in Clec16a KO mice. *Sci Rep* 2021;**11**:7372. doi:10.1038/s41598-021-86493-8

181 Vomero M, Caliste M, Barbati C, *et al.* Ab0145 the Inhibition of Jak Pathway Was Associated with Reduction of Autophagy in Synoviocytes from Rheumatoid Arthritis Patients. *Annals of the Rheumatic Diseases* 2019;**78**:1530–1. doi:10.1136/annrheumdis-2019-eular.5445

182 Wang Y, Gao W. Effects of TNF-α on autophagy of rheumatoid arthritis fibroblast-like synoviocytes and regulation of the NF-κB signaling pathway. *Immunobiology* 2021;**226**:152059. doi:10.1016/j.imbio.2021.152059

183 Taylor W, Gladman D, Helliwell P, *et al.* Classification criteria for psoriatic arthritis: development of new criteria from a large international study. *Arthritis and Rheumatism* 2006;**54**:2665–73. doi:10.1002/art.21972

184 Krenn V, Morawietz L, Häupl T, *et al.* Grading of Chronic Synovitis—A Histopathological Grading System for Molecular and Diagnostic Pathology1. *Pathology-Research and Practice* 2002;**198**:317–25.

185 Krenn V, Morawietz L, Burmester G-R, *et al.* Synovitis score: discrimination between chronic low-grade and high-grade synovitis. *Histopathology* 2006;**49**:358–64. doi:10.1111/j.1365-2559.2006.02508.x

186 Krenn V, Perino G, Rüther W, *et al.* 15 years of the histopathological synovitis score, further development and review: A diagnostic score for rheumatology and orthopaedics. *Pathol Res Pract* 2017;**213**:874–81. doi:10.1016/j.prp.2017.05.005

187 Najm A, Le Goff B, Orr C, *et al.* Standardisation of synovial biopsy analyses in rheumatic diseases: a consensus of the EULAR Synovitis and OMERACT Synovial Tissue Biopsy Groups. *Arthritis Research & Therapy* 2018;**20**:265. doi:10.1186/s13075-018-1762-1

188 Moll JMH, Wright V. Psoriatic arthritis. *Seminars in Arthritis and Rheumatism* 1973;**3**:55–78. doi:10.1016/0049-0172(73)90035-8

189 Husted JA, Gladman DD, Long JA, *et al.* A modified version of the Health Assessment Questionnaire (HAQ) for psoriatic arthritis. *Clin Exp Rheumatol* 1995;**13**:439–43.

190 Schoels MM, Aletaha D, Alasti F, *et al.* Disease activity in psoriatic arthritis (PsA): defining remission and treatment success using the DAPSA score. *Annals of the Rheumatic Diseases* 2016;**75**:811–8. doi:10.1136/annrheumdis-2015-207507

191 Healy PJ, Helliwell PS. Measuring clinical enthesitis in psoriatic arthritis: Assessment of existing measures and development of an instrument specific to psoriatic arthritis. *Arthritis Care & Research* 2008;**59**:686–91. doi:10.1002/art.23568

192 Gossec L, McGonagle D, Korotaeva T, *et al.* Minimal Disease Activity as a Treatment Target in Psoriatic Arthritis: A Review of the Literature. *The Journal of Rheumatology* 2018;**45**:6–13. doi:10.3899/jrheum.170449

193 Coates LC, Fransen J, Helliwell PS. Defining minimal disease activity in psoriatic arthritis: a proposed objective target for treatment. *Annals of the Rheumatic Diseases* 2010;**69**:48–53. doi:10.1136/ard.2008.102053

194 Wallace AB. The exposure treatment of burns. *Lancet* 1951;**1**:501–4.

195 Ficjan A, Husic R, Gretler J, *et al.* Ultrasound composite scores for the assessment of inflammatory and structural pathologies in Psoriatic Arthritis (PsASon-Score). *Arthritis Res Ther* 2014;**16**. doi:10.1186/s13075-014-0476-2

196 Möller I, Janta I, Backhaus M, *et al.* The 2017 EULAR standardised procedures for ultrasound imaging in rheumatology. *Annals of the Rheumatic Diseases* 2017;**76**:1974–9. doi:10.1136/annrheumdis-2017-211585

197 Wakefield RJ, Balint PV, Szkudlarek M, *et al.* Musculoskeletal ultrasound including definitions for ultrasonographic pathology. *The Journal of Rheumatology* 2005;**32**:2485–7.

198 Naredo E, Möller I, Cruz A, *et al.* Power doppler ultrasonographic monitoring of response to anti–tumor necrosis factor therapy in patients with rheumatoid arthritis. *Arthritis & Rheumatism* 2008;**58**:2248–56. doi:10.1002/art.23682

199 Harris PA, Taylor R, Thielke R, *et al.* Research electronic data capture (REDCap)--a metadata-driven methodology and workflow process for providing translational research informatics support. *J Biomed Inform* 2009;**42**:377–81. doi:10.1016/j.jbi.2008.08.010

200 D'Agostino M-A, Wakefield RJ, Berner-Hammer H, *et al.* Value of ultrasonography as a marker of early response to abatacept in patients with rheumatoid arthritis and an inadequate response to methotrexate: results from the APPRAISE study. *Ann Rheum Dis* 2016;**75**:1763–9. doi:10.1136/annrheumdis-2015-207709

201 D'Agostino M-A, Terslev L, Aegerter P, *et al.* Scoring ultrasound synovitis in rheumatoid arthritis: a EULAR-OMERACT ultrasound taskforce-Part 1: definition and development of a standardised, consensus-based scoring system. *RMD Open* 2017;**3**:e000428. doi:10.1136/rmdopen-2016-000428

202 Meric De Bellefon L, Lazarou I. US-Guided Biopsies: Overarching Principles. *Frontiers in Medicine* 2019;**6**. doi:10.3389/fmed.2019.00001

203 Humby FC. Synovial Tissue Sampling in Rheumatological Practice—Past Developments and Future Perspectives. *Frontiers in Medicine* 2019;**6**. doi:10.3389/fmed.2019.00004

204 Koski J, Helle M. Ultrasound guided synovial biopsy using portal and forceps. *Ann Rheum Dis* 2005;**64**:926–9. doi:10.1136/ard.2004.027409

205 Scirè CA, Epis O, Codullo V, *et al.* Immunohistological assessment of the synovial tissue in small joints in rheumatoid arthritis: validation of a minimally invasive ultrasound-guided synovial biopsy procedure. *Arthritis Res Ther* 2007;**9**:R101. doi:10.1186/ar2302

206 Kelly S, Humby F, Filer A, *et al.* Ultrasound-guided synovial biopsy: a safe, well-tolerated and reliable technique for obtaining high-quality synovial tissue from both large and small joints in early arthritis patients. *Annals of the Rheumatic Diseases* 2015;**74**:611–7. doi:10.1136/annrheumdis-2013-204603

207 Najm A, Orr C, Heymann M-F, *et al.* Success Rate and Utility of Ultrasound-guided Synovial Biopsies in Clinical Practice. *The Journal of Rheumatology* 2016;**43**:2113–9. doi:10.3899/jrheum.151441

208 Rosengren S, Corr M, Firestein GS, *et al.* The JAK inhibitor CP-690,550 (tofacitinib) inhibits TNF-induced chemokine expression in fibroblast-like synoviocytes: autocrine role of type I interferon. *Annals of the Rheumatic Diseases* 2012;**71**:440–7. doi:10.1136/ard.2011.150284

209 Rosengren S, Boyle DL, Firestein GS. Acquisition, Culture, and Phenotyping of Synovial Fibroblasts. ;:11.

210 Kuo D, Ding J, Cohn IS, *et al.* HBEGF $^{+}$ macrophages in rheumatoid arthritis induce fibroblast invasiveness. *Science Translational Medicine* 2019;**11**:eaau8587. doi:10.1126/scitranslmed.aau8587

211 Tang Y, Wang B, Sun X, *et al.* Rheumatoid arthritis fibroblast-like synoviocytes co-cultured with PBMC increased peripheral CD4+CXCR5+ICOS+ T cell numbers. *Clinical & Experimental Immunology* 2017;**190**:384–93. doi:10.1111/cei.13025

212 Schindelin J, Arganda-Carreras I, Frise E, *et al.* Fiji: an open-source platform for biological-image analysis. *Nat Methods* 2012;**9**:676–82. doi:10.1038/nmeth.2019

213 Divakaruni AS, Paradyse A, Ferrick DA, *et al.* Analysis and interpretation of microplate-based oxygen consumption and pH data. *Methods Enzymol* 2014;**547**:309–54. doi:10.1016/B978-0-12-801415-8.00016-3

214 Patergnani S, Pinton P. Mitophagy and mitochondrial balance. *Methods Mol Biol* 2015;**1241**:181–94. doi:10.1007/978-1-4939-1875-1_15

215 Hawerkamp HC, Domdey A, Radau L, *et al.* Tofacitinib downregulates antiviral immune defence in keratinocytes and reduces T cell activation. *Arthritis Res Ther* 2021;**23**:144. doi:10.1186/s13075-021-02509-8

216 Wechalekar M.D., Najm A., Veale D.J., *et al.* The 2018 OMERACT synovial Tissue Biopsy special interest group report on standardization of synovial biopsy analysis. *J Rheumatol* 2019;**46**:1365–8. doi:10.3899/jrheum.181062

217 Ingegnoli F, Coletto LA, Scotti I, *et al.* The Crucial Questions on Synovial Biopsy: When, Why, Who, What, Where, and How? *Frontiers in Medicine* 2021;**8**:1232. doi:10.3389/fmed.2021.705382

218 Small A, Wechalekar MD. Synovial biopsies in inflammatory arthritis: precision medicine in rheumatoid arthritis. *Expert Review of Molecular Diagnostics* 2019;**0**:null. doi:10.1080/14737159.2020.1707671

219 Gerlag DM, Tak PP. How to perform and analyse synovial biopsies. *Best Practice & Research Clinical Rheumatology* 2013;**27**:195–207. doi:10.1016/j.berh.2013.03.006

220 Lazarou I, D'Agostino M-A, Naredo E, *et al.* Ultrasound-guided synovial biopsy: a systematic review according to the OMERACT filter and recommendations for minimal reporting standards in clinical studies. *Rheumatology (Oxford)* 2015;**54**:1867–75. doi:10.1093/rheumatology/kev128

221 Lazarou I, Kelly S, Humby F, *et al.* Ultrasound-guided synovial biopsy of the wrist does not alter subsequent clinical or ultrasound disease activity assessments: a prospective study for incorporation of imaging in clinical trials. *Clin Exp Rheumatol* 2016;**34**:802–7.

222 Humby F, Kelly S, Bugatti S, *et al.* Evaluation of Minimally Invasive, Ultrasound-guided Synovial Biopsy Techniques by the OMERACT Filter--Determining Validation Requirements. *J Rheumatol* 2016;**43**:208–13. doi:10.3899/jrheum.141199

223 Maeshima K, Yamaoka K, Kubo S, *et al.* The JAK inhibitor tofacitinib regulates synovitis through inhibition of interferon-γ and interleukin-17 production by human CD4+ T cells. *Arthritis & Rheumatism* 2012;**64**:1790–8. doi:10.1002/art.34329

224 Migita K, Komori A, Torigoshi T, *et al.* CP690,550 inhibits oncostatin M-induced JAK/STAT signaling pathway in rheumatoid synoviocytes. *Arthritis Research & Therapy* 2011;**13**:R72. doi:10.1186/ar3333

225 Bucala R, Ritchlin C, Winchester R, *et al.* Constitutive production of inflammatory and mitogenic cytokines by rheumatoid synovial fibroblasts. *J Exp Med* 1991;**173**:569–74. doi:10.1084/jem.173.3.569

226 Zou Q-F, Li L, Han Q-R, *et al.* Abatacept alleviates rheumatoid arthritis development by inhibiting migration of fibroblast-like synoviocytes via MAPK pathway. *Eur Rev Med Pharmacol Sci* 2019;**23**:3105–11. doi:10.26355/eurrev_201904_17594

227 Huang W, Zhang L, Cheng C, *et al.* Parallel comparison of fibroblast-like synoviocytes from the surgically removed hyperplastic synovial tissues of rheumatoid arthritis and osteoarthritis patients. *BMC Musculoskeletal Disorders* 2019;**20**. doi:10.1186/s12891-019-2977-2

228 Andersen M, Boesen M, Ellegaard K, *et al.* Association between IL-6 production in synovial explants from rheumatoid arthritis patients and clinical and imaging response to biologic treatment: A pilot study. *PLoS One* 2018;**13**. doi:10.1371/journal.pone.0197001

229 Kawashiri S-Y, Kawakami A, Iwamoto N, *et al.* Proinflammatory Cytokines Synergistically Enhance the Production of Chemokine Ligand 20 (CCL20) from Rheumatoid Fibroblast-like Synovial Cells in vitro and Serum CCL20 Is Reduced in vivo by Biologic Disease-modifying Antirheumatic Drugs. *The Journal of Rheumatology* 2009;**36**:2397–402. doi:10.3899/jrheum.090132

230 Bürger C, Shirsath N, Lang V, *et al.* Blocking mTOR Signalling with Rapamycin Ameliorates Imiquimod-induced Psoriasis in Mice. *Acta Derm Venereol* 2017;**97**:1087–94. doi:10.2340/00015555-2724

231 Chen J, Long F. mTOR signaling in skeletal development and disease. *Bone Res* 2018;**6**:1. doi:10.1038/s41413-017-0004-5

232 Raychaudhuri SK, Raychaudhuri SP. mTOR Signaling Cascade in Psoriatic Disease: Double Kinase mTOR Inhibitor a Novel Therapeutic Target. *Indian J Dermatol* 2014;**59**:67–70. doi:10.4103/0019-5154.123499

233 Mitra A, Raychaudhuri SK, Raychaudhuri SP. IL-22 induced cell proliferation is regulated by PI3K/Akt/mTOR signaling cascade. *Cytokine* 2012;**60**:38–42. doi:10.1016/j.cyto.2012.06.316

234 Clarke AJ, Ellinghaus U, Cortini A, *et al.* Autophagy is activated in systemic lupus erythematosus and required for plasmablast development. *Annals of the Rheumatic Diseases* 2015;**74**:912–20. doi:10.1136/annrheumdis-2013-204343

235 Alessandri C, Barbati C, Vacirca D, *et al.* T lymphocytes from patients with systemic lupus erythematosus are resistant to induction of autophagy. *FASEB J* 2012;**26**:4722–32. doi:10.1096/fj.12-206060

236 Patergnani S, Bouhamida E, Leo S, *et al.* Mitochondrial Oxidative Stress and "Mito-Inflammation": Actors in the Diseases. *Biomedicines* 2021;**9**:216. doi:10.3390/biomedicines9020216

237 Eisner V, Picard M, Hajnóczky G. Mitochondrial dynamics in adaptive and maladaptive cellular stress responses. *Nat Cell Biol* 2018;**20**:755–65. doi:10.1038/s41556-018-0133-0

238 Kim H-R, Kim K-W, Kim B-M, *et al.* N-acetyl-l-cysteine controls osteoclastogenesis through regulating Th17 differentiation and RANKL in rheumatoid arthritis. *Korean J Intern Med* 2019;**34**:210–9. doi:10.3904/kjim.2016.329

239 Croft AP, Campos J, Jansen K, *et al.* Distinct fibroblast subsets drive inflammation and damage in arthritis. *Nature* 2019;:1. doi:10.1038/s41586-019-1263-7

240 Dennis G, Holweg CT, Kummerfeld SK, *et al.* Synovial phenotypes in rheumatoid arthritis correlate with response to biologic therapeutics. *Arthritis Res Ther* 2014;**16**:R90. doi:10.1186/ar4555

241 Humby F, Lewis M, Ramamoorthi N, *et al.* Synovial cellular and molecular signatures stratify clinical response to csDMARD therapy and predict radiographic progression in early rheumatoid arthritis patients. *Annals of the Rheumatic Diseases* 2019;**78**:761–72. doi:10.1136/annrheumdis-2018-214539

242 Alivernini S, Tolusso B, Gessi M, *et al.* Inclusion of Synovial Tissue–Derived Characteristics in a Nomogram for the Prediction of Treatment Response in Treatment-Naive Rheumatoid Arthritis Patients. *Arthritis Rheumatol* 2021;**73**:1601–13. doi:10.1002/art.41726

Acknowledgments

E. Silvagni would like to thank the clinicians and nurses of the Rheumatology Unit, Ferrara University, for their help in the clinical evaluation of patients with chronic inflammatory arthropathies, as well as all the personnel of the Paolo Pinton Lab__Signal Transduction, Department of Medical Sciences, University of Ferrara, and the personnel of the Pathology Division, Department of Translational Medicine, University of Ferrara. He is grateful to Carlo Alberto Scirè for his strenuous help and continuous support.

Conflicts of interest

E. Silvagni has received research support from AbbVie, and consulting/speaker's fees from AbbVie, Pfizer, and Novartis.

Funding

The author declares the present study was partially supported by local funds from the University of Ferrara.